The DUNE Far Detector Interim Design Report

Volume 1: Physics, Technology & Strategies

Deep Underground Neutrino Experiment (DUNE)

This document was prepared by Deep Underground Neutrino Experiment (DUNE) using the resources of the Fermi National Accelerator Laboratory (Fermilab), a U.S. Department of Energy, Office of Science, HEP User Facility. Fermilab is managed by Fermi Research Alliance, LLC (FRA), acting under Contract No. DE-AC02-07CH11359. Fermilab-Design-2018-02

DUNE
DEEP UNDERGROUND NEUTRINO EXPERIMENT

FERMILAB-DESIGN-2018-02

Cover design: Diana Brandonisio, Fermilab Creative Services, July 2018
Cover photo: "Inside ProtoDUNE" by Maximilien Brice, ©CERN, November 2017

Authors

B. Abi,[125] R. Acciarri,[54] M. A. Acero,[8] M. Adamowski,[54] C. Adams,[62] D. Adams,[15] P. Adamson,[54] M. Adinolfi,[14] Z. Ahmad,[165] C. H. Albright,[54] L. Aliaga Soplin,[54] T. Alion,[152] S. Alonso Monsalve,[20] M. Alrashed,[89] C. Alt,[47] J. Anderson,[5] K. Anderson,[54] C. Andreopoulos,[99] M. P. Andrews,[54] R. A. Andrews,[54] A. Ankowski,[140] J. Anthony,[27] M. Antonello,[58] M. Antonova,[68] S. Antusch,[10] A. Aranda Fernandez,[34] A. Ariga,[11] T. Ariga,[11] D. Aristizabal Sierra,[154] E. Arrieta Diaz,[150] J. Asaadi,[157] M. Ascencio,[135] D. Asner,[15] M. S. Athar,[1] M. Auger,[11] A. Aurisano,[32] V. Aushev,[94] D. Autiero,[79] F. Azfar,[125] A. Back,[82] H. Back,[126] J. Back,[170] C. Backhouse,[100] P. Baesso,[14] L. Bagby,[54] X. Bai,[147] M. Baird,[167] B. Balantekin,[173] S. Balasubramanian,[175] B. Baller,[54] P. Ballett,[46] L. Balleyguier,[79] B. Bambah,[66] H. Band,[175] M. Bansal,[129] S. Bansal,[129] G. Barenboim,[68] G. J. Barker,[170] C. Barnes,[108] G. Barr,[125] J. Barranco Monarca,[60] N. Barros,[132] J. Barrow,[155] A. Bashyal,[123] V. Basque,[105] M. Bass,[15] F. Bay,[160] K. Bays,[26] J. L. Bazo,[135] J. F. Beacom,[122] E. Bechetoille,[79] B. R. Behera,[129] L. Bellantoni,[54] G. Bellettini,[133] V. Bellini,[28] O. Beltramello,[20] D. Belver,[21] N. Benekos,[20] P. A. Benetti,[130] A. Bercellie,[139] E. Berman,[54] P. Bernardini,[164] R. Berner,[11] H.-G. Berns,[23] R. H. Bernstein,[54] S. Bertolucci,[74] M. Betancourt,[54] V. Bhatnagar,[129] M. Bhattacharjee,[71] B. Bhuyan,[71] S. Biagi,[96] J. Bian,[24] K. Biery,[54] B. Bilki,[81] M. Bishai,[15] A. Bitadze,[105] T. Blackburn,[152] A. Blake,[97] B. Blanco Siffert,[51] F. Blaszczyk,[13] E. Blaufuss,[106] G. C. Blazey,[113] M. Blennow,[88] E. Blucher,[30] V. Bocean,[54] F. Boffelli,[130] J. Boissevain,[101] S. Bolognesi,[19] T. Bolton,[89] M. Bonesini,[73] T. Boone,[36] A. Booth,[152] C. Booth,[143] S. Bordoni,[20] A. Borkum,[152] T. Boschi,[46] P. Bour,[39] B. Bourguille,[67] S. B. Boyd,[170] D. Boyden,[113] J. Bracinik,[12] D. Brailsford,[97] A. Brandt,[157] J. Bremer,[20] S. J. Brice,[54] C. Bromberg,[109] G. Brooijmans,[37] J. Brooke,[14] G. Brown,[157] N. Buchanan,[36] H. Budd,[139] P. C. de Holanda,[49] T. Cai,[139] D. Caiulo,[79] P. Calafiura,[98] A. Calatayud,[135] J. Calcutt,[109] C. Callahan,[132] E. Calligarich,[130] E. Calvo,[21] L. Camilleri,[37] A. Caminata,[56] M. Campanelli,[100] G. Cancelo,[54] K. Cankocak,[81] C. Cantini,[47] D. Caratelli,[54] B. Carlus,[79] M. Carneiro,[123] I. Caro Terrazas,[36] T. J. Carroll,[158] M. P. Carvallo,[151] M. Cascella,[100] C. Castromonte,[114] E. Catano-Mur,[82] M. Cavalli-Sforza,[67] F. Cavanna,[54] E. Cazzato,[10] S. Centro,[128] G. Cerati,[54] A. Cervelli,[74] A. Cervera Villanueva,[68] T. Cervi,[130] M. Chalifour,[20] A. Chappuis,[95] A. Chatterjee,[157] S. Chattopadhyay,[54] S. Chattopadhyay,[165] J. Chaves,[132] H. Chen,[15] M.-C. Chen,[24] S. Chen,[159] D. Cherdack,[36] C.-Y. Chi,[37] S. Childress,[54] K. Cho,[92] S. Choubey,[61] B. C. Choudhary,[43] A. Christensen,[36] D. Christian,[54] G. Christodoulou,[99] C.-A. Christofferson,[147] E. Church,[126] P. Clarke,[48] T. E. Coan,[150] A. Cocco,[115] G. H. Collin,[107] E. Conley,[45] J. M. Conrad,[107] M. Convery,[140] R. Corey,[147] L. Corwin,[147] P. Cotte,[19] L. Cremonesi,[100] J. I. Crespo-Anadón,[37] J. Creus Prats,[20] E. Cristaldo,[163] P. Crivelli,[47] D. Cronin-Hennessy,[112] C. Crowley,[54] C. Cuesta,[21] A. Curioni,[73] D. Cussans,[14] M. Dabrowski,[15] D. Dale,[76] H. Da Motta,[18] T. Davenne,[141] E. Davenport,[157] G. S. Davies,[78] J. Davies,[152] S. Davini,[56] J. Dawson,[4] K. De,[157] M. P. Decowski,[119] P. Dedin Neto,[49] I. de Icaza Astiz,[152] A. Delbart,[19] D. Delepine,[60] M. Delgado,[3] A. Dell,[20] J. de Mello Neto,[51] D. DeMuth,[166] Z. Deng,[159] S. Dennis,[99] C. Densham,[141] I. De Bonis,[95] A. De Gouvêa,[120] P. De Jong,[119] P. De Lurgio,[5] S. De Rijck,[158] A. De Roeck,[20] J. J. de Vries,[27] R. Dharmapalan,[5] N. Dhingra,[129] M. Diamantopoulou,[7] F. Diaz,[135] J. S. Díaz,[78] G. Diaz Bautista,[139] P. Ding,[54] C. Distefano,[96] M. Diwan,[15] S. Di Domizio,[56] L. Di Giulio,[20] S. Di Luise,[67] Z. Djurcic,[5] F. Doizon,[79] N. Dokania,[151] M. J. Dolinski,[44] R. Dong,[81] J. dos Anjos,[18] D. Douglas,[109] G. Drake,[5] D. Duchesneau,[95] K. Duffy,[54] B. Dung,[158] D. Dutta,[61] M. Duvernois,[173] H. Duyang,[145] O. Dvornikov,[63] D. A. Dwyer,[98] S. Dye,[63] A. S. Dyshkant,[113] S. Dytman,[134] M. Eads,[113] B. Eberly,[140] D. Edmunds,[109] J. Eisch,[82] A. Elagin,[30] S. Elliott,[101] W. Ellsworth,[64] M. Elnimr,[24] S. Emery,[19] S. Eno,[106] A. Ereditato,[11] C. O. Escobar,[54] L. Escudero Sanchez,[27] J. J. Evans,[105] A. Ezeribe,[143] K. Fahey,[54] A. Falcone,[157] L. Falk,[152] A. Farbin,[157] C. Farnese,[128] Y. Farzan,[75] M. Fasoli,[73] A. Fava,[54] J. Felix,[60] E. Fernandez-Martinez,[104] P. Fernandez Menendez,[68] F. Ferraro,[56] F. Feyzi,[54] L. Fields,[54] A. Filkins,[172] F. Filthaut,[119] A. Finch,[97] O. Fischer,[10] M. Fitton,[141] R. Fitzpatrick,[108] W. Flanagan,[41] B. T. Fleming,[175] R. Flight,[139] T. Forest,[76] J. Fowler,[45] W. Fox,[78] J. Franc,[39] K. Francis,[113] P. Franchini,[170] D. Franco,[175] J. Freeman,[54] J. Freestone,[105] J. Fried,[15] A. Friedland,[140] S. Fuess,[54] I. Furic,[55] A. Furmanski,[105] A. M. Gago,[135] H. Gallagher,[161] A. Gallego-Ros,[21] V. Galymov,[79] E. Gamberini,[20] S. Gambetta,[20] T. Gamble,[143] R. Gandhi,[61] R. Gandrajula,[109] S. Gao,[15] D. Garcia-Gamez,[105] S. Gardiner,[23] D. Gastler,[13] J. Gehrlein,[104] B. Gelli,[49] A. Gendotti,[47] Z. Ghorbani-Moghaddam,[23] A. Ghosh,[154] D. Gibin,[128] I. Gil-Botella,[21] C. Girerd,[79] A. K. Giri,[72] S. Glavin,[132] D. Goeldi,[11] O. Gogota,[94] M. Gold,[117] S. Gollapinni,[155] K. Gollwitzer,[54] R. A. Gomes,[57] L. Gomez,[142] L. V. Gomez Bermeo,[142] J. J. Gomez Cadenas,[68] H. Gong,[159] F. Gonnella,[12] J. A. Gonzalez-Cuevas,[163] M. Goodman,[5] O. Goodwin,[105] D. Gorbunov,[80] S. Goswami,[127] E. Goudzovski,[12] C. Grace,[98] N. Graf,[134] N. Graf,[140] M. Graham,[140] E. Gramellini,[175] R. Gran,[111] A. Grant,[42] C. Grant,[13] N. Grant,[170] V. Greco,[28] S. Green,[27] H. Greenlee,[54] L. Greenler,[173] M. Greenwood,[123] J. Greer,[14] W. C. Griffith,[152] M. Groh,[78]

J. Grudzinski,[5] K. Grzelak,[168] G. Guanghua,[159] E. Guardincerri,[101] V. Guarino,[5] G. P. Guedes,[53] R. Guenette,[62] A. Guglielmi,[128] B. Guo,[145] S. Gupta,[84] V. Gupta,[71] K. K. Guthikonda,[91] R. Gutierrez,[3] P. Guzowski,[105] M. M. Guzzo,[49] A. Habig,[111] R. W. Hackenburg,[15] A. Hackenburg,[175] B. Hackett,[63] H. Hadavand,[157] R. Haenni,[11] A. Hahn,[54] J. Haigh,[170] T. Haines,[101] J. Haiston,[147] T. Hamernik,[54] P. Hamilton,[153] J. Han,[134] T. Handler,[155] S. Hans,[15] D. A. Harris,[54] J. Hartnell,[152] T. Hasegawa,[87] R. Hatcher,[54] A. Hatzikoutelis,[155] S. Hays,[54] E. Hazen,[13] M. Headley,[148] A. Heavey,[54] K. Heegerv,[175] J. Heise,[148] K. Hennessy,[99] S. Henry,[139] A. Hernandez,[3] J. Hernandez-Garcia,[104] K. Herner,[54] J. Hewes,[32] J. Hignight,[109] A. Higuera,[64] T. Hill,[76] S. Hillier,[12] A. Himmel,[54] C. Hohl,[10] A. Holin,[100] E. Hoppe,[126] S. Horikawa,[47] G. Horton-Smith,[89] M. Hostert,[46] A. Hourlier,[107] B. Howard,[78] R. Howell,[139] J. Huang,[158] J. Hugon,[102] P. Hurh,[54] J. Hylen,[54] R. Illingworth,[54] J. Insler,[44] G. Introzzi,[130] A. Ioannisian,[176] A. Izmaylov,[68] D. E. Jaffe,[15] C. James,[54] E. James,[54] C.-H. Jang,[31] F. Jediny,[39] Y. S. Jeong,[6] A. Jhingan,[129] W. Ji,[15] A. Jipa,[16] S. Jiménez,[21] C. Johnson,[36] M. Johnson,[54] R. Johnson,[32] J. Johnstone,[54] B. Jones,[157] S. Jones,[100] J. Joshi,[15] H. Jostlein,[54] C. K. Jung,[151] T. Junk,[54] A. Kaboth,[141] I. Kadenko,[94] F. Kamiya,[52] Y. Kamyshkov,[155] G. Karagiorgi,[37] D. Karasavvas,[7] Y. Karyotakis,[95] S. Kasai,[93] S. Kasetti,[102] K. Kaur,[129] B. Kayser,[54] N. Kazaryan,[176] E. Kearns,[13] P. Keener,[132] E. Kemp,[49] C. Kendziora,[54] W. Ketchum,[54] S. H. Kettell,[15] M. Khabibullin,[80] A. Khotjantsev,[80] D. Kim,[20] B. Kirby,[15] M. Kirby,[54] J. Klein,[132] Y.-J. Ko,[31] T. Kobilarcik,[54] B. Kocaman,[160] L. W. Koerner,[64] S. Kohn,[22] G. Koizumi,[54] P. Koller,[11] A. Kopylov,[80] M. Kordosky,[172] L. Kormos,[97] T. Kosc,[79] U. Kose,[20] V. A. Kostelecký,[78] K. Kothekar,[14] M. Kramer,[22] F. Krennrich,[82] I. Kreslo,[11] K. Kriesel,[173] W. Kropp,[24] Y. Kudenko,[80] V. A. Kudryavtsev,[143] S. Kulagin,[80] J. Kumar,[63] L. Kumar,[129] A. Kumar,[129] S. Kumbhare,[157] C. Kuruppu,[145] V. Kus,[39] T. Kutter,[102] R. LaZur,[36] K. Lande,[132] C. Lane,[44] K. Lang,[158] T. Langford,[175] F. Lanni,[15] P. Lasorak,[152] D. Last,[132] C. Lastoria,[21] A. Laundrie,[173] I. Lazanu,[16] T. Le,[161] J. Learned,[63] P. Lebrun,[54] D. Lee,[101] G. Lehmann Miotto,[20] M. A. Leigui de Oliveira,[52] Q. Li,[54] S. Li,[15] S. W. Li,[140] X. Li,[151] Y. Li,[15] Z. Li,[45] H.-Y. Liao,[89] S.-K. Lin,[36] C-J. S. Lin,[98] R. Linehan,[140] V. Linhart,[39] J. Link,[167] Z. Liptak,[35] D. Lissauer,[15] L. Littenberg,[15] B. Littlejohn,[69] J. Liu,[146] T. Liu,[150] L. LoMonaco,[28] J. M. LoSecco,[121] S. Lockwitz,[54] N. Lockyer,[54] T. Loew,[98] M. Lokajicek,[17] K. Long,[77] K. Loo,[86] J. P. Lopez,[35] D. Lorca,[11] T. Lord,[170] M. Losada,[3] W. C. Louis,[101] M. Luethi,[11] K.-B. Luk,[22] T. Lundin,[54] X. Luo,[175] N. Lurkin,[12] T. Lux,[67] V. P. Luzio,[52] J. Lykken,[54] J. Maalampi,[86] R. MacLellan,[146] A. A. Machado,[52] P. Machado,[54] C. T. Macias,[78] J. Macier,[54] P. Madigan,[22] S. Magill,[5] G. Mahler,[15] K. Mahn,[109] M. Malek,[143] J. A. Maloney,[40] F. Mammoliti,[62] S. K. Mandal,[43] G. Mandrioli,[74] L. Manenti,[100] S. Manly,[139] A. Mann,[161] A. Marchionni,[54] W. Marciano,[15] S. Marcocci,[54] D. Marfatia,[63] C. Mariani,[167] J. Maricic,[63] F. Marinho,[162] A. D. Marino,[35] M. Marshak,[112] C. Marshall,[98] J. Marshall,[27] J. Marteau,[79] J. Martin-Albo,[125] D. Martinez,[69] N. Martinez,[137] H. Martinez,[142] K. Mason,[161] A. Mastbaum,[30] M. Masud,[68] H. Mathez,[79] S. Matsuno,[63] J. Matthews,[102] C. Mauger,[132] N. Mauri,[74] K. Mavrokoridis,[99] R. Mazza,[73] A. Mazzacane,[54] E. Mazzucato,[19] N. McCauley,[99] E. McCluskey,[54] N. McConkey,[143] K. McDonald,[136] K. S. McFarland,[139] C. McGivern,[54] A. McGowan,[139] C. McGrew,[151] R. McKeown,[172] A. McNab,[105] D. McNulty,[76] R. McTaggart,[149] V. Meddage,[89] A. Mefodiev,[80] P. Mehta,[85] D. Mei,[146] O. Mena,[68] S. Menary,[177] H. Mendez,[137] D. P. Mendez,[152] A. Menegolli,[130] G. Meng,[128] M. Messier,[78] W. Metcalf,[102] M. Mewes,[78] H. Meyer,[171] T. Miao,[54] J. Migenda,[143] R. Milincic,[63] J. Miller,[154] W. Miller,[112] J. Mills,[161] C. Milne,[76] O. Mineev,[80] O. Miranda,[33] C. S. Mishra,[54] S. R. Mishra,[145] A. Mislivec,[112] B. Mitrica,[65] D. Mladenov,[20] I. Mocioiu,[131] K. Moffat,[46] N. Moggi,[74] R. Mohanta,[66] N. Mokhov,[54] J. Molina,[163] L. Molina Bueno,[47] A. Montanari,[74] C. Montanari,[130] D. Montanari,[54] L. Montano Zetina,[33] J. Moon,[107] M. Mooney,[36] C. Moore,[54] D. Moreno,[3] B. Morgan,[170] G. F. Moroni,[54] C. Morris,[64] W. Morse,[15] C. Mossey,[54] C. A. Moura,[52] J. Mousseau,[108] L. Mualem,[26] M. Muether,[171] S. Mufson,[78] F. Muheim,[48] H. Muramatsu,[112] S. Murphy,[47] J. Musser,[78] J. Nachtman,[81] M. Nalbandyan,[176] R. Nandakumar,[141] D. Naples,[134] S. Narita,[83] G. Navarro,[3] J. Navarro,[8] D. Navas-Nicolás,[21] N. Nayak,[24] M. Nebot-Guinot,[48] M. Needham,[48] K. Negishi,[83] J. Nelson,[172] M. Nessi,[20] D. Newbold,[14] M. Newcomer,[132] R. Nichol,[100] T. C. Nicholls,[141] E. Niner,[54] A. Norman,[54] B. Norris,[54] J. Norris,[76] P. Novella,[68] E. Nowak,[20] J. Nowak,[97] M. S. Nunes,[49] H. O'Keeffe,[97] M. Oberling,[5] A. Olivares Del Campo,[46] A. Olivier,[139] Y. Onel,[81] Y. Onishchuk,[94] T. Ovsjannikova,[80] S. Ozturk,[20] L. Pagani,[23] S. Pakvasa,[63] O. Palamara,[54] J. Paley,[54] M. Pallavicini,[56] C. Palomares,[21] J. Palomino,[151] E. Pantic,[23] A. Paolo,[64] V. Paolone,[134] V. Papadimitriou,[54] R. Papaleo,[96] S. Paramesvaran,[14] J. Park,[167] S. Parke,[54] Z. Parsa,[15] S. Pascoli,[46] J. Pasternak,[77] J. Pater,[105] L. Patrizii,[74] R. B. Patterson,[26] S. J. Patton,[98] T. Patzak,[4] A. Paudel,[89] B. Paulos,[173] L. Paulucci,[52] Z. Pavlovic,[54] G. Pawloski,[112] P. Payam,[75] D. Payne,[99] V. Pec,[143] S. J. M. Peeters,[152] E. Pennacchio,[79] A. Penzo,[81] G. N. Perdue,[54] O. l. G. Peres,[49] L. Periale,[47] K. Petridis,[14] G. Petrillo,[140] R. Petti,[145] P. Picchi,[130] L. Pickering,[109] F. Pietropaolo,[128] J. Pillow,[170] P. Plonski,[169] R. Plunkett,[54] R. Poling,[112] X. Pons,[20] N. Poonthottathil,[82]

M. Popovic,[54] R. Pordes,[54] S. Pordes,[54] M. Potekhin,[15] R. Potenza,[28] B. Potukuchi,[84] S. Poudel,[64] J. Pozimski,[77] M. Pozzato,[74] T. Prakasj,[98] R. Preece,[141] O. Prokofiev,[54] N. Pruthi,[129] P. Przewlocki,[116] F. Psihas,[78] D. Pugnre,[79] D. Pushka,[54] K. Qi,[151] X. Qian,[15] J. L. Raaf,[54] R. Raboanary,[2] V. Radeka,[15] J. Rademacker,[14] V. Radescu,[20] B. Radics,[47] A. Radovic,[172] A. Rafique,[89] M. Rajaoalisoa,[2] I. Rakhno,[54] H. T. Rakotondramanana,[2] L. Rakotondravohitra,[2] Y. A. Ramachers,[170] R. A. Rameika,[54] M. A. Ramirez Delgado,[60] J. Ramsey,[101] B. J. Ramson,[54] A. Rappoldi,[130] G. L. Raselli,[130] P. Ratoff,[97] S. Ravat,[20] O. Ravinez,[114] H. Razafinime,[2] B. Rebel,[54] D. Redondo,[21] C. Regenfus,[47] M. Reggiani-Guzzo,[49] T. Rehak,[44] J. Reichenbacher,[147] D. Reitzner,[54] M. H. Reno,[81] A. Renshaw,[64] S. Rescia,[15] F. Resnati,[20] A. Reynolds,[125] G. Riccobene,[96] L. C. J. Rice,[113] K. Rielage,[101] K. Riesselmann,[54] Y. - A. Rigaut,[47] D. Rivera,[132] L. Rochester,[140] M. Roda,[99] P. Rodrigues,[125] M. J. Rodriguez Alonso,[20] B. Roe,[108] A. J. Roeth,[45] R. M. Roser,[54] M. Ross-Lonergan,[46] M. Rossella,[130] J. Rout,[85] S. Roy,[61] A. Rubbia,[47] C. Rubbia,[59] R. Rucinski,[54] B. Russell,[175] J. Russell,[140] D. Ruterbories,[139] M. R. Vagins,[90] R. Saakyan,[100] N. Sahu,[72] P. Sala,[110] G. Salukvadze,[20] N. Samios,[15] F. Sanchez,[67] M. C. Sanchez,[82] C. Sandoval,[3] B. Sands,[136] S. U. Sankar,[70] S. Santana,[137] L. M. Santos,[49] G. Santucci,[151] N. Saoulidou,[7] P. Sapienza,[96] C. Sarasty,[32] I. Sarcevic,[6] G. Savage,[54] A. Scaramelli,[130] A. Scarpelli,[4] T. Schaffer,[111] H. Schellman,[123] P. Schlabach,[54] C. M. Schloesser,[47] D. W. Schmitz,[30] J. Schneps,[161] K. Scholberg,[45] A. Schukraft,[54] E. Segreto,[49] S. Sehrawat,[61] J. Sensenig,[132] I. Seong,[24] J. A. Sepulveda-Quiroz,[82] A. Sergi,[12] F. Sergiampietri,[151] D. Sessumes,[157] K. Sexton,[15] L. Sexton-Kennedy,[54] D. Sgalaberna,[20] M. H. Shaevitz,[37] S. Shafaq,[85] J. S. Shahi,[129] S. Shahsavarani,[157] P. Shanahan,[54] H. R. Sharma,[84] R. Sharma,[15] R. K. Sharma,[138] T. Shaw,[54] S. Shin,[30] I. Shoemaker,[146] D. Shooltz,[109] R. Shrock,[151] N. Simos,[15] J. Sinclair,[11] G. Sinev,[45] V. Singh,[9] J. Singh,[103] J. Singh,[103] I. Singh,[129] J. Singh,[129] R. Sipos,[20] F. W. Sippach,[37] G. Sirri,[74] K. Siyeon,[31] D. Smargianaki,[151] A. Smith,[27] A. Smith,[45] E. Smith,[78] P. Smith,[78] J. Smolik,[39] M. Smy,[24] E. L. Snider,[54] P. Snopok,[69] J. Sobczyk,[174] H. Sobel,[24] M. Soderberg,[153] C. J. Solano Salinas,[114] N. Solomey,[171] W. Sondheim,[101] M. Sorel,[68] J. A. Soto-Oton,[21] A. Sousa,[32] K. Soustruznik,[29] F. Spagliardi,[125] M. Spanu,[130] J. Spitz,[108] N. J. C. Spooner,[143] R. Staley,[12] M. Stancari,[54] L. Stanco,[128] A. Stefanik,[54] H. M. Steiner,[98] J. Stewart,[15] J. Stock,[147] F. Stocker,[20] S. Stoica,[65] J. Stone,[13] J. Strait,[54] M. Strait,[112] T. Strauss,[54] S. Striganov,[54] A. Stuart,[34] G. Sullivan,[106] M. Sultana,[139] Y. Sun,[63] A. Surdo,[164] V. Susic,[10] L. Suter,[54] C. M. Sutera,[28] R. Svoboda,[23] B. Szczerbinska,[156] A. M. Szelc,[105] S. Söldner-Rembold,[105] N. Tagg,[124] R. Talaga,[5] H. Tanaka,[140] B. Tapia Oregui,[158] S. Tariq,[54] E. Tatar,[76] R. Tayloe,[78] M. Tenti,[74] K. Terao,[140] C. Ternes,[68] F. Terranova,[73] G. Testera,[56] A. Thea,[141] L. F. Thompson,[143] J. Thompson,[143] C. Thorn,[15] A. Timilsina,[15] S. C. Timm,[54] J. Todd,[32] A. Tonazzo,[4] T. Tope,[54] D. Torbunov,[112] M. Torti,[73] M. Tortola,[68] F. Tortorici,[28] M. Toups,[54] C. Touramanis,[99] J. Trevor,[26] M. Tripathi,[23] W. Tromeur,[79] I. Tropin,[54] W. H. Trzaska,[86] Y.-T. Tsai,[140] K. V. Tsang,[140] A. Tsaris,[54] S. Tufanli,[175] C. Tull,[98] J. Turner,[46] M. Tzanov,[102] E. Tziaferi,[7] Y. Uchida,[77] J. Urheim,[78] T. Usher,[140] G. A. Valdiviesso,[50] E. Valencia,[172] L. Valerio,[54] Z. Vallari,[151] J. Valle,[68] R. Van Berg,[132] R. Van de Water,[101] F. Varanini,[128] G. Varner,[63] J. Vasel,[78] G. Vasseur,[19] K. Vaziri,[54] G. Velev,[54] S. Ventura,[128] A. Verdugo,[21] M. Vermeulen,[119] E. Vernon,[15] M. Verzocchi,[54] T. Viant,[47] C. Vignoli,[58] S. Vihonen,[86] C. Vilela,[151] B. Viren,[15] P. Vokac,[39] T. Vrba,[39] T. Wachala,[118] D. Wahl,[173] M. Wallbank,[32] H. Wang,[25] J. Wang,[23] T.-C. Wang,[46] B. Wang,[150] Y. Wang,[151] Z. Wang,[159] K. Warburton,[82] D. Warner,[36] M. O. Wascko,[77] D. Waters,[100] A. Watson,[12] A. Weber,[125, 141] M. Weber,[11] H. Wei,[15] W. Wei,[146] A. Weinstein,[82] D. Wenman,[173] M. Wetstein,[82] M. While,[147] A. White,[157] L. H. Whitehead,[20] D. Whittington,[153] K. Wierman,[126] M. Wilking,[151] C. Wilkinson,[11] J. Willhite,[54] Z. Williams,[157] R. J. Wilson,[36] P. Wilson,[54] P. Wittich,[38] J. Wolcott,[161] T. Wongjirad,[161] K. Wood,[151] L. Wood,[126] E. Worcester,[15] M. Worcester,[15] S. Wu,[47] W. Wu,[54] W. Xu,[146] C. Yanagisawa,[151] S. Yang,[32] T. Yang,[54] G. Yang,[151] J. Ye,[150] M. Yeh,[15] N. Yershov,[80] K. Yonehara,[54] L. Yoshimura,[163] B. Yu,[15] J. Yu,[157] J. Zalesak,[17] L. Zambelli,[95] B. Zamorano,[152] A. Zani,[20] K. Zaremba,[169] L. Zazueta,[172] G. P. Zeller,[54] J. Zennamo,[54] C. Zhang,[15] C. Zhang,[146] M. Zhao,[15] Y.-L. Zhou,[46] G. Zhu,[122] E. D. Zimmerman,[35] M. Zito,[19] S. Zucchelli,[74] J. Zuklin,[17] V. Zutshi,[113] and R. Zwaska[54]

(The DUNE Collaboration)

[1] *Aligarh Muslim University, Department of Physics, Aligarh-202002, India*
[2] *University of Antananarivo, BP 566, Antananarivo 101, Madagascar*
[3] *Universidad Antonio Nariño, Cra 3 Este No 47A-15, Bogota, Colombia*
[4] *APC, AstroParticule et Cosmologie, Universit Paris Diderot, CNRS/IN2P3, CEA/lrfu, Observatoire de Paris, Sorbonne Paris Cit, 10, rue Alice Domon et Lonie Duquet, 75205 Paris Cedex 13, France*
[5] *Argonne National Laboratory, Argonne, IL 60439, USA*
[6] *University of Arizona, 1118 E. Fourth Street Tucson, AZ 85721, USA*
[7] *University of Athens, University Campus, Zografou GR 157 84, Greece*
[8] *Universidad del Atlantico, Carrera 30 Nmero 8- 49 Puerto Colombia - Atlntico, Colombia*
[9] *Banaras Hindu University, Department of Physics, Varanasi - 221 005, India*

[10] University of Basel, Klingelbergstrasse 82, CH-4056 Basel, Switzerland
[11] University of Bern, Sidlerstrasse 5, CH-3012 Bern, Switzerland
[12] University of Birmingham, Edgbaston, Birmingham B15 2TT, United Kingdom
[13] Boston University, Boston, MA 02215, USA
[14] University of Bristol, H. H. Wills Physics Laboratory, Tyndall Avenue Bristol BS8 1TL, United Kingdom
[15] Brookhaven National Laboratory, Upton, NY 11973, USA
[16] University of Bucharest, Faculty of Physics, Bucharest, Romania
[17] Institute of Physics, Czech Academy of Sciences, Na Slovance 2, 182 21 Praha 8, Czech Republic
[18] Centro Brasileiro de Pesquisas Físicas, Rio de Janeiro, RJ 22290-180, Brazil
[19] CEA/Saclay, IRFU (Institut de Recherche sur les Lois Fondamentales de l'Univers), F-91191 Gif-sur-Yvette CEDEX, France
[20] CERN, European Organization for Nuclear Research 1211 Geneve 23, Switzerland, CERN
[21] CIEMAT, Centro de Investigaciones Energéticas, Medioambientales y Tecnológicas, Av. Complutense, 40, E-28040 Madrid, Spain
[22] University of California (Berkeley), Berkeley, CA 94720, USA
[23] University of California (Davis), Davis, CA 95616, USA
[24] University of California (Irvine), Irvine, CA 92697, USA
[25] University of California (Los Angeles), Los Angeles, CA 90095, USA
[26] California Institute of Technology, Pasadena, CA 91125, USA
[27] University of Cambridge, JJ Thomson Avenue, Cambridge CB3 0HE, United Kingdom
[28] University of Catania, INFN Sezione di Catania, Via Santa Sofia 64, I-95123 Catania, Italy
[29] Institute of Particle and Nuclear Physics of the Faculty of Mathematics and Physics of the Charles University in Prague, V Holešovičkách 747/2, 180 00 Praha 8-Libeň, Czech Republic
[30] University of Chicago, Chicago, IL 60637, USA
[31] Chung-Ang University, Dongjak-Gu, Seoul 06974, South Korea
[32] University of Cincinnati, Cincinnati, OH 45221, USA
[33] Cinvestav, Apdo. Postal 14-740, 07000 Ciudad de Mexico, Mexico
[34] Universidad de Colima, 340 Colonia Villa San Sebastian Colima, Colima, Mexico
[35] University of Colorado (Boulder), Boulder, CO 80309, USA
[36] Colorado State University, Fort Collins, CO 80523, USA
[37] Columbia University, New York, NY 10027, USA
[38] Cornell University, Ithaca, NY 14853, USA
[39] Czech Technical University in Prague, Břehová 78/7, 115 19 Prague 1, Czech Republic
[40] Dakota State University, Madison, SD 57042, USA
[41] University of Dallas, Irving, TX 75062-4736, USA
[42] Daresbury Laboratory, Daresbury Warrington, Cheshire WA4 4AD, United Kingdom
[43] University of Delhi, Department of Physics and Astrophysics, Delhi 110007, India
[44] Drexel University, Philadelphia, PA 19104, USA
[45] Duke University, Durham, NC 27708, USA
[46] University of Durham, South Road, Durham DH1 3LE, United Kingdom
[47] ETH Zurich, Institute for Particle Physics, Zurich, Switzerland
[48] University of Edinburgh, Edinburgh EH8 9YL, UK, United Kingdom
[49] Universidade Estadual de Campinas, Campinas - SP, 13083-970, Brazil
[50] Universidade Federal de Alfenas, Poços de Caldas - MG, 37715-400, Brazil
[51] Universidade Federal do Rio de Janeiro, Rio de Janeiro - RJ, 21941-901, Brazil
[52] Universidade Federal do ABC, Santo André, SP 09210-580, Brazil
[53] UEFS/DFIS - State University of Feira de Santana, Feira de Santana - BA, 44036-900, Brazil
[54] Fermi National Accelerator Laboratory, Batavia, IL 60510, USA
[55] University of Florida, PO Box 118440 Gainesville, FL 32611-8440, USA
[56] University of Genova, 16126 Genova GE, Italy
[57] Universidade Federal de Goias, Goiania, GO 74690-900, Brazil
[58] Laboratori Nazionali del Gran Sasso, I-67010 Assergi, AQ, Italy
[59] Gran Sasso Science Institute, Viale Francesco Crispi 7, L'Aquila, Italy
[60] Universidad de Guanajuato, Gto., C.P. 37000, Mexico
[61] Harish-Chandra Research Institute, Jhunsi, Allahabad 211 019, India
[62] Harvard University, 17 Oxford St. Cambridge, MA 02138, USA
[63] University of Hawaii, Honolulu, HI 96822, USA
[64] University of Houston, Houston, TX 77204, USA
[65] Horia Hulubei National Institute of Physiscs and Nuclear Engineering, Strada Reactorului 30, Măgurele, Romania
[66] University of Hyderabad, Gachibowli, Hyderabad - 500 046, India
[67] Institut de Fisica d'Altes Energies (IFAE), Campus UAB, Facultat Ciences Nord, 08193 Bellaterra, Barcelona, Spain
[68] Instituto de Fisica Corpuscular, Catedratico Jose Beltran, 2 E-46980 Paterna (Valencia), Spain
[69] Illinois Institute of Technology, Chicago, IL 60616, USA
[70] Indian Institute of Technology Bombay, Department of Physics Mumbai 400 076, India
[71] Indian Institute of Technology Guwahati, Guwahati, 781 039, India

[72]Indian Institute of Technology Hyderabad, Hyderabad, 502285, India
[73]Sezione INFN Milano Bicocca and University of Milano Bicocca, Milano, Italy
[74]INFN Universit degli Studi di Bologna, 40127 Bologna BO, Italy
[75]Institute for Research in Fundamental Sciences (IPM), Farmanieh St. Tehran, 19538-33511, Iran
[76]Idaho State University, Department of Physics, Pocatello, ID 83209, USA
[77]Imperial College of Science Technology & Medicine, Blackett Laboratory Prince Consort Road, London SW7 2BZ, United Kingdom
[78]Indiana University, Bloomington, IN 47405, USA
[79]Institut de Physique Nucleaire de Lyon (IPNL), Rue E. Fermi 4 69622 Villeurbanne, France
[80]Institute for Nuclear Research of the Russian Academy of Sciences (INR RAS), 60th October Anniversary Prosp. 7a Moscow, 117312, Russia
[81]University of Iowa, Department of Physics and Astronomy 203 Van Allen Hall Iowa City, IA 52242, USA
[82]Iowa State University, Ames, Iowa 50011, USA
[83]Iwate University, Morioka, Iwate 020-8551, Japan
[84]University of Jammu, Physics Department, JAMMU-180006, India
[85]Jawaharlal Nehru University, Jawaharlal Nehru University, New Delhi 110067, India
[86]University of Jyvaskyla, P.O. Box 35, FI-40014, Finland
[87]High Energy Accelerator Research Organization (KEK), Ibaraki, 305-0801, Japan
[88]KTH Royal Institute of Technology, Roslagstullsbacken 21, SE-106 91 Stockholm, Sweden
[89]Kansas State University, Manhattan, KS 66506, USA
[90]Kavli Institute for the Physics and Mathematics of the Universe (WPI), Kashiwa, Chiba 277-8583, Japan
[91]Department of Physics, K L E F, Green Fields, Guntur - 522 502, AP, India
[92]Korea Institute for Science and Technology Information, Daejeon, 34141, South Korea
[93]National Institute of Technology, Kure College, Hiroshima, 737-8506, Japan
[94]Kyiv National University, 64, 01601 Kyiv, Ukraine
[95]Laboratoire d'Annecy-le-Vieux de Physique des Particules, CNRS/IN2P3 and Université Savoie Mont Blanc, 74941 Annecy-le-Vieux, France
[96]INFN - Laboratori Nazionali del Sud (LNS), Via S. Sofia 62, 95123 Catania, Italy
[97]Lancaster University, Bailrigg, Lancaster LA1 4YB, United Kingdom
[98]Lawrence Berkeley National Laboratory, Berkeley, CA 94720, USA
[99]University of Liverpool, L69 7ZE, Liverpool, United Kingdom
[100]University College London, London, WC1E 6BT, United Kingdom
[101]Los Alamos National Laboratory, Los Alamos, NM 87545, USA
[102]Louisiana State University, Baton Rouge, LA 70803, USA
[103]University of Lucknow, Lucknow 226007, Uttar Pradesh, India
[104]Madrid Autonoma University, Ciudad Universitaria de Cantoblanco 28049 Madrid, Spain
[105]University of Manchester, Oxford Road, Manchester M13 9PL, United Kingdom
[106]University of Maryland, College Park, MD 20742, USA
[107]Massachusetts Institute of Technology, Cambridge, MA 02139, USA
[108]University of Michigan, Ann Arbor, MI 48109, USA
[109]Michigan State University, East Lansing, MI 48824, USA
[110]INFN Milano, INFN Sezione di Milano, I-20133 Milano, Italy
[111]University of Minnesota (Duluth), Duluth, MN 55812, USA
[112]University of Minnesota (Twin Cities), Minneapolis, MN 55455, USA
[113]Northern Illinois University, Department of Physics, DeKalb, Illinois 60115, USA
[114]Universidad Nacional de Ingeniería, Av. Tupac Amaru 210, Lima 25, Peru
[115]Istituto Nazionale di Fisica Nucleare - Sezione di Napoli, Complesso Universitario di Monte S. Angelo, I-80126 Napoli, Italy
[116]National Centre for Nuclear Research, A. Soltana 7, 05 400 Otwock, Poland
[117]University of New Mexico, 1919 Lomas Blvd. N.E. Albuquerque, NM 87131, USA
[118]H. Niewodniczanski Institute of Nuclear Physics, Polish Academy of Sciences, Cracow, Poland
[119]Nikhef National Institute of Subatomic Physics, Science Park, Amsterdam, Netherlands
[120]Northwestern University, Evanston, Il 60208, USA
[121]University of Notre Dame, Notre Dame, IN 46556, USA
[122]Ohio State University, 191 W. Woodruff Ave. Columbus, OH 43210, USA
[123]Oregon State University, Corvallis, OR 97331, USA
[124]Otterbein University, One South Grove Street Westerville, OH 43081, USA
[125]University of Oxford, Oxford, OX1 3RH, United Kingdom
[126]Pacific Northwest National Laboratory, Richland, WA 99352, USA
[127]Physical Research Laboratory, Ahmedabad 380 009, India
[128]University of Padova, Dip. Fisica e Astronomia G. Galilei and INFN Sezione di Padova, I-35131 Padova, Italy
[129]Panjab University, Chandigarh, 160014 U.T., India
[130]University of Pavia, INFN Sezione di Pavia, I-27100 Pavia, Italy
[131]Pennsylvania State University, University Park, PA 16802, USA
[132]University of Pennsylvania, Philadelphia, PA 19104, USA

[133] University di Pisa, Theor. Division; Largo B. Pontecorvo 3, Ed. B-C, I-56127 Pisa, Italy
[134] University of Pittsburgh, Pittsburgh, PA 15260, USA
[135] Pontificia Universidad Católica del Perú, Apartado 1761, Lima, Peru
[136] Princeton University, Princeton, New Jersey 08544, USA
[137] University of Puerto Rico, Mayaguez, 00681, USA
[138] Punjab Agricultural University, Department of Math. Stat. & Physics, Ludhiana 141004, India
[139] University of Rochester, Rochester, NY 14627, USA
[140] SLAC National Acceleratory Laboratory, Menlo Park, CA 94025, USA
[141] STFC Rutherford Appleton Laboratory, OX11 0QX Harwell Campus, Didcot, United Kingdom
[142] University Sergio Arboleda, Cll 74 -14 -14, 11022 Bogotá, Colombia
[143] University of Sheffield, Department of Physics and Astronomy, Sheffield S3 7RH, United Kingdom
[144] University of Sofia, 5 James Bourchier Blvd., Sofia, Bulgaria
[145] University of South Carolina, Columbia, SC 29208, USA
[146] University of South Dakota, Vermillion, SD 57069, USA
[147] South Dakota School of Mines and Technology, Rapid City, SD 57701, USA
[148] South Dakota Science And Technology Authority, Lead, SD 57754, USA
[149] South Dakota State University, Brookings, SD 57007, USA
[150] Southern Methodist University, Dallas, TX 75275, USA
[151] Stony Brook University, Stony Brook, New York 11794, USA
[152] University of Sussex, Brighton, BN1 9RH, United Kingdom
[153] Syracuse University, Syracuse, NY 13244, USA
[154] Universidad Tecnica Federico Santa Maria, Department de Fisica, Casino 110-V, Valparaiso, Chile
[155] University of Tennessee at Knoxville, TN, 37996, USA
[156] Texas A&M University (Corpus Christi), Corpus Christi, TX 78412, USA
[157] University of Texas (Arlington), Arlington, TX 76019, USA
[158] University of Texas (Austin), Austin, TX 78712, USA
[159] Tsinghua University, Haidian District, Beijing 100084, China
[160] TUBITAK Space Technologies Research Institute, TR-06800, Ankara, Turkey
[161] Tufts University, Medford, MA 02155, USA
[162] Universidade Federal de São Carlos, Araras - SP, 13604-900, Brazil
[163] Universidade Nacional de Asuncion, 585540/2 Interno 1068 CC: 910, Asunción, Paraguay
[164] Università del Salento - INFN, Via Provinciale per Arnesano, 73100 - Lecce , Italy
[165] Variable Energy Cyclotron Centre, 1/AF, Bidhannagar Kolkata - 700 064 West Bengal, India
[166] Valley City State University, Valley City, ND 58072, USA
[167] Virginia Tech, Blacksburg, VA 24060, USA
[168] University of Warsaw, Faculty of Physics ul. Pasteura 5 02-093 Warsaw, Poland
[169] Warsaw University of Technology, Nowowiejska 15/19, 00-665 Warszawa Poland, Poland
[170] University of Warwick, Coventry CV4 7AL, United Kingdom
[171] Wichita State University, Physics Division, Wichita, KS 67260, USA
[172] William and Mary, Williamsburg, VA 23187, USA
[173] University of Wisconsin (Madison), Madison, WI 53706, USA
[174] Wroclaw University, Plac Maxa Borna 9, 50-204 Wroclaw, Poland
[175] Yale University, New Haven, CT 06520, USA
[176] Yerevan Institute for Theoretical Physics and Modeling, Halabian Str. 34, Yerevan 0036, Armenia
[177] York University, Physics and Astronomy Department, 4700 Keele St. Toronto M3J 1P3, Canada

Contents

Contents i

List of Figures iii

List of Tables 1

1 Executive Summary 2
- 1.1 Overview . . . 2
- 1.2 Primary Science Goals . . . 4
- 1.3 The LBNF Facility . . . 5
- 1.4 The DUNE Experiment . . . 7
- 1.5 International Organization and Responsibilities . . . 9
- 1.6 DUNE Organization and Management . . . 10
- 1.7 Schedule and Milestones . . . 12
- 1.8 The DUNE Interim Design Report Volumes . . . 13

2 DUNE Physics 15
- 2.1 Introduction: Scientific Goals . . . 16
  - 2.1.1 The Primary Science Program . . . 16
  - 2.1.2 The Ancillary Science Program . . . 16
  - 2.1.3 Context for Discussion of Science Capabilities in this Document . . . 17
  - 2.1.4 Strategies . . . 17
- 2.2 Long-Baseline Neutrino Oscillation physics program . . . 19
  - 2.2.1 Experimental Context: Baseline, Configuration and Staging Scenario . . . 19
  - 2.2.2 Mass Hierarchy . . . 21
  - 2.2.3 CP Violation . . . 22
  - 2.2.4 Precision Measurement of Mixing Parameters . . . 23
- 2.3 Nucleon Decay and the GeV Scale Non-Accelerator Physics Program . . . 24
  - 2.3.1 Nucleon Decay . . . 24
  - 2.3.2 Atmospheric neutrinos . . . 25
- 2.4 Supernova-Neutrino Physics and Astrophysics . . . 26
- 2.5 Precision Measurements with the DUNE Near Detector Complex . . . 29
- 2.6 Opportunities in Beyond the Standard Model Physics . . . 29
  - 2.6.1 New Particle Searches . . . 29
  - 2.6.2 Searches for Deviations from the PMNS Neutrino Mixing Paradigm . . . 30
- 2.7 Summary . . . 32

3 DUNE Software and Computing **33**
3.1 Overview . . . 33
3.1.1 Detectors . . . 33
3.1.2 Physics Challenges . . . 35
3.1.3 Summary . . . 37
3.2 Building the Computing Model . . . 37
3.2.1 Infrastructure . . . 38
3.2.2 Algorithms . . . 38
3.2.3 Adaptability . . . 39
3.2.4 Downstream Activities . . . 39
3.3 Planning Inputs . . . 40
3.3.1 Running Experiments . . . 40
3.3.2 ProtoDUNE . . . 41
3.3.3 Data Challenges . . . 42
3.3.4 Monte Carlo Challenges . . . 43
3.3.5 Reconstruction tests . . . 43
3.4 Resource Planning and Prospects . . . 44

4 DUNE Calibration Strategy **45**
4.1 Calibration Strategy . . . 46
4.1.1 Physics Driven Calibration Requirements . . . 46
4.1.2 A Staged Approach . . . 48
4.2 Inherent Sources and External Measurements . . . 51
4.3 Proposed Systems . . . 53
4.3.1 Laser Systems . . . 53
4.3.2 Radioactive Source Deployment System . . . 55
4.3.3 Pulsed Neutron Source . . . 56
4.3.4 External Muon Tracker . . . 56
4.3.5 Configuration of Proposed Systems . . . 57
4.4 Summary . . . 58

Glossary **60**

References **64**

List of Figures

1.1 DUNE collaboration global map . . . 3
1.2 LBNF/DUNE project: beam from Illinois to South Dakota . . . 5
1.3 Underground caverns for DUNE in South Dakota . . . 6
1.4 Neutrino beamline and DUNE near detector hall in Illinois . . . 6
1.5 Structure for oversight of the DUNE and LBNF projects. . . . 11

2.1 Summary of mass hierarchy sensitivities . . . 21
2.2 CP-violation sensitivity and δ_{CP} resolution as a function of exposure . . . 22
2.3 Characteristics of the neutrino signal from core-collapse supernovae . . . 28

4.1 Categories of measurements provided by Calibration. . . . 48
4.2 Sample distortion that may be difficult to detect with cosmic rays . . . 53
4.3 Top view of the SP module cryostat showing various penetrations . . . 57

List of Tables

2.1 Required exposures to reach oscillation physics milestones 23
2.2 Atmospheric neutrino rates 26

3.1 Uncompressed data volumes/year for one single-phase (SP) module. 36
3.2 Uncompressed data volumes/year for one dual-phase (DP) module. 36
3.3 Computing tasks 39
3.4 Parameters for the ProtoDUNE-SP run at CERN 42
3.5 Parameters for a six month ProtoDUNE-DP cosmic run at CERN 42

4.1 Calibration systems and sources of the nominal DUNE FD calibration design 49
4.2 Annual rates for classes of cosmic-ray events useful for calibration 52
4.3 Key calibration milestones leading to first detector installation 59

Chapter 1

Executive Summary

1.1 Overview

The Deep Underground Neutrino Experiment (DUNE) will be a world-class neutrino observatory and nucleon decay detector designed to answer fundamental questions about the nature of elementary particles and their role in the universe. The international DUNE experiment, hosted by the U.S. Department of Energy's Fermilab, will consist of a far detector to be located about 1.5 km underground at the Sanford Underground Research Facility (SURF) in South Dakota, USA, at a distance of 1300 km from Fermilab, and a near detector to be located at Fermilab in Illinois. The far detector will be a very large, modular liquid argon time-projection chamber (LArTPC) with a 40 kt (40 Gg) fiducial mass. This LAr technology will make it possible to reconstruct neutrino interactions with image-like precision and unprecedented resolution.

The far detector will be exposed to the world's most intense neutrino beam originating at Fermilab. A high-precision near detector, located 575 m from the neutrino source on the Fermilab site, will be used to characterize the intensity and energy spectrum of this wide-band beam. The Long-Baseline Neutrino Facility (LBNF), also hosted by Fermilab, provides the infrastructure for this complex system of detectors at the Illinois and South Dakota sites. LBNF assumes the responsibility for the neutrino beam, the deep-underground site, and the infrastructure for the DUNE detectors.

The DUNE collaboration is a truly global organization including more than 1000 scientists and engineers from 32 countries (Figure 1.1). It represents the culmination of several worldwide efforts that developed independent paths toward a next-generation long-baseline (LBL) neutrino experiment over the last decade. It was formed in April 2015, combining the strengths of the LBNE project in the USA and the LBNO project in Europe, adding many new international partners in the process. DUNE thus represents the convergence of a substantial fraction of the worldwide neutrino-physics community around the opportunity provided by the large investment planned by the U.S. Department of Energy (DOE) and Fermilab to support a significant expansion of the underground infrastructure at SURF in South Dakota, and to create a megawatt neutrino-beam facility at Fermilab by 2026. The Proton Improvement Plan-II (PIP-II) upgrade at Fermilab [2]

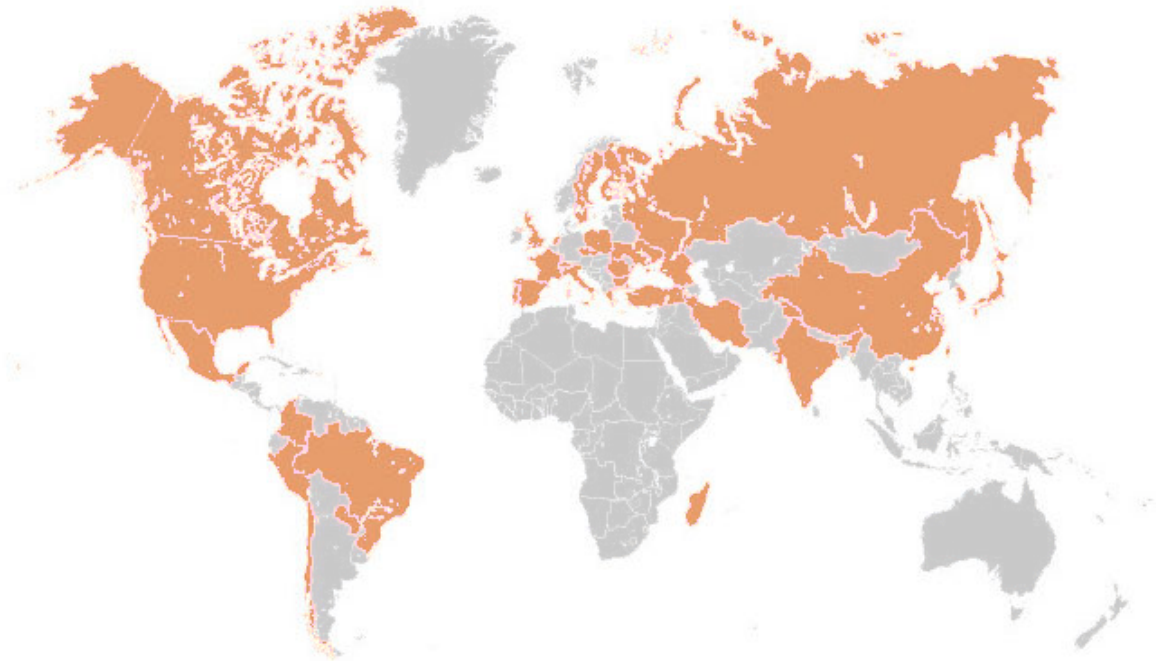

Figure 1.1: The international DUNE collaboration. Countries with DUNE membership are shown in orange.

will enable the accelerator to drive the new neutrino beamline with a 80 GeV primary proton beam at a beam power up to 1.2 MW. A further planned upgrade of the accelerator complex will enable it to provide up to 2.4 MW of beam power by 2030.

The LBNF/DUNE project (the *project*) strategy presented in this interim design report (IDR) has been developed to meet the requirements set out in the report of the Particle Physics Project Prioritization Panel (P5 in 2014). It also takes into account the recommendations of the European Strategy for Particle Physics (ESPP) adopted by the CERN Council in 2013, which classified the long-baseline (LBL) neutrino program as one of the four scientific objectives that require international infrastructure.

The P5 report [3] set the goal of reaching a sensitivity to charge-parity symmetry violation (CPV) of better than three standard deviations (3σ) over more than 75% of the range of possible values of the unknown CP-violating phase δ_{CP}. Based partly on this goal, they stated that "the minimum requirements to proceed are the identified capability to reach an exposure of 120 kt $\cdot$ MW $\cdot$ year by the 2035 time frame, the far detector situated underground with cavern space for expansion to at least 40 kt LAr fiducial volume, and 1.2 MW beam power upgradeable to multi-megawatt power. The experiment should have the demonstrated capability to search for supernova neutrino bursts (SNBs) and for proton decay, providing a significant improvement in discovery sensitivity over current searches for the proton lifetime." The strategy and design presented in this IDR meet these requirements.

This document serves as the IDR for the DUNE far detector (FD). The IDR is intended to provide

a clear statement of the physics goals and methods of the DUNE experiment, and to describe the detector technologies that have been designed to achieve these goals. Introductions to each chapter are intended to be useful and informative to technical specialists who serve in national science agencies. The body of the document is intended to be useful and informative to members of the international high energy physics community. The IDR deliberately emphasizes the connections between the physics and technologies of the DUNE FD modules. Very important project related tasks are presented in summary form. No information about cost is included, and schedule information appears only in the form of high-level milestones. The IDR forms the nucleus of the technical design report (TDR), which will be presented to international science agencies and the high energy physics (HEP) community in 2019.

1.2 Primary Science Goals

The DUNE experiment will combine the world's most intense neutrino beam, a deep underground site, and massive LAr detectors to enable a broad science program addressing some of the most fundamental questions in particle physics.

The primary science goals of DUNE, described in detail in Chapter 2, are to:

- Carry out a comprehensive program of neutrino oscillation measurements using ν_μ and $\bar{\nu}_\mu$ beams from Fermilab. This program includes measurements of the charge parity (CP) phase, determination of the neutrino mass ordering (the sign of $\Delta m^2_{31} \equiv m^2_3 - m^2_1$), measurement of the mixing angle θ_{23} and the determination of the octant in which this angle lies, and sensitive tests of the three-neutrino paradigm. Paramount among these is the search for CPV in neutrino oscillations, which may give insight into the origin of the matter-antimatter asymmetry, one of the fundamental questions in particle physics and cosmology.

- Search for proton decay in several important decay modes. The observation of proton decay would represent a ground-breaking discovery in physics, providing a key requirement for grand unification of the forces.

- Detect and measure the ν_e flux from a core-collapse supernova within our galaxy, should one occur during the lifetime of the DUNE experiment. Such a measurement would provide a wealth of unique information about the early stages of core-collapse, and could even signal the birth of a black hole.

The intense neutrino beam from LBNF, the massive DUNE LArTPC far detector, and the high-resolution DUNE near detector will also provide a rich ancillary science program, beyond the primary goals of the experiment. The ancillary science program includes

- other accelerator-based neutrino flavor transition measurements with sensitivity to beyond the standard model (BSM) physics, such as non-standard interactions (NSIs), Lorentz violation, CPT violation, sterile neutrinos, large extra dimensions, heavy neutral leptons; and measurements of tau neutrino appearance;

- measurements of neutrino oscillation phenomena using atmospheric neutrinos;
- a rich neutrino interaction physics program utilizing the DUNE near detector, including a wide-range of measurements of neutrino cross sections, studies of nuclear effects;
- searches for dark matter.

Further advancements in the LArTPC technology during the course of the DUNE far detector construction may open up the opportunity to observe very low-energy phenomena such as solar neutrinos or even the diffuse supernova neutrino flux.

1.3 The LBNF Facility

The Long-Baseline Neutrino Facility (LBNF), hosted by Fermilab, is separate from the DUNE collaboration and is intended to enable the construction and operation of the DUNE detectors in South Dakota and Illinois. The DUNE collaboration will construct a deep-underground neutrino observatory in South Dakota based on four independent 10 kt LArTPCs. LBNF will provide facilities in Illinois and South Dakota to enable the scientific program of DUNE. These facilities are geographically separated into the near site facilities, those to be constructed at Fermilab, and the far site facilities, located at SURF. Figure 1.2 shows a schematic of the facilities at the two sites, and Figure 1.3 shows the cavern layout.

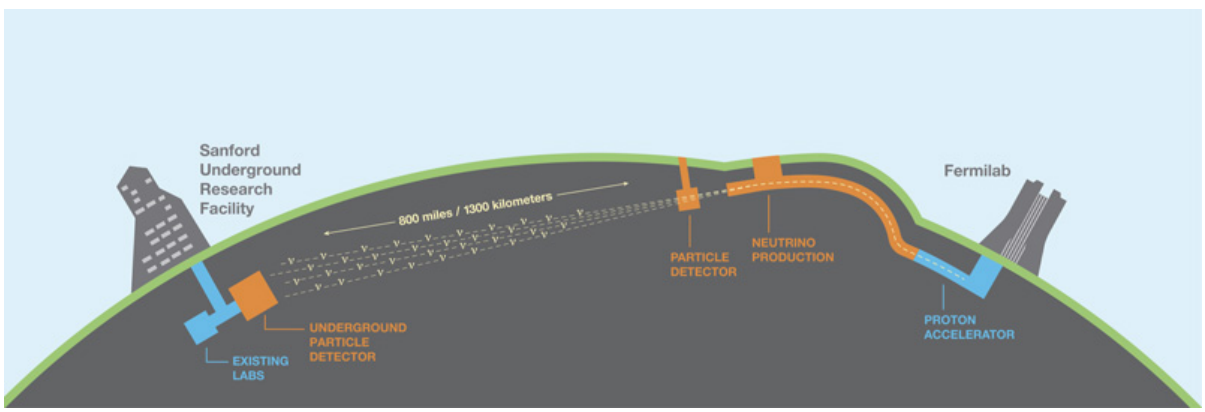

Figure 1.2: LBNF/DUNE project: beam from Illinois to South Dakota.

Specifically, the Long-Baseline Neutrino Facility (LBNF) provides

- the technical and conventional facilities for a powerful 1.2 MW neutrino beam utilizing the PIP-II upgrade of the Fermilab accelerator complex, to become operational by 2026 at the latest, and to be upgradable to 2.4 MW with the proposed PIP-III upgrade;
- the civil construction, or conventional facilities (CF), for the near detector systems at Fermilab; (see Figure 1.4);

- the excavation of four underground caverns at SURF, planned to be completed by 2021 under a single contract, with each cavern to be capable of housing a cryostat with a minimum 10 kt fiducial mass LArTPC; and

- surface, shaft, and underground infrastructure to support the outfitting of the caverns with four free-standing, steel-supported cryostats and the required cryogenics systems. The first cryostat will be available for filling, after installation of the detector components, by 2023, enabling a rapid deployment of the first two 10 kt far detector modules. The intention is to install the third and fourth cryostats as rapidly as funding will allow.

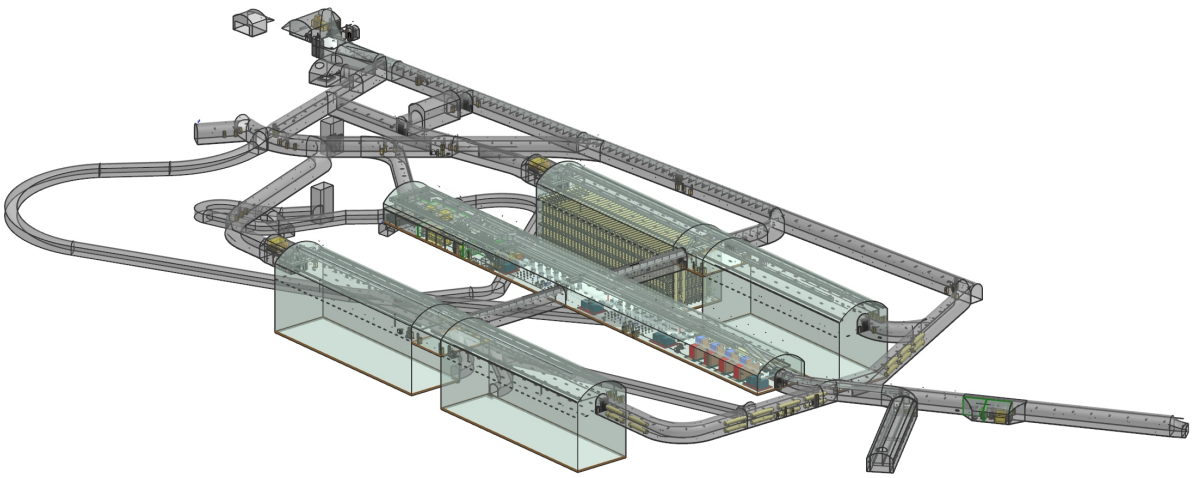

Figure 1.3: Underground caverns for DUNE far detectors and cryogenic systems at SURF, in South Dakota.

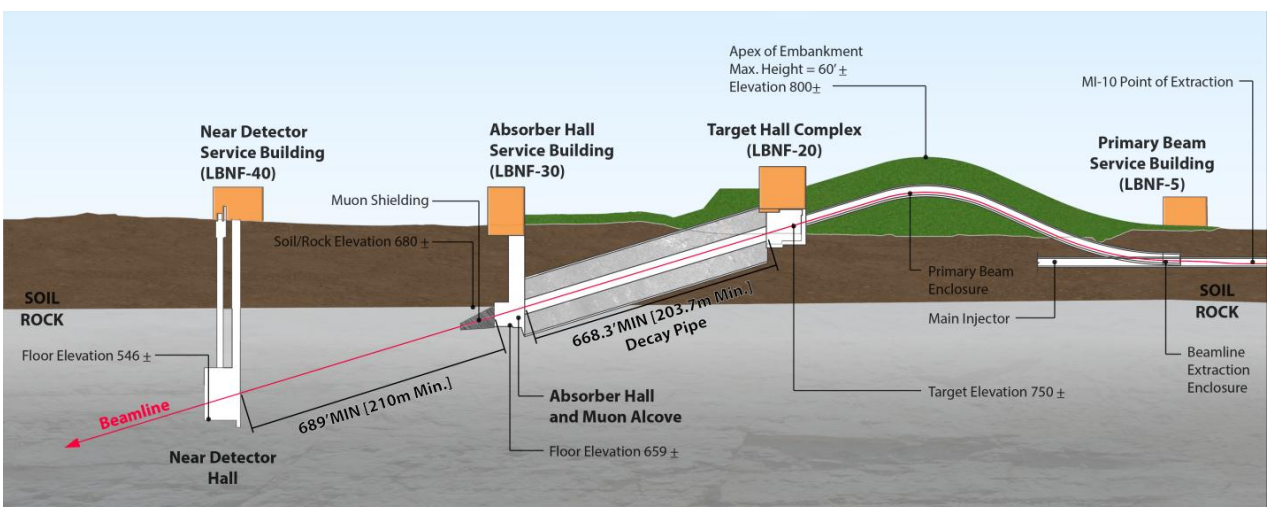

Figure 1.4: Neutrino beamline and DUNE near detector hall at Fermilab, in Illinois

The success of the DUNE project depends on the successful realization of the LBNF facilities. This IDR focuses on the DUNE physics program that is enabled by the first three FD modules, which are expected to be based on the single-phase (SP) and dual-phase (DP) LAr technologies.

1.4 The DUNE Experiment

The DUNE experiment includes a precision near detector at the edge of the Fermilab site, in Batavia, Illinois, and a very large, modular far detector about 1.5 km underground at SURF in Lead, South Dakota, 1300 km (800 miles) from Fermilab. The DUNE far detector is the focus of this IDR.

The near detector will be located 575 m from the target. It will consist of a LArTPC followed by a fine-grained magnetic spectrometer. The LArTPC will use pixel readout to deal with the high occupancy from neutrino events in the intense LBNF beam. The details of the magnetic spectrometer will be resolved in the near future. The goal for the near detector group is to produce a conceptual design report (CDR) at the time of the FD TDR. The near detector CDR will provide information critical to establishing the physics reach for the primary neutrino oscillation program of DUNE. The near detector TDR will follow the FD TDR by approximately one year, consistent with the near detector construction schedule.

The DUNE FD will consist of four similar LArTPCs, each with fiducial mass of at least 10 kt, installed about 1.5 km underground. Each detector will be installed in a cryostat with internal dimensions 14.0 m (W) $\times$ 14.1 m (H) $\times$ 62.0 m (L), and will contain a total LAr mass of about 17.5 kt. The LArTPC technology provides excellent tracking and calorimetry performance, making it an ideal choice for the DUNE far detectors. The four identically sized cryostats give flexibility for staging and evolution of the LArTPC technology.

DUNE is planning for and prototyping two LArTPC technologies:

- Single-phase (SP): This technology was pioneered by the ICARUS project, and after several decades of worldwide R&D, is now a mature technology. It is the technology used for Fermilab's currently operating MicroBooNE, and the planned SBND. In the SP technology, ionization charges are drifted horizontally in LAr and read out on wires in the liquid. The maximum drift length in the DUNE SP module is 3.53 m and the nominal drift field is 500 V/cm, corresponding to a cathode high voltage of 180 kV. There is no signal amplification in the liquid, so readout with good signal-to-noise requires very low-noise electronics.

- Dual-phase (DP): This technology was pioneered at large scale by the WA105 DP demonstrator collaboration. It is less established than the SP technology but offers a number of potential advantages and challenges. Here, ionization charges are drifted vertically in LAr and transferred into the gas above the liquid. The signal charges are then amplified in the gas phase using large electron multipliers (LEMs). This gain reduces the requirements on the electronics, and makes it possible for the DP module to have a longer drift, which requires a correspondingly higher voltage. The maximum drift length in the DP module is 12 m and the nominal drift field is 500 V/cm, corresponding to a cathode high voltage of 600 kV.

The plans for the single and dual-phase TPCs are described in detail in Volumes 2 and 3 of this IDR.

The DUNE collaboration is committed to deploying both technologies. For planning purposes,

DUNE assumes the first detector module to be SP and the second to be DP. The actual sequence of detector module installation will depend on results from the prototype detectors, described below, and on available resources.

The collaboration is in now in the final stages of constructing two large prototype detectors (called ProtoDUNEs), one employing SP readout (ProtoDUNE-SP) and the other employing DP readout (ProtoDUNE-DP). Each is approximately one-twentieth of a DUNE detector module, but uses components identical in size to those of the full-scale module. ProtoDUNE-SP has the same 3.53 m maximum drift length as the full SP module. ProtoDUNE-DP has a 6 m maximum drift length, half of that planned for the DP module.

These large-scale prototypes will allow us to validate key aspects of the TPC designs, test engineering procedures, and collect valuable calibration data using a hadron test beam. The following list includes the key goals of the ProtoDUNE program:

1. Test production of components:
    - stress testing of the production and quality assurance processes of detector components,
    - mitigation of the associated risks for the far detector.
2. Validate installation procedures:
    - test of the interfaces between the detector elements,
    - mitigation of the associated risks for the far detector.
3. Detector operation with cosmic rays:
    - validation of the detector designs and performance.
4. Collection of test beam data:
    - measurements of essential physics response of the detector.

Items 1 to 3 are required as input to the TDR. Item 4, collection and the corresponding analysis of test beam data, will be vital to DUNE's physics program, but is not required for the TDR.

The full DUNE far detector requires four modules. For the TDR, we will describe plans for at least the first two of these modules. Based on our current expectations, we hope to present a plan for two SP modules, one of which will be the first module installed, and one DP module. At the time of the TDR, it is likely that resources for the fourth detector module will remain to be identified.

1.5 International Organization and Responsibilities

DUNE is the first science project of this scale in the USA that will be built with large international participation and as an international collaboration. This requires a new organizational and governance model that takes into account the international nature of the project. The model used by CERN for managing the construction and exploitation of the Large Hadron Collider (LHC) and its experiments served as a starting point for the joint management of LBNF and the DUNE experimental program. LBNF, which is responsible for the facilities, comprising the neutrino beam, the near site at Fermilab and the far site at SURF, is organized as a DOE-Fermilab project incorporating international partners. DUNE is a fully international project organized by the DUNE collaboration with appropriate oversight from all international stakeholders. The DUNE collaboration is responsible for

- the definition of the scientific goals and corresponding scientific and technical requirements on the detector systems and neutrino beamline;
- the design, construction, commissioning, and operation of the detectors; and
- the scientific research program conducted with the DUNE detectors.

A set of organizational structures has been established to provide coordination among the participating funding agencies; oversight of the LBNF and DUNE projects; and coordination and communication between the two. These structures and the relationships among them are shown in Figure 1.5. They comprise the following committees:

- International Neutrino Council (INC)

  The INC is composed of regional representatives, such as CERN, and representatives of funding agencies making major contributions to LBNF infrastructure and to DUNE. The INC acts as the highest-level international advisory body to the U.S. Department of Energy (DOE) and the Fermilab directorate. The INC facilitates high-level global coordination across the entire enterprise (LBNF and DUNE). The INC is chaired by the DOE Office of Science associate director for high energy physics and includes the Fermilab director in its membership. The council meets and provides pertinent advice to the LBNF and DUNE projects through the Fermilab director as needed.

- Resources Review Board (RRB)

  The RRB is composed of representatives of all funding agencies that sponsor LBNF, DUNE, and PIP-II, and the Fermilab management. The RRB provides focused monitoring and detailed oversight of the DUNE collaboration, and also monitors the progress of LBNF and PIP-II. The Fermilab director, in consultation with the international funding partners for the projects, defines the membership of the RRB. A representative from the Fermilab directorate chairs the RRB and organizes regular meetings to facilitate coordination and to monitor the progress of the projects. The management teams from the DUNE collaboration and the LBNF project participate in the RRB meetings and make regular reports to the RRB on

technical, managerial, financial and administrative matters, as well as reporting on the status and progress of the DUNE collaboration.

- Long-Baseline Neutrino Committee (LBNC)

  The LBNC is composed of internationally prominent scientists with relevant expertise. It provides regular external scientific peer review of DUNE, and provides regular reports to the Fermilab directorate and the RRB. The LBNC reviews the scientific, technical and managerial decisions of the DUNE experiment. The LBNC will review the TDR for DUNE and will provide a recommendation to the Fermilab directorate and the RRB on whether to endorse the TDR.

  Upon request from the Fermilab director, the LBNC may employ additional DUNE and LBNF scrutiny groups for more detailed reports and evaluations.

- Neutrino Cost Group (NCG)

  Like the LBNC, the NCG is composed of internationally prominent scientists with relevant experience. The NCG reviews the cost, schedule, and associated risks for the DUNE experiment, and provides regular reports to the Fermilab directorate and the RRB. The NCG will review the TDR for DUNE and will provide a recommendation to the Fermilab directorate and the RRB on whether to endorse the TDR.

- Experiment-Facility Interface Group (EFIG)

  Close and continuous coordination between DUNE and LBNF is required to ensure the success of the combined enterprise. The EFIG oversees the interfaces between the two projects and ensures the required coordination during the design and construction phases and the operational phase of the program. This group covers areas including interfaces between the near and far detectors and the corresponding conventional facilities; interfaces between the detector systems provided by DUNE and the technical infrastructure provided by LBNF; design of the LBNF neutrino beamline and neutrino beamline operational issues that impact both LBNF and DUNE.

1.6 DUNE Organization and Management

All aspects of DUNE are organized and managed by the DUNE collaboration. Stakeholders include the collaborating institutions, the funding agencies participating in DUNE, and Fermilab as the host laboratory. All collaborating institutions have a representative on the DUNE Institutional Board (IB). The collaboration is responsible for the design, construction, installation, commissioning, and operation of the detectors and prototypes used to pursue the scientific program. The DUNE Executive Board (EB), described below, is the main management body of the collaboration and approves all significant strategic and technical decisions.

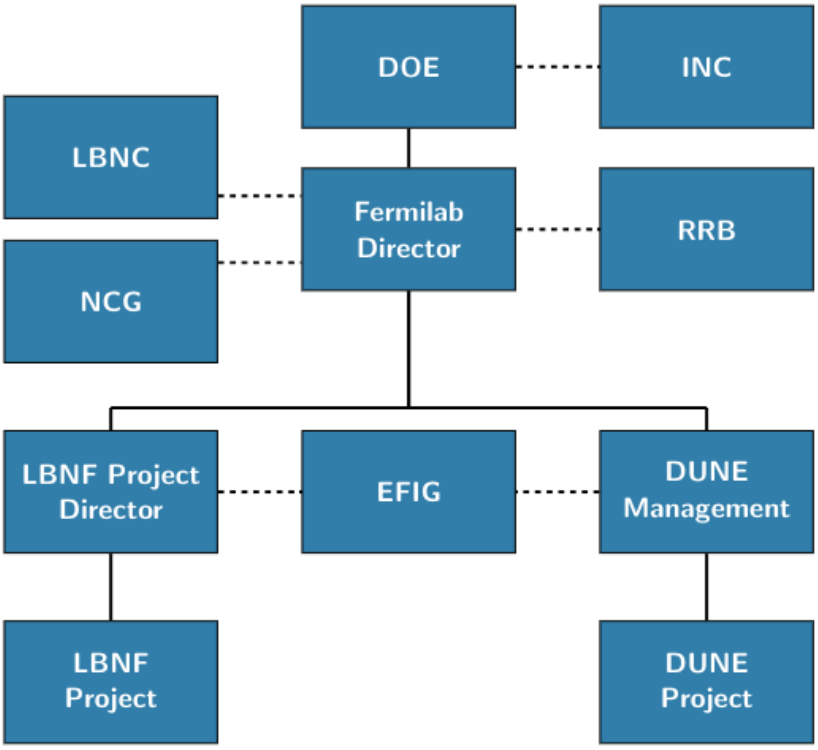

Figure 1.5: Top-level organization structure for oversight of the DUNE and LBNF projects.

The top-level DUNE management team consists of two elected co-spokespersons, the technical coordinator (TC), and the resource coordinator (RC). The TC and RC are selected jointly by the co-spokespersons and the Fermilab director. The management team is responsible for the day-to-day management of the collaboration, and for developing the overall collaboration strategy, which is presented for approval to the executive board. The executive board consists of the leaders of the main collaboration activities. The composition of the EB, currently including the DUNE management team, IB chair, physics coordinator, beam interface coordinator, computing coordinator, near detector coordinator, and leaders of the FD consortia, described below, is intended to ensure that all stakeholders in the collaboration have a voice in the decision-making process. In the post-TDR phase of DUNE, the intention is that the consortium leaders and the coordinators of the other major collaboration activities will become elected positions.

To carry out design and construction work for the DUNE far detector, DUNE has formed consortia of institutions that have taken responsibility for different detector subsystems. A similar structure will be formed for the DUNE near detector once the detector concept is selected. For the DUNE FD, there are currently nine consortia, including three specific to SP, three specific to DP, and three common to both technologies:

- (SP) anode plane assemblies (APAs),
- (SP) TPC cold electronics (CE),

- (SP) photon detection system (PDS),
- (DP) charge-readout planes (CRPs),
- (DP) TPC electronics,
- (DP) photon detection system (PDS),
- high voltage (HV) system,
- data acquisition (DAQ) system,
- cryogenic instrumentation and slow controls (CISC) system.

It is possible that additional consortia may be added depending on the organization of computing and calibration systems. Each consortium has an overall leader, a technical lead, and a consortium board with representatives from each consortium institution. The consortia have full responsibility for their subsystems, including developing a full work breakdown structure (WBS), understanding and documenting all interfaces with other systems, preparing final technical designs, and writing their respective sections of the IDR and the TDR. Following approval of the TDR, they will be responsible for construction of their detector systems.

1.7 Schedule and Milestones

LBNF and DUNE are working toward three international project milestones:

- 2019: Start main cavern excavation in South Dakota;
- 2022: Start installation of first FD module;
- 2026: Beam operation with two detector modules.

It is expected that these dates will be adjusted when the project baseline is defined. The key milestones to reach baseline status are:

- 2018 - Collect data with both ProtoDUNE detectors.
- April 2019 - Submit TDR for far detector modules.
- July 2019 - Complete LBNC and NCG review of TDR.
- September 2019 - Present TDR to RRB.
- October 2019 - Conduct conceptual design (DOE CD-2/3b) review of LBNF and the USA

scope of DUNE.

The TDR for the near detector is expected to follow the FD TDR by approximately one year.

The schedule for the design and construction work for LBNF and DUNE has two critical parallel paths: one for the far site (South Dakota) another for the near site (Illinois). The schedule for the initial work is driven by the CF design and construction at each site.

During the initial phase of the project, the far site CF is advanced first. The Ross Shaft rehabilitation work at SURF was recently halted at the 4850 level due to safety concerns, which have led to delays of two to four months. Early site preparation is timed to be completed in time to start excavation when the Ross Shaft rehabilitation work finishes. As each detector cavern is excavated and sufficient utilities are installed, the cryostat and cryogenics system work proceeds, followed by detector installation, filling and commissioning. The first detector module is to be operational by 2024, with the second and third modules completed one and two years later, respectively.

The DOE project management process requires approvals at critical decision (CD) milestones that allow the LBNF/DUNE project to move to the next step. In spring 2018 LBNF near site CF will seek CD-3b construction approval for Advanced Site Preparation to build the embankment. In 2020 LBNF and DUNE will seek to baseline the LBNF/DUNE scope of work, cost and schedule, as well as construction approval for the balance of the project scope of work.

The project concludes with CD-4 approval to start operations.

1.8 The DUNE Interim Design Report Volumes

The DUNE IDR describes the proposed physics program and technical designs of the far detector in preparation for the full TDR to be published in 2019. It is intended as an intermediate milestone on the path to a full TDR, justifying the technical choices that flow down from the high-level physics goals through requirements at all levels of the Project. These design choices will enable the DUNE experiment to make the ground-breaking discoveries that will help to answer fundamental physics questions.

The IDR is composed of three volumes. Volume 1 contains this executive summary, which describes the general aims of this document. The remainder of this first volume provides a more detailed description of the DUNE physics program that drives the choice of detector technologies. It also includes concise outlines of two overarching systems that have not yet evolved to consortium structures: computing and calibration. Volumes 2 and 3 describe, for the SP and DP, respectively, each module's subsystems, the technical coordination required for its design, construction, installation, and integration, and its organizational structure.

This IDR represents the state of the design for the first three DUNE far detector modules at this moment in time. The fourth module could employ a different LArTPC technology, taking into account potential advances in technology to further optimize the sensitivity for physics discoveries.

It is beyond the scope of this proposal. Also not covered in this proposal is the DUNE Near Detector, which constitutes an integral but less well developed portion of the experiment's physics program. Separate TDRs for these detector systems will be provided in the future.

Chapter 2

DUNE Physics

DUNE will address fundamental questions key to our understanding of the universe. These include:

- **What is the origin of the matter-antimatter asymmetry in the universe?** Immediately after the Big Bang, matter and antimatter were created equally, but now matter dominates. By studying the properties of neutrino and antineutrino oscillations, LBNF/DUNE will pursue the current most promising avenue for understanding this asymmetry.

- **What are the fundamental underlying symmetries of the universe?** The patterns of mixings and masses between the particles of the standard model is not understood. By making precise measurements of the mixing between the neutrinos and the ordering of neutrino masses and comparing these with the quark sector, LNBF/DUNE could reveal new underlying symmetries of the universe.

- **Is there a Grand Unified Theory of the Universe?** Results from a range of experiments suggest that the physical forces observed today were unified into one force at the birth of the universe. Grand Unified Theories (GUTs), which attempt to describe the unification of forces, predict that protons should decay, a process that has never been observed. DUNE will search for proton decay in the range of proton lifetimes predicted by a wide range of GUT models.

- **How do supernovae explode and what new physics will we learn from a neutrino burst?** Many of the heavy elements that are the key components of life were created in the super-hot cores of collapsing stars. DUNE would be able to detect the neutrino bursts from core-collapse supernovae within our galaxy (should any occur). Measurements of the time, flavor and energy structure of the neutrino burst will be critical for understanding the dynamics of this important astrophysical phenomenon, as well as bringing information on neutrino properties and other particle physics.

2.1 Introduction: Scientific Goals

The DUNE scientific objectives are categorized into: the *primary science program*, addressing the key science questions highlighted by the particle physics project prioritization panel (P5); a high-priority *ancillary science program* that is enabled by the construction of LBNF and DUNE; and *additional scientific objectives*, that may require further developments of the LArTPC technology. A detailed description of the physics objectives of DUNE is provided in Volume 2 of the DUNE conceptual design report (CDR)[1].

2.1.1 The Primary Science Program

The primary science program of DUNE focuses on fundamental open issues in neutrino and astroparticle physics:

- Precision measurements of the parameters that govern $\nu_\mu \to \nu_e$ and $\overline{\nu}_\mu \to \overline{\nu}_e$ oscillations with the goal of

  – measuring the charge-parity (CP) violating phase δ_{CP}, where a value differing from zero or π would represent the discovery of CP violation in the leptonic sector, providing a possible explanation for the matter-antimatter asymmetry in the universe;

  – determining the neutrino mass ordering (the sign of $\Delta m^2_{31} \equiv m^2_3 - m^2_1$), often referred to as the neutrino *mass hierarchy*; and

  – precision tests of the three-flavor neutrino oscillation paradigm through studies of muon neutrino disappearance and electron neutrino appearance in both ν_μ and $\overline{\nu}_\mu$ beams, including the measurement of the mixing angle θ_{23} and the determination of the octant in which this angle lies.

- Search for proton decay in several important decay modes. The observation of proton decay would represent a ground-breaking discovery in physics, providing a portal to Grand Unification of the forces; and

- Detection and measurement of the ν_e flux from a core-collapse supernova within our galaxy, should one occur during the lifetime of the DUNE experiment.

2.1.2 The Ancillary Science Program

The intense neutrino beam from LBNF, the massive DUNE LArTPC far detector and the high-resolution DUNE near detector provide a rich ancillary science program, beyond the primary

[1] `http://arxiv.org/abs/1512.06148`.

mission of the experiment. The ancillary science program includes

- other accelerator-based neutrino flavor transition measurements with sensitivity to the beyond the standard model (BSM) physics, such as: non-standard interactions (NSIs); Lorentz violation, CPT violation, the search for sterile neutrinos at both the near and far sites, large extra dimensions, heavy neutral leptons; and measurements of tau neutrino appearance;
- measurements of neutrino oscillation phenomena using atmospheric neutrinos;
- a rich neutrino interaction physics program utilizing the DUNE near detector, including: a wide range of measurements of neutrino cross sections and studies of nuclear effects; and
- the search for signatures of dark matter.

Furthermore, a number of previous breakthroughs in particle physics have been serendipitous, in the sense that they were beyond the original scientific objectives of an experiment. The intense LBNF neutrino beam and novel capabilities for both the DUNE near and far detectors will probe new regions of parameter space for both the accelerator-based and astrophysical frontiers, providing the opportunity for discoveries that are not currently anticipated.

2.1.3 Context for Discussion of Science Capabilities in this Document

The sections that follow highlight the projected capabilities of DUNE to realize the science program summarized above. These are documented in detail in Volume 2 of the DUNE Conceptual Design Report and in the following section. Since publication of the CDR in late 2015, the DUNE science collaboration has undertaken a campaign to develop data analysis tools and strategies to aid in detector design optimization as well as to obtain a more rigorous understanding of experimental sensitivity. This campaign is in progress as of this writing, and the outcomes will be reported as a component of the DUNE technical design report (TDR) now in development. Additionally, with currently-operating experiments beginning to reach peak fractional rates of integrated exposure, the rapid evolution of the world-wide experimental landscape in neutrino physics is particularly acute at present. Thus, for the purposes of the present report, the discussion of capabilities here will reflect what is documented within the CDR unless otherwise noted. In addition, the following section describes the status of the simulation and reconstruction strategies used to assess the physics requirements for DUNE.

2.1.4 Strategies

2.1.4.1 Simulation and Reconstruction Strategies

Liquid argon time projection chambers (LArTPCs) provide a robust and elegant method for measuring the properties of neutrino interactions above a few tens of MeV by providing three-

dimensional (3D) event imaging with excellent spatial and energy resolution. The state of the art in LArTPC event reconstruction and particle identification is evolving rapidly and will continue to do so for many years. The adoption of the common framework LArSoft[2] by several LArTPC experiments facilitates the exchange of tools and ideas.

The DUNE experimental design and physics program to be presented in the TDR will be, in the main, based on a realistic end-to-end simulation and reconstruction chain. This is in contrast to the highly parametrized methods used in the CDR. Note that the science case summarized in Chapter 2 of this interim design report (IDR) is still based on CDR-era studies, as we intend to carry out the full refresh of the DUNE science case using our modern tools on the TDR timeline (2019). The primary exception to this strategy are sensitivity studies for BSM physics, which will largely continue to use parametrized analyses with updated assumptions to reflect our latest understanding. A full description of the DUNE simulation and reconstruction tools will be included in the TDR. In this section, we give a brief summary of the techniques now in use.

2.1.4.1.1 Simulation Chain

Simulated events are created in four stages: event generation, GEometry ANd Tracking, version 4 (Geant4) tracking, TPC and photon detection system (PDS) signal simulation, and digitization. The first step is unique to each sample type while the remaining steps are common for all samples. Beam neutrino, atmospheric neutrino, and nucleon decay events are generated using Generates Events for Neutrino Interaction Experiments (GENIE) appropriately configured for each. Supernova events are generated using the new low-energy, argon-specific MARLEY generator [4]. Cosmogenic events at depth are generated using MUSIC (Muon Simulation Code) [5] and MUSUN (Muon Simulations Underground) [6].

Particle 4-vectors generated in the event generator step are passed to a GEANT4-based detector simulation. Energy depositions are converted to ionization electrons and scintillation photons, with recombination, electron attenuation, and diffusion effects included. The response of the photon detectors is simulated using a "photon library" that has precalculated the likelihood for the propagation of photons from any point in the detector to any PDS element. The response of the TPC induction and collection wires is based on a detailed GARFIELD [7] simulation. Throughout, measurements from test stands or from operating LArTPC experiments such as ICARUS, LArIAT, and MicroBooNE are used to establish simulation parameters, where possible.

The raw signals on each wire are converted into analog-to-digital converter (ADC) versus time traces by convolution with the field response and electronics response. ASIC electronics response is simulated with the BNL SPICE [8] simulation. The photon detector electronics simulation separately generates waveforms for each channel of a photon detector that has been hit by photons, with dark noise and line noise added. The raw data are passed through hit finding algorithms that handle deconvolution and disambiguation to produce the basic data used by the downstream event reconstruction. PDS signals are reconstructed by searching for peaks on individual channels and then forming coincidences across channels. Techniques for matching the correct PDS signal to TPC signals to reconstruction t_0 are being developed, and early results from these tools can be

[2] LArSoft, `http://inspirehep.net/record/1598096/export/hx`.

seen in Volume 2: Single-Phase Module Chapter 5.

2.1.4.1.2 Reconstruction and Event Identification

Several approaches to LArTPC reconstruction are under active development in DUNE and in the community at large. En route to the TDR, efforts on all fronts have been supported. One reconstruction path ("TrajCluster" + "Projection Matching") forms two-dimensional (2D) trajectory clusters in each detector view and then stitches these together into 3D objects. Resulting objects are further characterized by, for instance, extracting dE/dx information or comparing to electromagnetic shower profiles. An alternative approach is provided by the Pandora reconstruction package [9], in which the reconstruction and pattern recognition task is broken down into a large number of decoupled algorithms, where each algorithm addresses a specific task or targets a particular topology. Two additional algorithms ("WireCell" and "SpacePointSolver") take a different approach and create 3D maps of energy depositions directly by solving a constrained system of equations governed by the geometry of the TPC wires. Finally, several analyses are using deep learning and convolutional neural networks with promising early success, as these techniques are well suited to the type of data produced by LArTPCs.

Energy reconstruction is based on electron-lifetime-corrected calorimetry except in the case of muons where energy is determined from track range or (for uncontained muons) multiple Coulomb scattering. Moving forward, more particle-specific energy estimators will be developed.

The output from all reconstruction algorithms is processed into standard "ntuple files" for use by analysis developers. In the special case of long-baseline oscillation measurements, the CAFAna fitting toolkit developed originally for NOνA is used to combine far detector and near detector information, to assess the impact of systematic uncertainties, and to ultimately produce neutrino oscillation sensitivities, discussed next.

2.2 Long-Baseline Neutrino Oscillation physics program

Precision neutrino oscillation measurements lie at the heart of the DUNE scientific program. The strengths of DUNE are (1) its discovery potential for charge-parity symmetry violation (CPV) in the neutrino sector, (2) its ability to resolve the neutrino mass ordering unambiguously, regardless of values of all other parameters governing neutrino oscillations, and (3) its unique ability to make high precision measurements of neutrino oscillations all within a single experiment.

2.2.1 Experimental Context: Baseline, Configuration and Staging Scenario

The 1300 km baseline, coupled with the wide-band high-intensity neutrino beam from LBNF, establishes one of DUNE's key strengths, namely sensitivity to the matter effect. This effect

leads to a discrete asymmetry in the $\nu_\mu \to \nu_e$ versus $\bar{\nu}_\mu \to \bar{\nu}_e$ oscillation probabilities, the sign of which depends on the presently unknown mass hierarchy (mass hierarchy (MH)). At 1300 km, the asymmetry,

$$\mathcal{A} = \frac{P(\nu_\mu \to \nu_e) - P(\bar{\nu}_\mu \to \bar{\nu}_e)}{P(\nu_\mu \to \nu_e) + P(\bar{\nu}_\mu \to \bar{\nu}_e)} \tag{2.1}$$

is approximately $\pm 40\%$ in the region of the peak flux in the absence of CP-violating effects. This is larger than the maximal possible CP-violating asymmetry associated with the CP-violating phase, δ_{CP}, of the three-flavor PMNS mixing matrix in the region of the peak flux. The CP asymmetry is larger in the energy regions below the peak flux while the matter asymmetry is smaller. As a result, the LBNF wide-band beam will allow unambiguous determination of both the MH and δ_{CP} with high confidence *within the same experiment*, i.e., DUNE.

The DUNE far detector will be built as four 10 kt modules, which will come online sequentially over the course of several years. This staged program enables an early scientific output from DUNE, initially focused on the observation of natural sources of neutrinos, searches for nucleon decay and measurements of backgrounds. Two years after commissioning the first two detector modules, the LBNF neutrino beam at Fermilab will begin sending neutrinos over the 1300 km baseline, commencing the LBL oscillation physics program with a beam power of up to 1.2 MW. Upgrades to increase the beam power to 2.4 MW are planned to be in place six years later. The early physics program will be statistically limited and constraints from comparison of the ν_μ disappearance spectrum with that from ν_e appearance will partially mitigate systematic uncertainties. The near detector is expected to come online in a timescale similar to that of the initial beam and will provide powerful constraints on the beam flux and neutrino interaction model, providing the necessary control of systematic uncertainties for the full exploitation of LBNF/DUNE.

The evolution of the projected DUNE sensitivities as a function of real time is estimated based on an assumed deployment plan with the following assumptions:

- Year 1: 20 kt far detector fiducial mass, 1.07 MW 80 GeV proton beam with 1.47×10^{21} protons-on-target per year and initial near detector constraints;
- Year 2: Addition of the third 10 kt far detector module, for a total far detector fiducial mass of 30 kt;
- Year 4: Addition of the fourth 10 kt far detector module, for a total far detector fiducial mass of 40 kt, and improved systematic constraints from near detector analysis;
- Year 7: Upgrade of beam power to 2.14 MW for a 80 GeV proton beam.

With regard to the sensitivities reported here, it is assumed that the knowledge from the near detector can be retroactively applied to previous data sets, such that each successive improvement in the knowledge of systematic uncertainties is applied to the full exposure up to that point.

2.2.2 Mass Hierarchy

As indicated above, unraveling the complex interplay of the matter effect with the degeneracies presented by multiple neutrino-mixing parameters with poorly known values will be a critical contribution from DUNE. Addressing the mass hierarchy question can be thought of as a first step toward this, one with intrinsic interest and import of its own. While significant progress on this is expected from currently running experiments, DUNE's ability to resolve the MH for all allowed values of mixing parameters is a key strength.

The discriminating power between the two MH hypotheses is quantified by the difference, denoted $\Delta\chi^2$, between the $-2\log\mathcal{L}$ values calculated for the normal and inverted hierarchies. As the sensitivity depends on the true value of the unknown CP-violating phase, $\delta_{\rm CP}$, all possible values of $\delta_{\rm CP}$ are considered. In terms of this test statistic[3], the MH sensitivity of DUNE for exposures of seven and ten years is illustrated in Figure 2.1 for the case of normal hierarchy and the NuFit 2016 [10] best-fit value of $\sin^2\theta_{23} = 0.44$. For this exposure, the DUNE determination of the MH will be definitive for the overwhelming majority of the $\delta_{\rm CP}$ and $\sin^2\theta_{23}$ parameter space. Even for unfavorable combinations of the parameters, a statistically ambiguous outcome is highly unlikely.

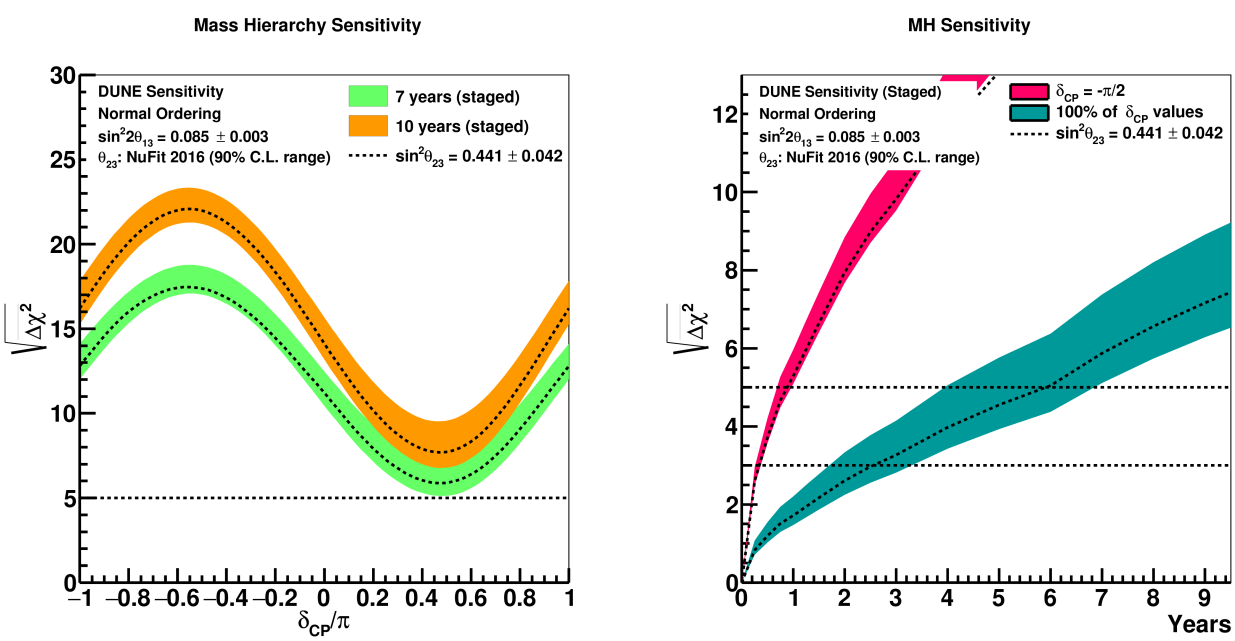

Figure 2.1: The square root of the mass hierarchy discrimination metric $\Delta\chi^2$ is plotted as a function of the unknown value of $\delta_{\rm CP}$ for exposures of seven and ten years (left). The minimum significance — the lowest point on the curve on the left — with which the mass hierarchy can be determined for all values of $\delta_{\rm CP}$ and the significance for a true value of $\delta_{\rm CP}$ =-$\pi/2$ as a function of years of running under the staging plan described in the text (right). The shaded regions represent the range in sensitivity corresponding to different true values of θ_{23}.

Figure 2.1 shows the evolution of the sensitivity to the MH determination as a function of years of

[3]For the case of the MH determination, the usual association of this test statistic with a χ^2 distribution for one degree of freedom is not strictly correct; additionally the assumption of a Gaussian probability density implicit in this notation is not exact.

operation, for the least favorable scenario (blue band), corresponding to the case in which the MH asymmetry is maximally offset by the leptonic CP asymmetry. An exposure of 209 kt · MW · year (which corresponds to approximately five years of operation) is required to distinguish between normal and inverted hierarchy with $|\Delta\chi^2| = \overline{|\Delta\chi^2|} = 25$. This corresponds to a $\geq 99.9996\%$ probability of determining the correct hierarchy. The dependence of the mass hierarchy sensitivity on systematics is still under evaluation, but current studies indicate only a weak dependence on the assumptions for the achievable systematic uncertainties. This indicates that a measurement of the unknown neutrino mass hierarchy with very high precision can be carried out during the first few years of operation. Concurrent analysis of the corresponding atmospheric-neutrino samples in an underground detector may improve the precision and speed with which the MH is determined.

2.2.3 CP Violation

DUNE will search for CP violation using the ν_μ to ν_e and $\bar{\nu}_\mu$ to $\bar{\nu}_e$ oscillation channels, with two objectives. First, DUNE aims to observe a signal for leptonic CP violation independent of the underlying nature of neutrino oscillation phenomenology. Such a signal will be observable in comparisons of $\nu_\mu \to \nu_e$ and $\bar{\nu}_\mu \to \bar{\nu}_e$ oscillations of the LBNF beam neutrinos in a wide range of neutrino energies over the 1300 km baseline. Second, DUNE aims to make a precise determination of the value of $\delta_{\rm CP}$ within the context of the standard three-flavor mixing scenario described by the PMNS neutrino mixing matrix. Together, the pursuit of these two goals provides a thorough and unprecedented test of the standard three-flavor scenario.

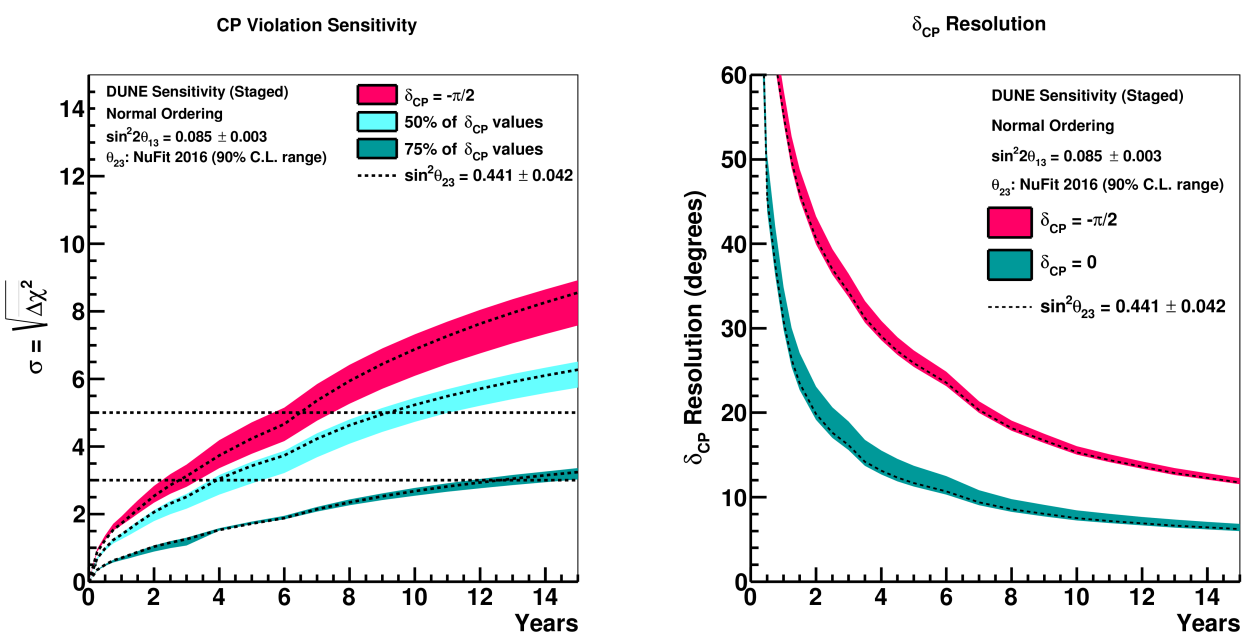

Figure 2.2: The significance with which CP violation can be determined for 75% and 50% of $\delta_{\rm CP}$ values and for $\delta_{\rm CP}$ =-$\pi/2$ (left) and the expected 1σ resolution (right) as a function of exposure in years using the proposed staging plan outlined in this chapter. The shaded regions represent the range in sensitivity corresponding to different true values of θ_{23}. The plots assume normal mass hierarchy.

Figure 2.2 shows, as a function of time, the expected sensitivity to CP violation expressed as the

minimum significance with which CP violation can be determined for 75% and 50% of $\delta_{\rm CP}$ values as well as the sensitivity when the true value of $\delta_{\rm CP}$ =-$\pi/2$. Also shown is the 1σ resolution for $\delta_{\rm CP}$ as a function of time for $\delta_{\rm CP} = 0$ (no CP violation) and $\delta_{\rm CP} = -90°$ (maximal CP violation). In both figures the staging scenario described previously is assumed. The exposure required to measure $\delta_{\rm CP} = 0$ with a precision better than 10° is 250 kt · MW · year or about six and a half years of operation. A full-scope LBNF/DUNE operating with multi-megawatt beam power can in time achieve a precision comparable to the current precision on the CP phase in the CKM matrix in the quark sector (5%).

Table 2.1 summarizes the exposures needed to achieve specific oscillation physics milestones, calculated for the current best-fit values of the known neutrino mixing parameters. For example, to reach 3σ sensitivity for 75% of the range of $\delta_{\rm CP}$, a DUNE exposure of 775 kt · MW · year or 12 years is needed. Changes in the assumed true value of θ_{23} impact CP-violation and MH sensitivities and can either reduce or increase the discovery potential for CP violation, as seen in Figure 2.2. To reach this level of sensitivity a highly capable near neutrino detector is required to control systematic uncertainties at a level lower than the statistical uncertainties in the far detector. No experiment can provide coverage at 100% of all $\delta_{\rm CP}$ values, since CP-violating effects vanish as $\delta_{\rm CP}$ $\rightarrow 0$ or π.

Table 2.1: The exposure in mass (kt) × proton beam power (MW) × time (years) and calendar years assuming the staging plan described in this chapter needed to reach certain oscillation physics milestones. The numbers are for normal hierarchy using the NuFit 2016 best fit values of the known oscillation parameters.

Physics milestone	Exposure (kt · MW · year)	Exposure (years)
1° θ_{23} resolution ($\theta_{23} = 42°$)	29	1
CPV at 3σ ($\delta_{\rm CP} = -\pi/2$)	77	3
MH at 5σ (worst point)	209	6
10° $\delta_{\rm CP}$ resolution ($\delta_{\rm CP} = 0$)	252	6.5
CPV at 5σ ($\delta_{\rm CP} = -\pi/2$)	253	6.5
CPV at 5σ 50% of $\delta_{\rm CP}$	483	9
CPV at 3σ 75% of $\delta_{\rm CP}$	775	12.5
Reactor θ_{13} resolution ($\sin^2 2\theta_{13} = 0.084 \pm 0.003$)	857	13.5

2.2.4 Precision Measurement of Mixing Parameters

In long-baseline experiments with ν_μ beams, the magnitude of ν_μ disappearance and ν_e appearance signals is proportional to $\sin^2 2\theta_{23}$ and $\sin^2 \theta_{13}$, respectively, in the standard three-flavor mixing scenario. Current ν_μ disappearance data are consistent with close to maximal mixing, $\theta_{23} = 45°$. To obtain the best sensitivity to both the magnitude of its deviation from 45° as well the θ_{23} octant, a combined analysis of the two channels is needed [11]. A DUNE detector with sufficient exposure will be able to resolve the θ_{23} octant at the 3σ level or better for θ_{23} values less than 43°

or greater than 48°. The full LBNF/DUNE scope will allow θ_{23} to be measured with a precision of 1° or less, even for values within a few degrees of 45°.

To summarize, DUNE has great prospects to discover CP violation or, in the absence of the effect, set stringent limits on the allowed values of δ_{CP}. DUNE will also determine the neutrino mass hierarchy with better than a 5σ C.L. and provide precision measurements of the mixing angles θ_{23} and θ_{13}.

2.3 Nucleon Decay and the GeV Scale Non-Accelerator Physics Program

2.3.1 Nucleon Decay

Unification of three of the fundamental forces in the universe, the strong, electromagnetic and weak interactions, is a central paradigm for the current world-wide program in particle physics. Grand Unified Theories (GUTs), aiming at extending the standard model of particle physics to include a unified force at very high energies (above 10^{15} GeV), predict a number of observable effects at low energies, such as nucleon decay [12, 13, 14, 15, 16, 17]. Several experiments have been searching for signatures of nucleon decay, with the best limits for most decay modes set by the Super-Kamiokande experiment [18], which features the largest sensitive mass to date.

The DUNE far detector, as the largest active volume of argon, will be highly sensitive to a number of possible nucleon decay modes, in many cases complementing the capabilities of large water detectors. In particular, the LArTPC technology is expected to be well-suited for observing nucleon decays into charged kaons, which can be identified with redundancy from their distinctive dE/dx signature as well as by their decays. A particularly interesting mode for the proton decay search with DUNE is $p \to K^+\bar{\nu}$, which is expected to have a lifetime of the order of $> 10^{33}$ years in SUSY models. This decay can be tagged in a LArTPC if a single kaon within a proper energy/momentum range can be reconstructed with its point of origin lying within the fiducial volume. Background events initiated by cosmic-ray muons can be controlled by requiring no activity close to the edges of the TPCs and by stringent single kaon identification within the energy range of interest. Atmospheric neutrino-induced background with real kaon production will either have an associated strange baryon (for reactions with $\Delta S = 0$) whose decay can be reconstructed, or an identifiable charged lepton (for reactions with $\Delta S = 1$). Atmospheric neutrino-induced background may also arise from misidentification of protons from abundant quasielastic interactions. Work is ongoing (see below) to understand in detail how to fully exploit the capabilities of the DUNE LArTPC FD modules to suppress the above backgrounds while maintaining the high acceptance necessary for discovery-level sensitivity. Similarly, the DUNE FD is expected to have good sensitivity to other compelling nucleon decay modes, such as $n \to K^+e$, $p \to l^+K^0$, and $p \to \pi^0e^+$, which are also under study.

As is the case for the entire non-accelerator based physics program of DUNE, nucleon decay searches require efficient triggering and event localization (within the far detector) capabilities.

Given the 1-GeV energy release, the requirements on tracking and calorimetry capabilities are similar to those for the beam-based neutrino oscillation program described in the previous section. Experimental challenges such as particle identification to separate protons from kaons, the impact of final state interactions (FSI) on proton decay kinematics, and full control of the potential background processes, are presently under study with realistic detector simulations. This includes opportunities for enhanced background rejection by using convolutional neural networks, as well as efforts to understand the uncertainty associated with the intra-nuclear cascade model used to simulate FSI. We expect that ProtoDUNE data taken with charged particle beams at CERN will provide important sample of events to train and improve on reconstruction algorithms and the resulting dE/dx resolution.

Baryon number non-conservation can also be manifested by neutron-antineutron oscillations leading to subsequent antineutron annihilation with a neutron or a proton. This annihilation event will have a distinct signature of a vertex with several emitted light hadrons, with total energy of twice the nucleon mass and net momentum zero. The ability to re-construct these hadrons correctly and measure their energies is key to the identification of the signal event. The main background for these $n\bar{n}$ annihilation events is caused by atmospheric neutrinos. Most commonly mis-classified events are neutral current deep inelastic scattering events without a lepton in the final state. As above, nuclear effects and final state interactions make the picture more complicated and are probably the major component of the systematic uncertainty for the sensitivity studies carried out thus far. Initial signal vs background discrimination studies have been performed using convolutional neural networks resulting in an equivalent sensitivity for the $n \to \bar{n}$ oscillation lifetime of 1.6×10^9 s at 90% confidence level, a factor of 5 improvement on the current limit from Super-Kamiokande. More information about particle identification and energy measurements will be provided by the ProtoDUNE experiment with charged particle beams.

2.3.2 Atmospheric neutrinos

Atmospheric neutrinos are a unique tool to study neutrino oscillations: the oscillated flux contains all flavors of neutrinos and antineutrinos, is very sensitive to matter effects and to both Δm^2 parameters, and covers a wide range of L/E. In principle, all oscillation parameters could be measured, with high complementarity to measurements performed with a neutrino beam. In addition, atmospheric neutrinos are available all the time, in particular before the beam becomes operational. The DUNE far detector, with its large mass and the overburden to protect it from atmospheric muon background, is an ideal tool for these studies. Given the strong overlap in event topology and energy scale with beam neutrino interactions, most requirements will necessarily be met by the far detector design. Additional requirements include the need to self-trigger since atmospheric neutrino events are asynchronous with respect to accelerator timing, and a more stringent demand on neutrino direction reconstruction.

The sensitivity to neutrino oscillation parameters has been evaluated with a dedicated, but simplified, simulation, reconstruction and analysis chain. The fluxes of each neutrino species at the far detector location were computed taking into account oscillations. Interactions in the LAr medium were simulated with the GENIE event generator. Detection thresholds and energy resolutions based on full simulations were applied to the outgoing particles, to take into account detector

effects. Events were classified as fully contained (FC) or partially contained (PC) by placing the vertex at a random position inside the detector and tracking the lepton until it reached the detector edges. The number of events expected for each flavor and category is summarized in Table 2.2.

Table 2.2: Atmospheric neutrino event rates per year in 40 kt fiducial mass of the DUNE FD.

Sample	Yearly Event Rate
Fully contained atmospheric e-like	1.6×10^3
Fully contained atmospheric μ-like	2.4×10^3
Partly contained atmospheric μ-like	7.9×10^2

When neutrinos travel through the Earth, the MSW resonance influences electron neutrinos in the few-GeV energy range. More precisely, the resonance occurs for ν_e in the case of normal mass hierarchy (NH, $\Delta m^2 > 0$), and for $\bar{\nu}_e$ in the case of inverted mass hierarchy (IH, $\Delta m^2 < 0$). The mass hierarchy (MH) sensitivity can thus be greatly enhanced if neutrino and antineutrino events can be separated. The DUNE detector will not be magnetized; however, its high-resolution imaging offers possibilities for tagging features of events that provide statistical discrimination between neutrinos and antineutrinos. Two tags can be used to discriminate $\bar{\nu}$ and ν events: a proton tag (a signature of a likely neutrino interaction) and a positive muon decay tag (a signature of an antineutrino interaction since only 25% of negative muons will decay).

Unlike for beam measurements, the sensitivity to MH with atmospheric neutrinos is nearly independent of the CP-violating phase. The sensitivity comes from both electron neutrino appearance as well as muon neutrino disappearance, and is strongly dependent on the true value of θ_{23}. Despite the much smaller mass, DUNE would have comparable sensitivity to the Hyper–Kamiokande atmospheric neutrino analyses due to better event reconstruction.

These analyses will provide a complementary approach to beam neutrinos. Atmospheric neutrinos can help to lift degeneracies that can be present in beam analyses, for instance, through the fact that the MH sensitivity is essentially independent of δ_{CP}. Atmospheric neutrino data will be acquired even in the absence of the beam, and will provide a useful sample for the development of reconstruction software and analysis methodologies. Atmospheric neutrinos provide a window into a range of new physics scenarios, and can place limits on CPT violation [19], non-standard interactions, mass-varying neutrinos [20], sterile neutrinos [21], and Lorentz invariance violation [22].

2.4 Supernova-Neutrino Physics and Astrophysics

The neutrinos from a core-collapse supernova are emitted in a burst of a few tens of seconds duration, with about half the signal emitted in the first second. The neutrino energies are mostly in the range 5 to 50MeV, and the flux is divided roughly equally between the three known neutrino flavors. Current water and scintillator detectors are sensitive primarily to electron antineutrinos ($\bar{\nu}_e$), with detection through the inverse-beta decay process on free protons, which dominates the interaction rate in these detectors. Liquid argon has a unique sensitivity to the electron-neutrino

(ν_e) component of the flux, via the absorption interaction on ^{40}Ar,

$$\nu_e + {}^{40}\mathrm{Ar} \;\rightarrow\; e^- + {}^{40}\mathrm{K}^*.$$

This interaction can in principle be tagged via the coincidence of the emitted electron and the accompanying photon cascade from the ^{40}K* de-excitation. About 3000 events would be expected in a 40 kt fiducial mass liquid argon detector for a supernova at a distance of 10 kpc. In the neutrino channel, the oscillation features are in general more pronounced, since the ν_e spectrum is almost always significantly different from the ν_μ (ν_τ) spectrum in the initial core-collapse stages, to a larger degree than is the case for the corresponding $\bar{\nu}_e$ spectrum. While ν_e absorption should represent ∼90% of the signal, there are in addition other channels of interest, including $\bar{\nu}_e$ charged current, elastic scattering on electrons (which provides pointing information) and neutral-current interactions which result in final-state deexcitation γ's. Each channel has a distinctive signature in the detector, but in all cases, events appear as small (tens of cm scale) tracks and blips. Figure 2.3 shows an example of a simulated event. Section 2.1.4.1 describes reconstruction and calibration challenges for detecting these events.

Observation of the core-collapse neutrino burst in DUNE will provide critical information on key astrophysical phenomena [23]. These include the neutronization burst, for which the initial sharp, bright flash of ν_e from $p + e^- \rightarrow n + \nu_e$ heralds the formation of a compact neutron star remnant. The collapse of the proto-neutron star into a black hole would be signaled by a sharp cutoff in neutrino flux. Shock wave effects, shock instability oscillations, turbulence effects, and transitions to quark stars could all produce observable features in the energy, flavor and time structure of the neutrino burst. Furthermore, detection of the supernova burst neutrino signal in DUNE will provide information on neutrino properties: see reference [23]. Most notably, several features offer multiple signatures of mass ordering [24], likely the most robust being the level of suppression of the neutronization burst: see Figure 2.3. Because the neutronization burst is ν_e-rich, this mass ordering signature is especially clean in DUNE. "Collective effects", due to self-induced transitions driven by *neutrino-neutrino interactions* in the dense matter of the supernova, result in a rich phenomenology with multiple observables primarily at later times.

Because no beam trigger is available for a supernova, efficient triggering and continuous data collection is critical for supernova neutrino burst physics. To fully capitalize on the physics opportunities, the DUNE far detector must provide event timing capability at the sub-millisecond level, must have spatial readout granularity sufficient to track electrons down to 5 MeV with good energy resolution, and must operate at noise levels and thresholds that allow detection and energy measurement for deexcitation gammas and nucleons at the MeV level. The LArTPC technologies underlying the DUNE far detector conceptual designs is capable of meeting these requirements.

We note that information from DUNE will be highly complementary with neutrino burst information from other detectors, and furthermore multi-messenger astronomy information (from gravitational waves and a broad range of electromagnetic wavelengths) will combine to provide a full picture of a core-collapse event.

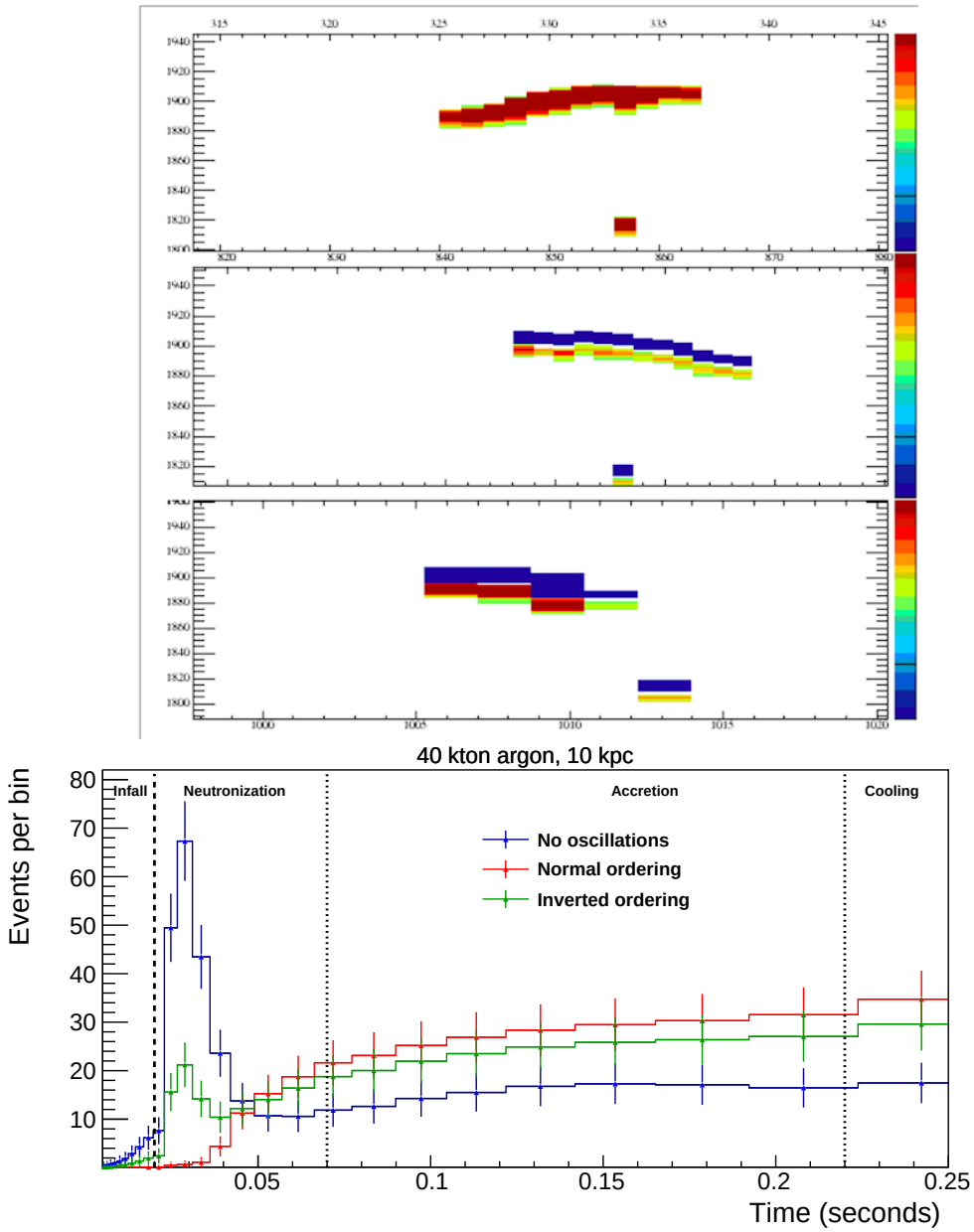

Figure 2.3: Top: Event display of a 30 MeV neutrino event simulated using MARLEY. Bottom: Expected event rates as a function of time for the electron-capture SNB model in [25] for 40 kt of argon during early stages of the event – the neutronization burst and early accretion phases, for which self-induced effects are unlikely to be important. Shown is the event rate for the unrealistic case of no flavor transitions (blue), the event rate including the effect of matter transitions for the normal (red) and inverted (green) hierarchies. Error bars are statistical, in unequal time bins.

2.5 Precision Measurements with the DUNE Near Detector Complex

The DUNE near detector will provide precision measurements of neutrino interactions that are essential for controlling the systematic uncertainties in the long-baseline neutrino oscillation physics program. The near detector will include argon targets and will measure the absolute flux and energy-dependent shape of all four neutrino species, ν_μ, $\bar{\nu}_\mu$, ν_e and $\bar{\nu}_e$, to accurately predict for each species the far/near flux ratio as a function of energy. It will also measure the four-momenta of secondary hadrons, such as charged and neutral mesons, produced in the neutral- and charged-current interactions that constitute the dominant backgrounds to the oscillation signals.

The near detector will also be the source of data for a rich program of neutrino-interaction physics in its own right. For an integrated beam intensity of 1×10^{20} protons-on-target at 120 GeV, the expected number of events per ton is 170,000 (59,000) ν_μ ($\bar{\nu}_\mu$) charged-current and 60,000 (25,000) neutral-current interactions in the ν ($\overline{\nu}$) beam. With PIP-II, the integrated protons-on-target per year is expected to be around 1.1×10^{21} at 120 GeV. The mass of the argon target in the low-mass tracker option for the DUNE near detector is expected to be approximately 80 tons. These numbers correspond to 10^5 neutrino interactions on argon per year for the range of beam configurations and near detector designs under consideration. Measurement of fluxes, cross sections and particle production over a large energy range of 0.5 GeV to 50 GeV are the key elements of this program. These data will also help constrain backgrounds to proton-decay signals from atmospheric neutrinos. Furthermore, very large samples of events will be amenable to precision reconstruction and analysis, and will be exploited for sensitive studies of electroweak physics and nucleon structure, as well as for searches for new physics in unexplored regions, such as heavy sterile neutrinos, high-Δm^2 oscillations, and light Dark Matter particles.

2.6 Opportunities in Beyond the Standard Model Physics

The unique combination of the high-intensity LBNF neutrino beam with DUNE's near detector and massive LArTPC far detector modules at a 1300 km baseline enables a variety of probes of BSM physics, either novel or with unprecedented sensitivity. This section describes a selection of such topics, and briefly summarizes how DUNE can make leading contributions in this arena.

2.6.1 New Particle Searches

Search for Low-mass Dark Matter. Various cosmological and astrophysical observations strongly support the existence of dark matter (DM) representing ≈27% of the mass-energy of the universe, but its nature and potential non-gravitational interactions with regular matter remain undetermined. The lack of evidence for weakly interacting massive particles (WIMP) at direct detection and the LHC experiments has resulted in a reconsideration of the WIMP paradigm. For instance, if dark matter has a mass which is much lighter than the electroweak scale (e.g., below the GeV

level), it motivates theories for dark matter candidates that interact with ordinary matter through a new "vector portal" mediator. High flux neutrino beam experiments, such as DUNE, have been shown to provide coverage of DM+*mediator* parameter space which cannot be covered by either direct detection or collider experiments. Dark matter particles can be detected in the near detector through neutral-current-like interactions either with electrons or nucleons in the detector material. The neutrino-induced backgrounds can be suppressed using timing and the kinematics of the scattered electron. These enable DUNE's search for light dark matter be competitive and complementary to other experiments.

Search for Boosted Dark Matter Using its large far detector, DUNE will be able to search for boosted dark matter. A representative model is composed of heavy and light dark matter components and the lighter one can be produced from the annihilation of the heavier one in e.g., the nearby sun or galactic centers. Due to the large mass difference between the two dark matter components, the lighter one is produced relativistically. The incoming energy of the lighter dark matter component can be high enough above the expected energy thresholds of DUNE in a wide range of parameter space. A first attempt at observing the inelastic boosted dark matter signal with ProtoDUNE prior to running DUNE is proposed in Ref. [26] and the same analysis strategy can be used in DUNE.

Heavy Neutral Leptons. The high intensity of the LBNF neutrino beam and the production of charm and bottom mesons in the beam enables DUNE to search for a wide variety of lightweight long-lived, exotic particles, by looking for topologies of rare event interactions and decays in the fiducial volume of the DUNE near detector. These particles include weakly-interacting heavy neutral leptons – right-handed partners of the active neutrinos, vector, scalar, or axion portals to the Hidden Sector, and light super-symmetric particles. Assuming these heavy neutral leptons are the lighter particles of their hidden sector, they will only decay into standard model particles. The parameter space explored by the DUNE near detector extends into the cosmologically relevant region complementary to the LHC heavy-mass dark-matter searches through missing energy and mono-jets.

2.6.2 Searches for Deviations from the PMNS Neutrino Mixing Paradigm

Non-Standard Neutrino Interactions. Non-standard neutrino interactions, affecting neutrino propagation through the Earth, can significantly modify the data to be collected by DUNE as long as the new physics parameters are large enough [27]. Leveraging its very long baseline and wide-band beam, DUNE is uniquely sensitive to these probes. If the DUNE data are consistent with standard oscillations for three massive neutrinos, interaction effects of order 0.1 G_F can be ruled out at DUNE [28, 29]. We note that DUNE might improve current constraints on $\epsilon_{\tau e}$ and $\epsilon_{\mu e}$ by a factor 2-5 [30].

Non-Unitarity. A generic characteristic of most models explaining the neutrino mass pattern is the presence of heavy neutrino states, additional to the three light states of the standard model of particle physics [31, 32, 33, 34]. This implies a deviation from unitary of the 3×3 PMNS matrix, which can be particularly sizable the lower the mass of the extra states are [35, 36, 37, 38]. For

values of the unitarity deviations of order 10^{-2}, this would decrease the expected reach of DUNE to the standard parameters, although stronger bounds existing from charged leptons would be able to restore its expected performance [39, 40].

Violations of Lorentz or CPT Symmetry. CPT symmetry, the combination of charge conjugation, parity and time reversal, is a cornerstone of our model building strategy and therefore the repercussions of its potential violation will severely threaten the standard model of particle physics. DUNE can improve the present limits on Lorentz and CPT violation by several orders of magnitude [19, 22, 41, 42, 43], contributing as a very important experiment to test one of the deepest results of quantum field theory.

Active-Sterile Neutrino Mixing. Experimental results in tension with the three-neutrino-flavor paradigm [44, 45, 46, 47], which may be interpreted as mixing between the known active neutrinos and one or more *sterile* states, have led to a rich and diverse program of searches for oscillations into sterile neutrinos. DUNE is sensitive over a broad range of potential sterile neutrino mass splittings by looking for disappearance of CC and NC interactions over the long distance separating the near and far detectors, as well as over the short baseline of the near detector. With a longer baseline, a more intense beam, and a high-resolution large-mass far detector, compared to previous experiments, DUNE provides a unique opportunity to improve significantly on the sensitivities of the existing probes, and greatly enhance the ability to map the extended parameter space if a sterile neutrino is discovered.

Large Extra Dimensions. DUNE can search for or constrain the size of large extra-dimensions (LED) by looking for distortions of the oscillation pattern predicted by the three-flavor paradigm. These distortions arise through mixing between the right-handed neutrino Kaluza-Klein modes, which propagate in the compactified extra dimensions, and the active neutrinos, which exist only in the four-dimensional brane [48]. Searching for these distortions in, for instance, the ν_μ CC disappearance spectrum should provide significantly enhanced sensitivity over existing results from the MINOS/MINOS+ experiment [49].

Neutrino Trident Production. The intriguing possibility that neutrinos may be charged under new gauge symmetries beyond the standard model $SU(3)_c \times SU(2)_L \times U(1)_Y$, and interact with the corresponding new gauge bosons can be tested with unprecedented precision by DUNE through near detector measurements of neutrino-induced di-lepton production in the Coulomb field of a heavy nucleus, also known as neutrino trident interactions [50]. Although this process is extremely rare (SM rates are suppressed by a factor of $\sim 10^{-5} - 10^{-7}$ with respect to CC interactions), the CHARM-II collaboration [51] and the CCFR collaboration [52] both reported detection of several trident events (~ 40 events at CCFR) and quoted cross-sections in good agreement with the SM predictions. With a predicted annual rate of over 100 di-muon neutrino trident interactions at the near detector, DUNE will be able to measure deviations from the SM rates and test for the presence of new gauge symmetries.

2.7 Summary

In summary, the primary science goals of DUNE are drivers for the advancement of particle physics. DUNE's physics program brings together the international neutrino community as well as leading experts in nucleon decay and particle astrophysics to explore key questions at the forefront of particle physics and astrophysics.

The questions being addressed are of wide-ranging consequence: the origin of flavor and the generation structure of the fermions, the physical mechanism that provides the CP violation needed to generate the baryon asymmetry of the universe, and the high-energy physics that would lead to the instability of matter. Achieving these goals requires a dedicated, ambitious and long-term program. The staged implementation of the far detector as four 10 kt modules will enable exciting physics in the intermediate term, including a definitive mass hierarchy determination and possibly a measurement of the CP phase (assuming neutrinos are CP-violating), while providing the fastest route toward achieving the full range of DUNE's science objectives.

Chapter 3

DUNE Software and Computing

3.1 Overview

Offline computing for DUNE faces new and considerable challenges due to the large scale and diverse physics goals of the experiment. In particular, the advent of liquid argon time-projection chambers (LArTPCs) with exquisite resolution and sensitivity, combined with enormous physical volumes, creates challenges in acquiring and storing large data volumes and in analyzing and reducing them. The computing landscape is changing rapidly, with the traditional HEP architecture of individual cores running Linux being superseded by multi-core machines and GPUs. At the same time, algorithms for liquid argon (LAr) reconstruction are still in their infancy and developing rapidly. As a result, we have reason to be optimistic about the future, but we are not able to predict it accurately. The ProtoDUNE single and dual phase tests at CERN in the fall of 2018 will provide a wealth of data that will inform the future evolution of the DUNE computing models.

The DUNE offline computing challenges can be classified in several ways. We will start with the different detector and physics configurations that drive the large scale data storage and reconstruction. This discussion leans heavily on the data acquisition (DAQ) design described in Volume 2: Single-Phase Module and Volume 3: Dual-Phase Module of the DUNE interim design report (IDR).

3.1.1 Detectors

The DUNE experiment will consist of four 17.5 kt far detector (FD) modules located at SURF, using either single-phase (SP) or dual-phase (DP) LArTPCs, and a not fully specified near detector at Fermilab. The proposed FD SP module has an active mass of 10 kt and the DP module has an active mass of 12.096 kt.

3.1.1.1 Single-phase estimates

Each SP module will consist of three rows of anode planes with a cathode plane between each anode plane pair. The planes are spaced 3.5 m apart and operated at 180 kV for a 500 V/cm drift field. The anode planes are made up of anode plane assemblies (APAs) which are 6.3 m tall by 2.3 m wide and have 2,560 readout channels each. Each channel is sampled with 12-bit precision every 500 nsec. For modules of this size, drift times in the liquid argon are of order 2.5 ms and raw data sizes before compression are of order 6 GB per module per 5.4 ms readout window. With no triggering and no zero suppression or compression, the raw data volume for four modules would be of order 145 EB/year.

3.1.1.2 Dual-phase technology

For DP, electrons may traverse the full height of the cryostat, emerge from the liquid and be collected, after gas amplification, on a grid of instrumented strips at the top of the detector module. The WA105 DP demonstrator test of this technology ran successfully in the summer of 2017[53]. Each 12.096 kt module will have 153,600 channels. Drift time in the LAr is 7.5 ms. Given 20,000 samples in an 8 ms readout, the uncompressed event size is 4.2 GB (for one drift window). Due to gas amplification, the S/N ratio is quite high, allowing lossless compression to be applied at the front-end with a compression factor of ten, bringing the event size/module to 0.42 GB. Recording the entire module drift window can be considered a pessimistic figure, since events are normally contained in smaller detector regions. A FD module can be treated as 20 smaller detectors (witha similar number of readout channels to the prototype currently being constructed at CERN), running in parallel, each one defining a ROI. For beam or cosmic events it is possible to record only the interesting ROIs with the compressed size of a single ROI being 22 MB.

3.1.1.3 Beam coincident rates

Requiring coincidence with the Long-Baseline Neutrino Facility (LBNF) beam will reduce the effective live-time from the full 1.2-1.5 sec beam cycle to a 5.4 ms (8 ms for DP) readout window coincident with the 10 microsecond beam spill, leading to an uncompressed data rate for beam-coincident events of around 20 GB/sec for four 17 kT single-phase detector modules ($\sim$ 16 GB/s for dual-phase), still too high to record permanently. Only a few thousand true beam interactions in the far detectors are expected each year. Compression and conservative triggering based on photon detectors and ionization should reduce the data rate from beam interactions by several orders of magnitude without sacrificing efficiency.

3.1.1.4 Near detector

The near detector configuration is not yet defined but we do have substantial experience from T2K and MicroBooNE at lower energies, and MINERνA at the DUNE beam energies on cosmic and

beam interactions under similar conditions. We can expect that a near detector will experience 5 to 10 beam interactions per beam pulse and non-negligible rates of cosmic rays, spread over an area of a few square meters. MicroBooNE experience and ProtoDUNE simulations indicate compressed event sizes of 100-1000 MB, leading to yearly data volumes of 2-20 PB. Storing and disentangling this information will be challenging but comparable to the ProtoDUNE data expected in 2018.

3.1.2 Physics Challenges

DUNE physics will consist of several different processes with very different rates and event sizes.

3.1.2.1 Long-baseline neutrino oscillations

Neutrino oscillation measurements will require a near detector operating in a high rate environment and far detectors in which beam-coincident events are rare but in time with the beam spill and of sufficient energy to be readily recognizable. Studies discussed in the DAQ section of IDR Volumes 2 and 3 indicate that high efficiencies are achievable at an energy threshold of 10 MeV, leading to event rates for beam-initiated interactions of $\sim$6400/year and an uncompressed data volume of around 30 TB/year per 17.5 kt SP module.

Tables 3.1 and 3.2 summarize the event and data rates after appropriate filtering from the DAQ section of Volumes 2 and 3 of the IDR.

3.1.2.2 Processes not in synchronization with the beam spill

These include supernova physics, atmospheric neutrinos, proton decay, neutron conversion and solar neutrinos. These processes are generally at lower energy, making triggering more difficult, and asynchronous, thus requiring an internal or external trigger. In particular, supernovae signals will consist of a large number of low-energy interactions spread throughout the far detector volume over a time period of 1-30 seconds. Buffering and storing 10 seconds of data would require around 2000 readout windows, or around 50 TB per supernova readout. At a rate of one such event/month, this is 600 TB of uncompressed data per module/year.

3.1.2.3 Calibration

In addition to physics channels, continuous calibration of the detectors will be necessary. It is likely that, for the far detectors, calibration samples will dominate the data volume. Cosmic-ray muons and atmospheric neutrino interactions will provide a substantial sample for energy and position calibration. Dedicated runs with radioactive sources and laser calibration will also generate substantial and extremely valuable samples. Table 3.1 includes estimates for the single-phase far detector. Cosmic ray and atmospheric neutrino signals collected for calibration make

Table 3.1: Anticipated annual, uncompressed data rates for a single SP module (from the SP module IDR volume). The rates for normal (non-SNB triggers) assume a readout window of 5.4 ms. In reality, lossless compression will be applied which is expected to provide as much as a $4\times$ reduction in data volume for each SP module.

Event Type	Data Volume PB/year	Assumptions
Beam interactions	0.03	800 beam and 800 rock muons; 10 MeV threshold in coincidence with beam time; include cosmics
Supernova candidates	0.5	30 seconds full readout, average once per month
Cosmics and atmospherics	10	10 MeV threshold
Radiologicals (^{39}Ar and others.	$\leq$1	fake rate of $\leq$100 per year
Front-end calibration	0.2	Four calibration runs per year, 100 measurements per point
Radioactive source calibration	0.1	source rate $\leq$10 Hz; single fragment readout; lossless readout
Laser calibration	0.2	1×10^6 total laser pulses, lossy readout
Random triggers	0.06	45 per day
Trigger primitives	$\leq$6	all three wire planes; 12 bits per primitive word; 4 primitive quantities; ^{39}Ar-dominated

Table 3.2: Anticipated annual, uncompressed data rates for one DP module. The rates for normal (non-SNB triggers) assume a readout window 7.5 ms. These numbers do not include lossless compression which is expected to provide as much as a $10\times$ reduction in data volume.

Event Type	Data Volume PB/year	Assumptions
Beam interactions (DP)	0.007	800 beam and 800 rock muons; this becomes 700 GB/year if just 2 ROIs/event are dumped on disk
Supernova candidates (DP)	0.06	10 seconds full readout, all ROIs are dumped on disk
Cosmics/atmospherics (DP)	2.33	This becomes 230 TB/year if two ROIs/event are dumped on disk
Radiologicals (^{39}Ar and other).	$\leq$1	fake rate of $\leq$100 per year
Miscellaneous calibrations	0.5	similar to SP
Random triggers	0.02	45 per day
Trigger primitives	$\leq$6	similar to SP

up the bulk of the uncompressed SP data volume at ∼10 PB/year per 17 kT module and will dominate the rates from the far detectors.

3.1.2.4 Zero suppression

The data volumes discussed above are for un-zero-suppressed data. Efficient zero suppression mechanisms can substantially reduce the final data volume but previous experience in HEP indicates that signal processing must be done carefully and often happens well into data-taking when the data are well understood. Experience from MicroBooNE and the ProtoDUNE experiments will aid us in developing these algorithms, but it is likely that they will be applied later in the processing chain for single-phase. No zero-suppression is planned for dual-phase.

The constrained environment at SURF motivates a model where any further data reduction via zero-suppression is done downstream, either on the surface or after delivery to computing facilities at FNAL or elsewhere. This could be analogous to the HLT's used by LHC experiments. The relative optimization of data movement and processing location is an important consideration for the design of both the DAQ and offline computing.

3.1.3 Summary

In summary, uncompressed data volumes will be dominated by calibration for the far detector modules (∼10 PB/year/module SP or ∼3 PB/year/module DP) and by beam and cosmic ray interactions in the near detectors (2-20 PB/year). With four FD modules, but a conservative factor of four for compression, a total compressed data volume of 12-30 PB per year is anticipated.

Data transfer rate from the far detector to Fermilab is limited to 100 Gbit/s, which is consistent with projected network bandwidths in the mid 2020s and a limit of 30 PB/year raw data stored to tape.

3.2 Building the Computing Model

The DUNE computing model is a work in progress. Major advances will take place over the next year on several fronts, with data from ProtoDUNE and the full incorporation of lessons from MicroBooNE into LArSoft .

The overall model can be divided into several major parts: infrastructure, algorithms and adaption for the future. These are in different stages of planning and completion. An overarching theme is evaluating and using community codes and resources wherever possible.

3.2.1 Infrastructure

This category includes the wealth of databases, catalogs, storage systems, compute farms, and the software that drives them. HEP fortunately has already developed much of this technology and our plan is to adopt pre-existing systems wherever possible. As DUNE is a fully global experiment, integrating the resources of multiple institutions is both an opportunity and a logistical challenge.

Current plans have the primary raw data repository at Fermilab, with derived samples and processing distributed among collaborating data centers. For ProtoDUNE, raw data will also be stored at CERN. Data processing is being designed to run on HEP grid resources, with significant ongoing effort to containerize it so that DUNE can make use of heterogenous resources worldwide.

3.2.1.1 Core HEP code infrastructure

Shared HEP infrastructure will be used wherever possible, notably the ROOT[54] and GEometry ANd Tracking, version 4 (Geant4) [55, 56] frameworks. For event simulation, we plan to use and contribute to the broad range of available generators (e.g., GENIE [57], NuWro [58]) shared with the worldwide neutrino community.

In addition, we are using the infrastructure developed for the LHC and the Intensity Frontier experiments at Fermilab, notably grid infrastructure, the *art* framework and the sequential access via metadata (SAM) data catalog. The NOνA and MicroBooNE experiments are already using these tools for distributed computing and the ProtoDUNE data challenges are integrating CERN and Fermilab storage and CPU resources. We are now extending this integration to the institutions within the collaboration who have access to substantial storage and CPU resources.

3.2.2 Algorithms

This category includes the simulations, signal processing and reconstruction algorithms needed to reconstruct and understand our data. Algorithms are currently under development but are informed by existing general codes (for example GENIE and Geant4) and the experience of other liquid argon experiments as encoded in the shared LArSoft project. Simulations are quite advanced but full understanding of reconstruction algorithms will need real data from ProtoDUNE.

3.2.2.1 External products

The image-like nature of TPC data allows us to make use of external machine-learning systems such as TensorFlow[59], Keras[60] and Caffe[61]. Many of these are being evaluated for pattern recognition. While they encapsulate a wealth of experience, they are also somewhat volatile as they are driven by needs of non-HEP users. We must have access to and must preserve the underlying source codes in order to maintain reproducibility.

3.2.3 Adaptability

As the experiment will be expected to run at least two decades past the present we must be prepared for the inevitable and major shifts in the underlying technologies that will occur. The ability to keep operating over decades almost requires that we emphasize open source over proprietary technologies for most applications. DUNE should also plan to be able to utilize and support a large range of compute architectures in order to fully utilize the resources available to the collaboration.

Table 3.3 summarizes the responsibilities of the software and computing group and reconstruction and algorithms groups for both DUNE and ProtoDUNE.

Table 3.3: Computing Tasks - see the ProtoDUNE section for details on current status.

Task	Status
Code management	in place
Documentation and logging of DAQ and detector configurations	in design
Data movement	design rates achieved for short periods
Grid processing infrastructure	early version in use for data challenges
Data catalog	sam, in place
Beam instrumentation and databases	ifbeam, in test
Calibration and Alignment processing	needs development
Calibration and Alignment databases	needs development
Noise reduction	tested in simulation
Hit finding	tested in simulation
Pattern recognition algorithms	tested in simulation
Event simulation	use existing software
Analysis formats	no common format
Distribution of analysis samples to collaborators	needs development

3.2.4 Downstream Activities

The previous sections have concentrated on movement and recording of raw data, as that is most time-critical and drives the primary data storage requirements. Basic simulation and reconstruction algorithms are in place, but other components, in particular physics analysis models, are in a much earlier stage of development.

3.2.4.1 Simulation

Our simulation efforts will build on the combined experience of multiple neutrino experiments and theory groups for input. DUNE already has a solid foundation of event and detector simulation codes thanks to prior work by the LArSoft and event generator teams. However, even with good software in place, detector simulation in detectors of this high resolution is highly CPU and memory intensive and we are actively following projects intended to exploit HPCs for more efficiency. As simulation is much less I/O and database intensive than raw data reconstruction, (due in part to our ability to trigger efficiently on signal), we can anticipate resource contributions to this effort being distributed across the collaboration and grid resources worldwide. Simulation sample sizes orders of magnitude larger than the number of beam events in the far detector will be reasonably easy to achieve while near detector samples would need to be prohibitively large to equal the millions of events that will be collected every year.

3.2.4.2 Reconstruction

DUNE has working frameworks for large-scale reconstruction of simulated and real data in place thanks to the LArSoft effort. These, and the simulations, have been exercised in large scale data challenges. Optimization of algorithms awaits data from ProtoDUNE.

3.2.4.3 Data Analysis

The data analysis framework has not been defined yet. We are working to build a distributed model, where derived data samples are available locally and regionally, similar to the LHC experiments. Provision of samples of ProtoDUNE data and simulated samples for the technical design report (TDR) will help define the analysis models that are most useful to the collaboration. However, previous experience on the Tevatron experiments indicates that data analysis methods are often best designed by end-users rather than imposed by central software mandates.

3.3 Planning Inputs

3.3.1 Running Experiments

The Fermilab intensity frontier program experiments (MINOS[62], MINERνA[63], MicroBooNE[64] and NOνA[65]) have developed substantial computing infrastructure for the storage, reconstruction and analysis of data on size scales of order 5% that of full DUNE and comparable to the ProtoDUNE experiments. While the LArTPC technology requires unique algorithms, the underlying compute systems, frameworks and database structures already exist and are being adapted for use on both ProtoDUNE and DUNE.

For algorithms, the MicroBooNE[66] experiment has been running since 2015 with a LArTPC that shares many characteristics with the DUNE APAs. MicroBooNE has, over the past year, published studies of noise sources and signal processing [67, 68], novel pattern recognition strategies [69, 70] and calibration signatures such as Michel electrons and cosmic rays [71, 67]. DUNE shares both the LArSoft software framework and many expert collaborators with MicroBooNE and is taking direct advantage of their experience in developing simulations and reconstruction algorithms.

3.3.2 ProtoDUNE

The ProtoDUNE single and dual-phase experiments will run in the Fall of 2018. While the detectors themselves have only 4-5% of the channel count of the final far detectors, the higher beam rates (up to 100 Hz) and the presence of cosmic rays make the expected instantaneous data rates of 2.5 GB/sec from these detectors comparable to those from the full far detectors and similar to those expected for a near detector.

In addition, the entire suite of issues in transferring, cataloging, calibrating, reconstructing and analyzing these data are the same as for the full detectors and are driving the design and development of a substantial array of computing services necessary for both ProtoDUNE and DUNE.

Substantial progress is already being made on the infrastructure for computing, through a series of data challenges in late 2017 and early 2018. Development of reconstruction algorithms is currently restricted to simulation but is already informed by the experience with MicroBooNE data.

In summary, most of the important systems are already in place or are in development for full ProtoDUNE data analysis and should carry over to the full DUNE. We have indicated where infrastructure is in place in table 3.3.

3.3.2.1 Single-Phase ProtoDUNE

ProtoDUNE-SP utilizes six prototype anode plane assemblies with the full drift length envisioned for the final far detector. In the SP detector module, the readout planes are immersed in the LAr and no amplification occurs before the electronics. ProtoDUNE-SP is being constructed in the NP04 test beamline at CERN and should run with tagged beam for around six weeks in the fall of 2018. In addition cosmic ray commissioning beforehand and cosmic running after the end of beam are anticipated. Table 3.4 shows the anticipated data rates and sizes.

3.3.2.2 Dual-Phase ProtoDUNE

The ProtoDUNE-DP will either run in the NP02 beamline in late fall 2018, or run at high rate on cosmics soon thereafter. Given the most recent construction schedule for ProtoDUNE-DP is now likely that the collaboration will forgo beam data taking and focus on detector performance

Table 3.4: Parameters for the ProtoDUNE-SP run at CERN

Parameter	Value
Beam trigger rate	25 Hz
Cosmic trigger rate	1 Hz
Spill duration	2×4.5 s
SPS cycle	32 s
Average trigger rate	7.8 Hz
Readout time window	5.4 ms
# of APAs to be read out	6
Uncompressed single readout size (per trigger)	276 MB
Lossless compression factor	4
Instantaneous compressed data rate (in-spill)	1728 MB/s
Average compressed data rate	536 MB/s
Three-day buffer depth	300 TB
Planned total statistics of beam triggers in 42 beam days	18M
Planned overall storage size of beam events	1.25 PB
Requested storage envelope for ProtoDUNE-SP	5 PB at Fermilab, 1.5 PB at CERN

assessment with two charge-readout planes (CRPs) read out and cosmics only. ProtoDUNE-DP will then run with cosmics at a rate going from 20 to 100 Hz from late fall 2018 to at least April 2019. During six months of operation, with 50% efficiency, ProtoDUNE-DP is expected to collect about 300 million cosmic triggers at various rates, corresponing to a total data volume of 2.4 PB.

Table 3.5: Parameters for a six month ProtoDUNE-DP cosmic run at CERN

Parameter	Value
Trigger rate	20-100 Hz
CRPs read out	2
Uncompressed single readout size (per trigger)	80 MB
Lossless compression factor	10
Maximum data rate	≤800 MB/s
Cosmic rays over a 6 month run	300 M
Requested cosmic storage envelope for ProtoDUNE-DP	2.4 PB

3.3.3 Data Challenges

Computing and software is performing a series of data challenges to ensure that systems will be ready when the detectors become fully operational in the summer of 2018. To date we have performed challenges using simulated single and double-phase data and real data from cold-box

tests of single-phase electronics. DUNE anticipates average rates of $\sim$ 600 MB/sec but have set our design criteria at 2.5 GB/sec for data movement from the experiments to CERN Tier-0 storage and from there to Fermilab.

In data challenge 1.5 in mid-January 2018, dummy data based on non-zero-suppressed simulated events were produced at CERN's EHN1 and successfully transferred via 10-50 parallel transfers to the EOS (EOS) disk systems in the CERN Tier-0 data center at a sustained rate of 2 GB/sec. Transfers to dCache/Enstore at Fermilab achieved rates of 500 MB/sec.

Data challenge 2.0 was performed in early April 2018 is still being analyzed but preliminary estimated rates of 4 GB/sec from CERN's Experiment Hall North One (EHN1) to the tier-0 were achieved over several days. Rates to Fermilab disk cache were 2 GB/sec. Movement from FNAL disk cache to tape was substantially slower due to configuration for a lower number of drives than needed and contention for mounts with other running experiments. Fermilab is in the process of upgrading their tape facilities but we may require additional offsite buffer space if data rates from the experiments exceed the $\sim$ 600 MB/sec expected.

A subsample of the data was used for data quality monitoring at CERN and the full sample was reconstructed automatically on the grid using resources at multiple sites, including CERN. Our overall conclusion from this test is that most components for data movement and automated processing are in place. Remaining issues are integration of beam information, detector configuration and calibrations into the main processing stream, and faster tape access.

3.3.4 Monte Carlo Challenges

The collaboration has performed multiple Monte Carlo challenges to create samples for physics studies for the IDR and in preparation for the TDR in early 2019. In the last major challenge, MCC10 in early 2018, 17M events, taking up 252 TB of space were generated and catalogued automatically using the central DUNE production framework in response to requests by the Physics groups.

3.3.5 Reconstruction tests

Reconstruction tests have been performed on simulated single-phase ProtoDUNE test beam interactions with cosmic rays and an electronic noise simulation based on MicroBooNE experience. Hit finding and shaping is found to take around 2 minutes/event with a 2 GB memory footprint, leading to a reduction in data size of a factor of four. Higher-level pattern recognition occupies 10-20 minutes/event with a 4-6 GB memory footprint. For real data, calibration, electric field non-uniformities and other factors will likely raise the CPU needs per event. We will learn this when real data starts to arrive in late summer.

3.4 Resource Planning and Prospects

The DUNE computing effort relies heavily on the human and hardware resources of multiple organizations, with the bulk of hardware resources at CERN, and national facilities worldwide. The DUNE computing organization serves as an interface between the collaboration and those organizations. Computational resources are currently being negotiated on a yearly basis, with additional resources available opportunistically. Human assistance is largely on a per-project basis, with substantial support when needed but very few personnel as yet permanently assigned to the DUNE or ProtoDUNE efforts. We are working with the laboratories and funding agencies to identify and solidify multi-year commitments of dedicated personnel and resources for ProtoDUNE and DUNE, analogous to, but smaller than, those assigned to the LHC experiments. In-kind contributions of computing resources and people can also be an alternative way for institutions to make substantial contributions to DUNE.

The ProtoDUNE efforts in 2018-2019 will exercise almost all computing aspects of DUNE, although at smaller scale. Much of the infrastructure needed for full DUNE, in particular databases, grid configurations and code management systems need to be fully operational for ProtoDUNE. We believe that the systems in place (and tested) will be adequate for that purpose.

However, ProtoDUNE represents only 4-5% of the final volume of the far detectors and the near detector technology is, as yet, unknown. At the same time, computing technology is evolving rapidly with increased need for flexibility and the ability to parallelize codes. Liquid argon detectors, because of their reasonably simple geometry and image-like data, are already able to take advantage of parallelization and generic machine learning techniques. We have good common infrastructure such as the LArSoft suite and Geant4, and will have an excellent testbed with the ProtoDUNE data, but our techniques will need substantial adaption to scale to full DUNE and to take full advantage of new architectures. These scaling challenges are similar to those facing the LHC experiments as they move towards the High Luminosity LHC on a similar timescale. We look forward to working with them on shared solutions. Achieving full scale will be one of our major challenges – and one of our prime opportunities for collaboration – over the next five years.

Chapter 4

DUNE Calibration Strategy

The DUNE far detector (FD) presents a unique challenge for calibration in many ways. Not only because of its size—the largest liquid argon time-projection chamber (LArTPC) ever constructed – but also because of its depth. It differs both from existing long-baseline neutrino detectors, and existing LArTPCs (e.g. the deep underground location). While DUNE is expected to have a LArTPC as ND, DUNE is unlike previous long baseline experiments (MINOS, NOνA) in that the near detector will have significant differences (pile-up, readout) that may make extrapolation of detector characteristics non-trivial. Like any LArTPC, DUNE has the great advantage precision tracking and calorimetry, but, fully exploiting this capability requires a detailed understanding of the detector response. This challenge is driven by the inherently highly convolved detector response model and strong correlations that exist between various calibration quantities. For example, the determination of energy associated to an event of interest will depend on the simulation model, associated calibration parameters, non-trivial correlations between the parameters and spatial and temporal dependence of those parameters. These variations in parameters occur since the detector is not static. Changes can be abrupt (e.g. noise, a broken resistor in the field cage), or ongoing (e.g. exchange of fluid through volume, ion accumulation).

A convincing measurement of CP violation, or a resolution of the neutrino mass ordering, or supernova neutrino burst (SNB) detection will require a demonstration that the overall detector response is well understood. This chapter describes a strategy for detector calibration for both SP modules and DP modules using dedicated FD systems or existing calibration sources. A large portion of the calibration work reported here is done under the joint single-phase (SP) and dual-phase (DP) calibration task force formed in August 2017. Section 4.1 summarizes a calibration strategy currently envisioned for DUNE. The systematic uncertainties for the long baseline and low energy (supernova) program will determine how precisely each calibration parameter needs to be measured. For example, how precisely will the drift velocity need to be measured to know fiducial volume better than 1%? In general, the calibration program must provide measurements at the few percent or better level stably across an enormous volume and a long period of time. The calibration strategy must also provide sufficient redundancy in the measurement program.

Existing calibration sources for DUNE include beam or atmospheric neutrino-induced samples, cosmic rays, argon isotopes, and instrumentation devices such as liquid argon purity and tem-

perature monitors. It is important for calibration strategy to further separate these sources into those used to measure a response model parameter, and those used to test the response model. In addition to existing sources, external measurements prior to DUNE will validate techniques, tools and design of systems applicable to the DUNE calibration program; data from ProtoDUNE and SBND are essential to the success of the overall calibration program. Section 4.2 describes calibration from existing source of particles and external measurements.

Section 4.3 describes dedicated external calibration systems currently under consideration for DUNE to perform calibrations that cannot be achieved fully from existing sources or external measurements. All the systems proposed are currently being actively discussed in the calibration task force and were agreed as important systems by the DUNE collaboration. Under current assumptions, the calibration strategy and proposed calibration systems described in this document are applicable to both SP modules and DP modules. Finally, Section 4.4 provides a summary along with future steps for calibration and a path to the technical design report (TDR).

4.1 Calibration Strategy

DUNE has a broad physics program that includes long baseline neutrino oscillation physics, supernova physics, nucleon decay, and other searches for new physics. The physics processes that lead to the formation of these signals and the detector effects that influence their propagation must be carefully understood in order to perform adequate calibrations, as they ultimately affect the detector's energy response. Several other categories of effects can impact measurements of physical quantities such as the neutrino interaction model or reconstruction pathologies. These other effects are beyond the scope of the FD calibration effort and can only amplify the overall error budget. In the reminder of this section, we briefly describe the physics-driven calibration requirements, including the calibration sources and systems required for the different stages of the experiment.

4.1.1 Physics Driven Calibration Requirements

Long-baseline physics: In the physics volume of the DUNE CDR [72], Figure 3.23 shows that increasing the uncertainties on the ν_e event rate from 2% overall to 3% results in a 50% longer run period to achieve a 5σ determination of CP violation for 50% of possible values of charge-parity symmetry violation (CPV). The CDR also assumes that the fiducial volume is understood at the 1% level. Thus, calibration information needs to provide approximately 1-2% understanding of normalization, energy, and position resolution within the detector. Later studies [73] expanded the simple treatment of energy presented above. In particular, 1% bias on the lepton energy has a significant impact on the sensitivity to CPV. A 3% bias in the hadronic state (excluding neutrons) is important, as the inelasticity distribution for neutrinos and antineutrinos is quite different. A different fraction of the antineutrino's energy will go into the hadronic state. Finally, while studies largely consider a single, absolute energy scale, relative spatial differences across the enormous DUNE FD volume will need to be monitored and corrected; this is also true for changes that

occur in time. A number of in-situ calibration sources will be required to address these broad range of requirements. Michel electrons, neutral pions and radioactive sources (both intrinsic and external) are needed for calibrating detector response to electromagnetic activity in the tens to hundreds of MeV energy range. Stopping protons and muons from cosmic rays or beam interactions form an important calibration source for calorimetric reconstruction and particle identification. ProtoDUNE, as a dedicated test beam experiment, provides critical measurements to characterize and validate particle identification strategies in a 1 kt scale detector and will be an essential input to the overall program. Dedicated calibration systems, like lasers, will be useful to provide in-situ full volume measurements of electric field distortions. Measuring the strength and uniformity of the electric field is a key aspect of calibration, as estimates of calorimetric response and particle identification depend on electric field through recombination. The stringent physics requirements on energy scale and fiducial volume also put similarly stringent requirements on detector physics quantities such as electric field, drift velocity, electron lifetime, and the time dependences of these quantities.

Supernova burst and low-energy neutrino physics: For this physics, the signal events present specific reconstruction and calibration challenges and observable energy is shared between different charge clusters and types of energy depositions. Some of the primary requirements here include calibration of absolute energy scale and understanding and improving the nominal 20% energy resolution, important for resolving spectral features of SNB events, calibration of time and and light response of optical photon detectors, absolute timing of events and understanding of detector response to radiological backgrounds. Potential calibration sources in this energy range include Michel electrons from muon decays (successfuly utilized by ICARUS and MicroBooNE [71]), which have a well known spectrum up to $\sim$50 MeV. Radiological sources provide calibrations of photon, electron, and neutron response for energies below 10 MeV. It is more challenging to find "standard candles" between 50 MeV and 100 MeV, beyond cosmic-ray muon energy loss. ProtoDUNE could potentially be a test bed for various calibration strategies. One can imagine also ancillary studies of detector response using detectors such as LArIAT [74], MicroBooNE [66], and SBND [75].

Nucleon decay and other exotic physics: The calibration needs for nucleon decay and other exotic physics are comparable to the long-baseline (LBL) program as listed before. Signal channels for light dark matter and sterile neutrino searches will be neutral current interactions that are background to the LBL physics program. Based on the widths of dE/dx-based metrics of particle identification, qualitatively, we need to calibrate dE/dx across all drift and track orientations at the few percent level or better, which is a similar target of interest as the LBL effort.

Calibration Sources and Systems: Calibration sources and systems provide measurements of the detector response model parameters, or provide tests of the response model. Calibration measurements can also provide corrections applied to data, data-driven efficiencies, systematics and particle responses. Figure 4.1 shows the broad range of categories of measurements calibrations can provide and lists the critical calibration parameters for DUNE's detector response model applicable to both SP or DP. Due to the significant interdependencies of many parameters (e.g. recombination, electric field, liquid argon purity), a calibration strategy will either need to iteratively measure parameters, or find sources that break these correlations. Table 4.1 provides a list of various calibration sources and proposed calibration systems along with their primary usage which will comprise the currently envisioned nominal DUNE FD calibration design to adequately address the needs for physics. More details on each of the calibration sources and systems are provided in the

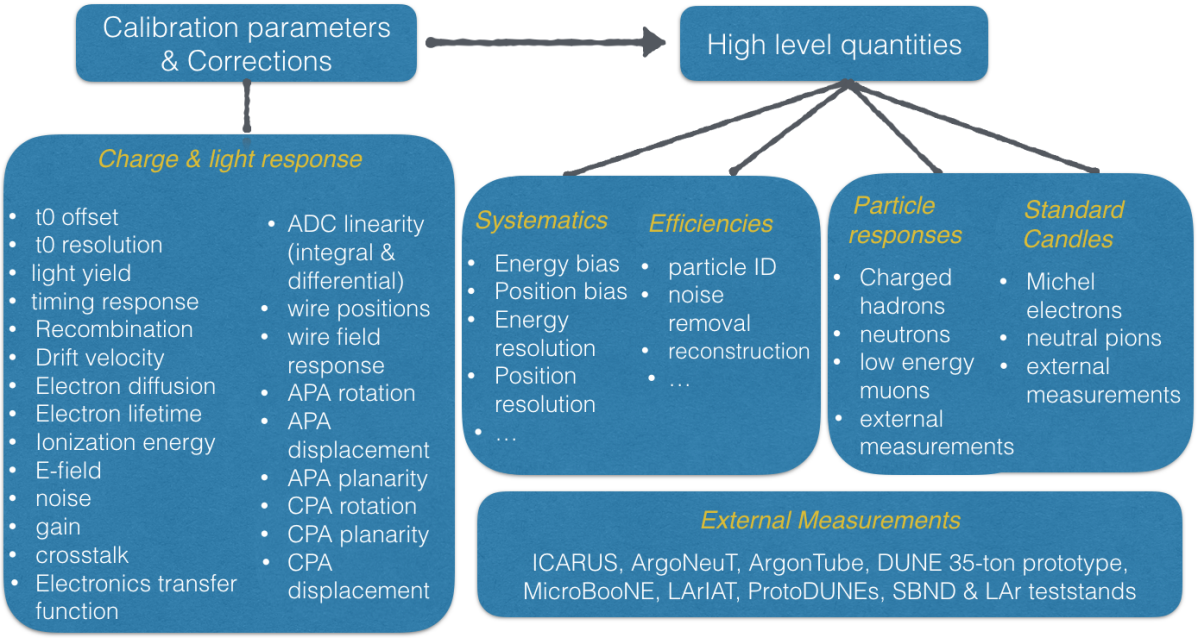

Figure 4.1: Categories of measurements provided by Calibration.

next sections. ProtoDUNE and previous measurements provide independent, tests of the response model, where the choice of parameterization and values correctly reproduces real detector data, however not all of the ex situ measurements will be directly extrapolatable to DUNE due to other detector effects and conditions. Only those that are believed to be universal (e.g., argon ionization energy) can be extrapolated. Also, while there are many existing calibration sources, each source comes with its own challenges. For example, electrons from muon decay (Michel electrons) are very useful to study the detector response to low-energy electrons (50 MeV). However, low-energy electrons present reconstruction challenges due to the loss of charge from radiative photons as demonstrated in MicroBooNE [71]. In terms of source category, Michel electrons are considered as an important, independent, and necessary test of the TPC energy response model, and not as a measurement of a particular response parameter.

4.1.2 A Staged Approach

The calibration strategy for DUNE will need to address the evolving operational and physics needs at every stage of the experiment in a timely manner using the primary sources and systems listed in Table 4.1. At the TDR stage, a clear and complete calibration strategy with necessary studies will be provided to demonstrate how the existing and proposed systems meet the physics requirements. Post-TDR, once the calibration strategy is set, necessary designs for calibration hardware along with tools and methods to be used with various calibration sources will need to be developed. To allow for flexibility in this process, the physical interfaces for calibration such as flanges or ports on the cryostat should be designed for a wide range of possible uses to accommodate the calibration hardware. As described in section 4.3.5, the calibration TF has made necessary accommodations for calibration systems for the SP module in terms of feedthrough penetration design and will soon

Table 4.1: Primary calibration systems and sources that comprise the nominal DUNE FD calibration design along with their primary usage.

System	Primary Usage
Existing Sources	**Broad range of measurements**
μ, predominantly from cosmic ray	Position (partial), angle (partial) velocity (timing), electron lifetime, wire response
Decay electrons, π^0 from beam, cosmic, atm ν	Test of electromagnetic response model
^{39}Ar	electron lifetime (x,y,z,t), diffusion
External Measurements	**Tests of detector model, calibration techniques and systems**
ArgoNeuT [76], ICARUS [77, 78, 79], MicroBooNE	Model parameters (e.g. recombination, diffusion)
DUNE 35 ton prototype [80]	Alignment and *t0* techniques
ArgonTUBE [81], MicroBooNE [66], SBND, ICARUS [82], ProtoDUNE [83]	Test of systems (e.g. Laser, external muon taggers)
ArgoNeuT [84], MicroBooNE [85, 86, 87, 71, 88, 76], ICARUS [89, 90, 91], ProtoDUNE	Test of calibration techniques and detector model (e.g., electron lifetime, Michel electrons, ^{39}Ar beta decays)
ProtoDUNE, LArIAT [74]	Test of particle response models and fluid flow models
LArTPC test stands [92, 93, 94, 95]	Light and LAr properties; signal processing techniques
Monitoring Systems	**Operation, Commissioning and Monitoring**
Purity Monitors	Electron lifetime
Photon Detection Monitoring System	photon detection system (PDS) response
Thermometers	Temperature, velocity; test of fluid flow model
Charge injection	Electronics response
Proposed Systems	**Targeted (near) independent, precision calibration**
Direct ionization via laser	Position, angle, electric field (x,y,z,t)
Photoelectric ejection via laser	Position, electric field (partial)
Radioactive source deployment	Test of SN signal model
Neutron injection	Test of SN signal, neutron capture model
External Muon Tracker	Position, angle, muon reconstruction efficiency

start finalizing the design and accommodations for calibration penetrations for the DP module.

As DUNE physics turns on at different rates and times, a calibration strategy at each stage for physics and data taking is described below. This strategy assumes that all systems are commissioned and deployed according to the nominal DUNE run plan.

Commissioning: When the detector is filled, data from various instrumentation devices will be needed to validate the argon fluid flow model and purification system. When the detector is filled and at desired high voltage, the detector immediately becomes live for supernovae and proton decay signals (beam and atmospheric neutrino physics will require a few years of data accumulation) at which stage it is critical for early calibration to track the space-time dependence of the detector. Noise data (taken with wires off) and pulser data (taken with signal calibration pulses injected into electronics) will be needed to understand the detector electronics response. Essential systems at this stage include temperature monitors, purity monitors, HV monitors, robust front-end charge injection system for cold electronics, and a PDS monitoring system for light. Additionally, as the ^{39}Ar data will be available immediately, readiness (in terms of reconstruction tools and methods) to utilize ^{39}Ar decays will be needed, both for understanding low energy response and space-time uniformity. External calibration systems as listed in Table 4.1 will be deployed and commissioned at this stage and commissioning data from these systems will be needed to verify expected configuration for each system and any possible adjustments needed to tune for data taking.

Early data taking: Since DUNE will not have all in-situ measurements of liquid argon properties at this stage, early calibration of the detector will utilize liquid argon physical properties from ProtoDUNE or SBND, and E fields from calculations tuned to measured HV. This early data will most likely need to be recalibrated at a later stage when other data sets become available. This is expected to improve from in-situ measurements as data taking progresses and with dedicated calibration runs. The detector response models in simulation will need to be tuned on ProtoDUNE and/or SBND data during this early phase, and the mechanism for performing this tuning needs to be ready. This together with cosmic ray muon analysis will provide an approximate energy response model that can be used for early physics. Analysis of cosmic ray muon data to develop methods and tools for muon reconstruction from MeV to TeV and a well-validated cosmic ray event generator with data will be essential for early physics. Cosmic ray or beam induced muon tracks tagged with an external muon tracker system will be very useful in these early stages to independently measure and benchmark muon reconstruction performance and efficiencies in the FD. Dedicated early calibration runs from external calibration systems will be needed to develop and tune calibration tools to data taking and correct for any space-time irregularities observed in the TPC system for early physics. Given the expected low rate of cosmic ray events at the underground location (see Section 4.2), calibration with cosmic rays are not possible over short time scales and will proceed from coarse-grained to fine-grained over the course of years as statistics is accumulated. The experiment will have to rely on external systems such as laser for calibrations that require an independent probe with reduced or removed interdependencies, fine-grained measurements (both in space and time) and detector stability monitoring in the time scales needed for physics. Additionally some measurements are not possible with cosmic rays (e.g. APA flatness or global alignment of all APAs).

Stable operations: Once the detector conditions are stabilized and the experiment is under

stable running, dedicated calibration runs, ideally before, during and after each run period, will be needed to ensure detector conditions have not significantly changed. As statistics are accumulated, standard candle data samples (e.g. Michel electrons and neutral pions) both from cosmic rays, beam induced and atmospheric neutrinos can be used to validate and improve the detector response models needed for precision physics. As DUNE becomes systematics limited, dedicated calibration campaigns using the proposed external systems will become crucial for precision calibration to meet the stringent physics requirements both for energy scale reconstruction and detector resolution. For example, understanding electromagnetic (EM) response in the FD will require both cosmic rays and external systems. The very high energy muons from cosmic rays at that depth that initiate EM showers (which would be rare at ProtoDUNE or SBND), will provide information to study EM response at high energies. External systems such as radioactive sources or neutron injection sources will provide low energy EM response at the precision required for low energy supernovae physics. Other calibration needs not addressed with existing sources and external systems, will be determined initially from the output of the ProtoDUNE and/or SBND program, and later from the DUNE ND if the design choice will be a LArTPC.

4.2 Inherent Sources and External Measurements

Existing sources of particles, external measurements and monitors are an essential part of the DUNE FD calibration program which we briefly summarize here.

Existing sources: Cosmic rays and neutrino-induced interactions provide commonly used "standard candles" like electrons from muon and pion decays, and neutral pions, which have characteristic energy spectra. Cosmic ray muons are also used to determine detector element locations (alignment), timing offsets or drift velocity, electron lifetime, and channel-by-channel response. The rates for cosmic rays events are summarized in Table 4.2, and certain measurements (e.g. channel-to-channel gain uniformity and cathode panel alignment) are estimated to take several months of data. The rates for atmospheric ν interactions can be found in Table 2.2 and are comparable to beam-induced events; both atmospheric and beam induced interactions do not have sufficient rates to provide meaningful spatial or temporal calibration and are expected to provide supplemental measurements only. Also, beam neutrinos may not contribute to the first module calibration during early data taking as the beam is expected to arrive later. The reconstructed energy spectrum of ^{39}Ar beta decays can be used to make a spatially and temporally precise electron lifetime measurement. It can also provide other necessary calibrations, such as measurements of wire-to-wire response variations and diffusion measurements using the signal shapes associated with the beta decays. The ^{39}Ar beta decay rate in commercially provided argon is about $1\,\mathrm{Bq\,kg^{-1}}$, so $O(50\mathrm{k})$ ^{39}Ar beta decays are expected in a single 5 ms event readout in an entire 10 kt detector module. The ^{39}Ar beta decay cut-off energy is 565 keV which is close to the energy deposited on a single wire by a minimum ionizing particle (MIP). However, there are several factors that can impact the observed charge spectrum from ^{39}Ar beta decays such as electronics noise, electron lifetime and recombination fluctuations.

Monitors: Several instrumentation and detector monitoring devices discussed in detail in Chapter 8 of Volume 2: Single-Phase Module and Volume 3: Dual-Phase Module of the interim design

Table 4.2: Annual rates for classes of cosmic-ray events described in this section assuming 100% reconstruction efficiency. Energy, angle, and fiducial requirements have been applied. Rates and geometrical features apply to the single-phase far detector design.

Sample	Annual Rate	Detector Unit
Inclusive	1.3×10^6	Per 10 kt module
Vertical-Gap crossing	3300	Per gap
Horizontal-Gap crossing	3600	Per gap
APA-piercing	2200	Per APA
APA-CPA piercing	1800	Per active APA side
APA-CPA piercing, CPA opposite to APA	360	Per active APA side
Collection-plane wire hits	3300	Per wire
Stopping Muons	11000	Per 10 kt module
π^0 Production	1300	Per 10 kt module

report (IDR) will provide valuable information for early calibrations and to track the space-time dependence of the detector. The instrumentation devices include liquid argon temperature monitors, LAr purity monitors, gaseous argon analyzers, cryogenic (cold) and inspection (warm) cameras, and liquid level monitors. The computational fluid dynamics (CFD) simulations play a key role for calibrations initially in the design of the cryogenics recirculation system, and later for physics studies when the cryogenics instrumentation data is used to validate the simulations. Other instrumentation devices essential for calibration such as drift high voltage (HV) current monitors and external charge injection systems are discussed in detail in Chapters 4 and 5, respectively, of Volume 2: Single-Phase Module and Volume 3: Dual-Phase Module of the IDR, respectively.

External measurements: External measurements here include both past measurements (e.g., ArgoNeuT, DUNE 35 ton prototype, MicroBooNE, ICARUS, SBND, LArIAT), anticipated measurements from ongoing and future experiments (e.g., MicroBooNE, ProtoDUNE) as well as from small scale LArTPC test stands. External measurements provide a test bed for proposed calibration hardware systems and techniques which are applicable to the DUNE FD. In particular, ProtoDUNE will provide validation of the fluid flow model using instrumentation data. Early calibration for physics in DUNE will utilize liquid argon physical properties from ProtoDUNE or SBN for tuning detector response models in simulation. Table 4.1 provides references for specific external measurements. The usability of ^{39}Ar has been demonstrated with MicroBooNE data. Use of ^{39}Ar and other radiological sources, including the DAQ readout challenges associated with their use, will be tested on the ProtoDUNE detectors. Proposed systems for DUNE, including the laser system below, are part of the MicroBooNE and SBND programs which will provide increased information of the use of the system and optimization of the design. Measurements from small-scale liquid argon test stands can also provide valuable information for DUNE. The liquid argon test stand planned at Brookhaven National Lab will provide important information for how field response is simulated and calibrated at DUNE.

Remaining Studies: In advance of the TDR, studies will be done to clarify the physics use limitations of the various sources presented in this section. For example, quantification of what can be achieved for electron lifetime measurements and the overall energy scale calibration from cosmic

rays, ^{39}Ar beta decays, long baseline interactions and atmospheric neutrinos, in terms of spatial and temporal granularity using decay electrons, π^0 samples; determining the relative importance of electromagnetic shower photons below pair production threshold. It is expected that combinations of information from cosmic-ray events with proposed and existing systems (laser-based, neutrino-induced events, and dedicated muon systems) will reduce the total uncertainties on mis-alignment. The impact of misalignments on the physics case needs to be studied, especially for alignment modes which are weakly constrained due to cosmic ray direction, as shown in Figure 4.2, including global shifts and rotations of all detector elements, and crumpling modes where the edges of the anode plane assemblies (APAs) hold together but angles are slightly different from nominal. The impact of the fluid model on physics needs require quantification via CFD simulations (e.g., overall temperature variation in the cryostat and impact on drift velocity; overall impurity variation across the detector module, and impact on energy scale especially for DP which has a 12 m long single drift path). The CFD studies will also be important in understanding how LAr flow can impact space charge from both ionization and non-ionization sources and ion accumulation (both positive and negative ions), separately for SP module and DP module designs.

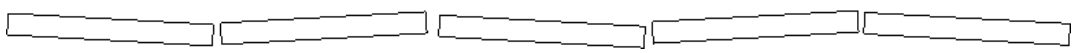

Figure 4.2: An example of a distortion that may be difficult to detect with cosmic rays. The APA frames are shown as rotated rectangles, as viewed from the top.

4.3 Proposed Systems

The nominal calibration design includes the existing sources, external measurements, and monitors listed in the previous section, and the following proposed systems: laser (Section 4.3.1), radioactive source deployment (Section 4.3.2), neutron injection (Section 4.3.3), and external muon tracker (Section 4.3.4). While the systems described previously are necessary they are not sufficient for the entire DUNE calibration program. The proposed systems discussed here are motivated as they supply necessary information beyond the reach of the existing systems.

4.3.1 Laser Systems

None of the systems discussed in the previous section can provide an independent, fine-grained estimate of the E field in space or time, which is a critical parameter for physics signals as it ultimately impacts the spatial resolution and energy response of the detector. The primary purpose of a laser system is to provide such a measurement. There are multiple sources which may distort the electric field temporally or spatially in the detector. Current simulation studies indicate that positive ion accumulation and drift (space charge) due to ionization sources such as cosmic rays or ^{39}Ar is small in the DUNE FD; however, not enough is known yet about the fluid flow pattern in the FD to exclude the possibility of stable eddies which may amplify the effect for both SP and DP modules. This effect can get further amplified significantly in DP module due to ion accumulation at the liquid-gas interface. Additionally, other sources in the detector (especially detector imperfections) can cause E field distortions. For example, field cage resistor failures,

non-uniform resistivity in the voltage dividers, CPA misalignment, CPA structural deformations, and APA and CPA offsets and deviations from flatness can create localized E field distortions. Each individual E field distortion may add in quadrature with other effects, and can reach 4% under certain conditions. Understanding all these effects require in-situ measurement of E field for proper calibration. Many useful secondary uses of laser include alignment (especially modes that are weakly constrained by cosmic rays; see Figure 4.2), stability monitoring, and diagnosing detector failures (e.g., HV).

Two laser-based systems have been considered to extract the electric field map. They fall into two categories: photoelectron from the LArTPC cathode and direct ionization of the liquid argon (LAr), both driven by a 266 nm laser system. The reference design uses direct ionization laser light with multiple laser paths, as it can provide field map information in (x, y, z, t); photoelectron only provides integral field across the drift. An ionization-based system has been used in the ARGONTUBE [96], MicroBooNE, CAPTAIN, and SBND experiments. Assuming multiple, steerable laser entry points as discussed in Section 4.3.5, the ionization-based system can characterize the electric field with fewer dependencies compared to other systems. Two "laser tracks" that cross in a detector volume element can be used to estimate the local E field in that volume. If two tracks enter the same spatial voxel ($10 \times 10 \times 10$ cm^3 volume) in the detector module, the relative position of the tracks provides an estimate of the local 3D E field. A scan of the full detector using 1 L volume elements would take a day, but it is expected that practically shorter runs could be done to investigate specific regions. The deviation from straighness of single "laser tracks" can also be used to constrain local E fields. The direct ionizing laser system may also be used to create photoelectrons from the cathode, even under low power operation.

A photoelectron-based calibration system was used in the T2K gaseous (predominantly Ar), TPCs [97]. Thin metal surfaces placed at surveyed positions on the cathode provided point-like and line sources of photoelectrons when illuminated by a laser. The T2K photoelectron system provided measurements of adjacent electronics modules' relative timing response, drift velocity with few ns resolution of 870 mm drift distance, electronics gain, transverse diffusion, and an integrated measurement of the electric field along the drift direction. For DUNE, the system would be similarly used as on T2K to diagnose electronics or TPC response issues on demand, and provide an integral field measurement and relative distortions of y, z positions with time, and of either x or drift velocity. Ejection of photoelectrons from the direct ionization laser system has also been observed, so it is likely this is a reasonable addition to the nominal design.

The remaining studies for the laser systems to be done prior to the TDR are:

- Determine a nominal design for photoelectric thin metal surfaces on the cathode. A survey in cold conditions is not possible for the SP system, and the photoelectric system could provide both known positions in the detector and information complementary to a survey or cosmic data.

- For the DP system, quantify the additional benefit of a photoejection system since it will be possible to survey the charge-readout planes (CRPs) externally under cold conditions.

- Determine whether the known classes of possible E field distortions warrant a mechanical penetration of the field cage (FC) (versus reduced sampling from projecting laser light inward

between FC elements) and further understand sensitivity of the laser to realistic E field distortions.

- Continue to study the range of possible E field distortions in order to further refine the estimation of overall variation of the E field in the detector module.

4.3.2 Radioactive Source Deployment System

Radioactive source deployment provides an in-situ source of the electrons and de-excitation gamma rays, which are directly relevant for physics signals from supernova or ^8B solar neutrinos. Secondary measurements from the source deployment include electromagnetic (EM) shower characterization for long-baseline ν_e CC events, electron lifetime as a function of detector module vertical position, and help determine radiative components of the electron energy spectrum from muon decays.

A composite source can be used that consists of ^{252}Cf, a strong neutron emitter, and ^{58}Ni, which, via the ^{58}Ni(n,γ)^{59}Ni process, converts one of the ^{252}Cf decay neutrons, suitably moderated, to a monoergetic 9 MeV photon [98]. The source is envisaged to be inside a cylindrical teflon moderator with mass of about 10 kg and a diameter of 20 cm such that it can be deployed via the multipurpose instrumentation ports discussed in Section 4.3.5. The activity of the radioactive source is chosen such that no more than one 9 MeV capture γ-event occurs during a single drift period. This allows one to use the arrival time of the measured light as a $t0$ and then measure the average drift time of the corresponding charge signal(s). This restricts the maximally permissible rate of 9 MeV capture γ-events occurring inside the radioactive source to be less than 1 kHz, given a spill-in efficiency into the active LAr of less than 10%. The sources would be deployed outside the FC within the cryostat to avoid regions with high electric field. Sources would be removed and stored outside the cryostat when not in use.

Assuming stable detector conditions, a radioactive source would be deployed every half year, before and after a given run period. If stability fluctuates for any reason (e.g., electronic response changes over time) at a particular location, it is desirable to deploy the source at that location once a month, or more often, depending on how bad the stability is. It would take of order eight hours to deploy the system at one feedthrough location, and a full radioactive source calibration campaign might take a week.

For the TDR, continued development of geometry and simulation tools of radioactive source system is necessary to demonstrate the usage of these sources, including studies of various radiological contaminants on detector response, and source event rate and methods to suppress them. In addition, a test will be performed at South Dakota School of Mines and Technology. A radioactive source deployment in a potential phase 2 of ProtoDUNE could be envisaged to demonstrate proof of principle of the radioactive source deployment. However, studies need to be performed to first understand how cosmic rays can be vetoed sufficiently well for a radioactive source measurement.

4.3.3 Pulsed Neutron Source

An external neutron generator system would provide a triggered, well defined neutron energy deposition that can be detected throughout the volume. Neutron capture is a critical component of signal processes for SNB and LBL physics.

A triggered pulse of neutrons can be generated outside the TPC, then injected via a dedicated opening in the insulation into the LAr, where it spreads through the entire volume to produce monoenergetic photons via the ^{40}Ar(n,γ)^{41}Ar capture process. The uniform population of neutrons throughout the detector module volume exploits a remarkable property of argon – the near transparency to neutrons with an energy near 57 keV due to a deep minimum in the cross section caused by the destructive interference between two high-level states of the ^{40}Ar nucleus. This cross section "anti-resonance" is about 10 keV wide, and 57 keV neutrons consequently have a scattering length of 859 m. For neutrons moderated to this energy the DUNE LArTPC is essentially transparent. The 57 keV neutrons that do scatter quickly leave the anti-resonance and thermalize, at which time they capture. Each neutron capture releases exactly the binding energy difference between ^{40}Ar and ^{41}Ar, about 6.1 MeV in the form of gamma rays.

The fixed, shielded deuterium-deuterium (DD) neutron generator would be located above a penetration in the hydrogenous insulation. Of order 100 μs pulse width commercially available DD generators exist that are about the size of a thermos bottle, and are cost competitive. Between the generator and the cryostat, layers of water or plastic and intermediate fillers will be included for sufficient degradation of the neutron energy. Initial simulations indicate that a single neutron injection point would illuminate the entire volume of one of the ProtoDUNE detectors and would be rapid (likely less than 30 min).

The remaining studies for the TDR for the external neutron source include an assessment of the full design: degrader materials, shielding, and the space and mounting (weight) considerations above the cryostat. Detailed simulation studies to understand the neutron transport process will be performed. In addition, the neutron capture gamma spectrum is also being characterized. In Nov 2017, the ACED[99] Collaboration took several hundred thousand neutron capture events at the DANCE[100] facility at LANSCE which will be used to prepare a database of the neutron capture gamma cascade chain.

4.3.4 External Muon Tracker

A external muon tracker (EMT), a dedicated fast tracking system, would provide track position, direction, and time information independent of TPC and PDS systems.

Rock muons from beam interactions in the rock surrounding the cryostat have similar energy and angular spectrum as CC ν_μ events. A nominal design of the EMT would cover the front face of the detector (approximately 14m $\times$ 12m) to provide an estimate of the initial position, and the time for a subset of these events, independent of the TPC and PDS systems. A second, similarly sized panel, 1 m away from the cryostat would provide directional information. Additional measurements

are possible elsewhere in the detector if the system is portable; it could be positioned on top of the cryostat to capture (nearly downward-going) cosmic rays during commissioning, or positioned along the side for rock muon-induced tracks along the drift direction. The EMT pixelization will be small enough that rock-muon statistics will allow determination of the center of each pixel to the same resolution as that expected for the detector (roughly 1 cm). So, for example, even with 50 one-cm-sized pixels, with about 1000 rock muons per year passing through the EMT, the achievable precision on average for the incident position (before subsequent multiple scattering) is about 5 mm.

The remaining studies for the EMT system prior to the TDR include continued study of the precision with which the EMT (including panels on the sides and bottom) can determine biases or other problems with the detector model. Optimization of EMT size and pixelization and possible cost-saving options including re-use of existing scintillators (e.g. MINOS) or counter systems (e.g., ProtoDUNE or SBN) will be investigated. The available space for the EMT around the cryostat needs more investigation. A plan for surveying the EMT relative to the anode plane assemblies also needs to be developed, to be coordinated with the APA consortium; error in such a survey could be misinterpreted as a reconstruction bias.

4.3.5 Configuration of Proposed Systems

The current cryostat design for the SP detector module with multi-purpose cryostat penetrations for various sub-systems is shown in Figure 4.3. The penetrations dedicated for calibrations are highlighted in black ovals. The placement of these penetrations is largely driven by the ionization track laser and radioactive source system requirements but would be usable for the neutron system as well. The ports that are closer to the center of the cryostat are placed near the anode plane assemblies (similarly to what is planned for SBND) to minimize any risks due to the HV discharge. For the far east and west ports, HV is not an issue as they are located outside the FC and the penetrations are located near mid-drift to meet radioactive source requirements.

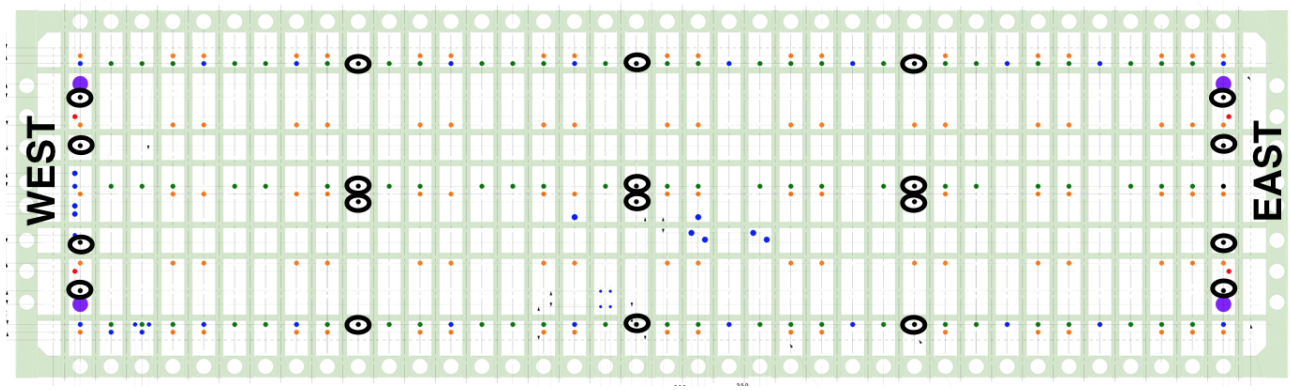

Figure 4.3: Top view of the SP module cryostat showing various penetrations. Highlighted in black ovals are multi-purpose calibration penetrations. The green ports are TPC signal cable penetrations. The orange ports are DSS penetrations. The blue ports are cryogenics penetrations. The larger purple ports at the four corners of the cryostat are human access tunnels.

Implementation of the ionization laser system, proposed in Section 4.3.1, requires 20 feedthroughs

to cover the four TPC drift volumes; this arrangement would provide (almost) full volume calibration of the electric field and associated diagnostics (e.g. HV). The crossing laser tracks are necessary to unambiguously construct the field map. A steerable plastic insulator laser head and fiber interface would be mounted on top of the cryostat in the feedthrough. Two options are under investigation: (1) the FC (but not the ground plane or the active volume) is penetrated, and (2) the FC is not penetrated. In the former case, the FC penetration has been shown to create a small distortion to the E field, for the benefit of full volume E field mapping. When the FC is not penetrated, the laser shines through the FC tubes, producing some regions that are not mappable by the laser, and it will not be possible to map the position of the track start making the analysis more difficult. This is the case for laser system which use the far east and west ports. The necessity of penetrating the FC has not been fully assessed yet. The photoelectron system would employ fixed fibers, and would not require a steering mechanism or mechnical FC penetrations.

The distance between any two consecutive feedthrough columns in Figure 4.3 is about 15 m, a plausible distance for the laser beam to travel. The maximum distance light would travel to the bottom corner of the detector, would be approximately 20 m. Direct-ionization tracks have been demonstrated at a maximum possible distance in MicroBooNE of 10 m. The Rayleigh scattering of the laser light is about 40 m, but additional optics effects, including self-focusing (Kerr) effects may limit the maximum practical range. Assuming these are not a limitation, this laser arrangement could illuminate the full volume with crossing track data. It is important to note that at this point in time, a maximum usable track length is unknown and it is possible that the full 60 m detector module length could be achieved by the laser system after optimization.

The calibration group focused on finalizing the cryostat penetrations for the SP detector module driven by the cryostat design timeline. A similar exercise will be done to finalize DP detector module penetrations for calibrations in the near future.

4.4 Summary

The physics requirements for the broad DUNE physics program places stringent requirements on calibration systems and sources. The aim of the upcoming TDR will be to demonstrate that the proposed calibration systems, in conjunction with existing sources, external measurements and monitors, will be sufficient for DUNE's calibration requirements. The proposed systems discussed here have been identified as important to DUNE's physics program. However, the multi-purpose ports also enable deployment of other possible calibrations systems in the future.

The calibration group has started establishing relevant connections to physics working groups and consortia as appropriate. The calibration group has started collaborating with the long-baseline physics group to develop the necessary tools and techniques to propagate detector physics effects into oscillation analyses and similar effort will occur to connect with other physics groups. The calibration group has also started working closely with the consortia and identified liaisons for each to ensure that calibration needs are strongly considered as each consortium develops its designs. For example, a preliminary list of DAQ calibration requirements are already in process and will be finalized in the coming months.

The calibration systems for DUNE, as presented in this document, will be further discussed and developed for the TDR within DUNE's management structure. Two options are currently favored for calibration, (1) formation of a new calibration consortium, or (2) inclusion of calibration in the cryogenic instrumentation and slow controls (CISC) consortium. This decision will depend on the scope of the proposed calibration systems presented in this document. The goal is to make and execute this decision in June 2018, shortly after the final IDR submission. The full design development for each calibration system, along with costing and risk mitigation, will follow.

Table 4.3: Key calibration milestones leading to first detector installation.

Date	Milestone
May 2018	IDR
June 2018	Finalize process of integrating calibration into consortium structure
Jan. 2019	Design validation of calibration systems using ProtoDUNE/SBN data (where applicable) and incorporate lessons learned into designs
Apr. 2019	Technical design report
Sep. 2022	Finish construction of calibration systems for Cryostat #1
May 2023	Cryostat 1 ready for TPC installation
Oct. 2023	All calibration systems installed in Cryostat #1

Glossary

35 ton prototype The 35 ton prototype cryostat and single-phase (SP) detector built at Fermilab before the ProtoDUNE detectors. 49, 52

analog-to-digital converter (ADC) A sampling of a voltage resulting in a discrete integer count corresponding in some way to the input. 18

anode plane assembly (APA) A unit of the SP detector module containing the elements sensitive to ionization in the LAr. It contains two faces each of three planes of wires, and interfaces to the cold electronics and photon detection system. 11, 34, 41, 53, 57

art A software framework implementing an event-based execution paradigm. 38

ASIC application-specific integrated circuit. 18

conceptual design report (CDR) A formal project document that describes the experiment at a conceptual level. 7, 16–18

cold electronics (CE) Refers to readout electronics that operate at cryogenic temperatures. 11

conventional facilities (CF) Pertaining to construction and operation of buildings or caverns and conventional infrastructure. 5, 13

cryogenic instrumentation and slow controls (CISC) A DUNE consortium responsible for the cryogenic instrumentation and slow controls components. 12, 59

CPT product of charge, parity and time-reversal transformations. 4, 17

charge-parity symmetry violation (CPV) Lack of symmetry in a system before and after charge and parity transformations are applied. 3, 4, 19, 46

charge parity (CP) Product of charge and parity transformations. 4

charge-readout plane (CRP) In the DP technology, a collection of electrodes in a planar arrangement placed at a particular voltage relative to some applied E field such that drifting electrons may be collected and their number and time may be measured. 12, 42, 54

data acquisition (DAQ) The data acquisition system accepts data from the detector FE electronics, buffers the data, performs a trigger decision, builds events from the selected data and delivers the result to the offline secondary DAQ buffer. 12, 33, 35, 37, 39

detector module The entire DUNE far detector is segmented into four modules, each with a nominal 10 kt fiducial mass. 8, 12, 13, 34, 54, 55, 63

secondary DAQ buffer A secondary DAQ buffer holds a small subset of the full rate as selected by a trigger command. This buffer also marks the interface with the DUNE Offline. 61

DP module dual-phase detector module. 7, 8, 33, 45, 46, 50, 53

dual-phase (DP) Distinguishes one of the DUNE far detector technologies by the fact that it operates using argon in both gas and liquid phases. i, 6, 33, 36, 37, 45, 47, 53

detector support system (DSS) The system used to support the SP detector within the cryostat. 57

DUNE Deep Underground Neutrino Experiment. 33–35, 37–41, 43, 44

Experiment Hall North One (EHN1) Location at CERN of the ProtoDUNE experiments. 43

EOS (EOS) The XRootD based distributed file system developed by CERN. 43

field cage (FC) The component of a LArTPC that contains and shapes the applied E field. 54, 55, 57, 58

far detector (FD) Refers to the 40 kt fiducial mass DUNE detector to be installed at the far site at SURF in Lead, SD, to be composed of four 10 kt modules. 3, 4, 6, 7, 11–13, 33, 34, 37, 45, 46, 53

GEometry ANd Tracking, version 4 (Geant4) A software toolkit for the simulation of the passage of particles through matter using Monte Carlo methods. 18, 38, 44

Generates Events for Neutrino Interaction Experiments (GENIE) Software providing an object-oriented neutrino interaction simulation resulting in kinematics of the products of the interaction. 18

HPC high-performance computing facilities; generally computing facilities emphasizing parallel computing with aggregate power of more than a teraflop. 40

high voltage (HV) Generally describes a voltage applied to drive the motion of free electrons through some media. 12, 52, 54, 57

LArSoft Liquid Argon Software (LArSoft), a shared base of physics software across LArTPC experiments. 37, 38, 40, 44

liquid argon time-projection chamber (LArTPC) A class of detector technology that forms the basis for the DUNE far detector modules. It typically entails observation of ionization activity by electrical signals and of scintillation by optical signals. 33, 45, 49, 52, 56

liquid argon (LAr) The liquid phase of argon. 33, 54–56

long-baseline (LBL) Refers to the distance between the neutrino source and the far detector. It can also refer to the distance between the near and far detectors. The "long" designation is an approximate and relative distinction. For DUNE, this distance (between Fermilab and SURF) is approximately 1300 km. 3, 47, 56

Long-Baseline Neutrino Facility (LBNF) The organizational entity responsible for developing the neutrino beam, the cryostats and cryogenics systems, and the conventional facilities for DUNE. 34

mass hierarchy (MH) Describes the separation between the mass squared differences related to the solar and atmospheric neutrino problems. 20–23, 26

MicroBooNE The LArTPC-based MicroBooNE neutrino oscillation experiment at Fermilab. 34, 35, 37, 38, 40, 41, 43, 47, 48, 52, 54

MINERνA The MINERνA neutrino cross sections experiment at Fermilab. 34, 40

minimum ionizing particle (MIP) Refers to a momentum traversing some medium such that the particle is losing near the minimum amount of energy per distance traversed. 51

NOνA The NOνA off-axis neutrino oscillation experiment at Fermilab. 38, 40, 45

ProtoDUNE-DP The DP ProtoDUNE detector. i, 8, 41, 42

ProtoDUNE-SP The SP ProtoDUNE detector. i, 8, 41, 42

photon detection system (PDS) The detector subsystem sensitive to light produced in the LAr. 12, 18, 49

ProtoDUNE Either of the two DUNE prototype detectors constructed at CERN and operated in a CERN test beam (expected fall 2018). One prototype implements SP and the other DP technology. 8, 12, 25, 30, 33, 35, 37–44, 46–52, 56, 57, 59, 60

ROI region of interest. 34

S/N signal-to-noise (ratio). 34

sequential access via metadata (SAM) A data-handling system to store and retrieve files and associated metadata, including a complete record of the processing that has used the files. 38

supernova neutrino burst (SNB) A prompt increase in the flux of low-energy neutrinos emitted in the first few seconds of a core-collapse supernova. It can also refer to a trigger command type that may be due to an SNB, or detector conditions that mimic its interaction signature. 3, 28, 36, 45, 47, 56

SP module single-phase detector module. iii, 7, 8, 33, 35, 36, 45, 46, 48, 53, 57

single-phase (SP) Distinguishes one of the DUNE far detector technologies by the fact that it operates using argon in its liquid phase only . i, 6, 33, 36, 37, 45, 47, 60

technical design report (TDR) A formal project document that describes the experiment at a technical level. 4, 7, 8, 10, 12–14, 17–19, 40, 43, 46, 52, 54–57, 63

interim design report (IDR) An intermediate milestone on the path to a full technical design report (TDR). 3, 4, 6, 7, 12, 13, 18, 33, 35, 36, 43, 51, 52, 59

trigger candidate Summary information derived from the full data stream and representing a contribution toward forming a trigger decision. 63

trigger command Information derived from one or more trigger candidates that directs elements of the detector module to read out a portion of the data stream. 61, 63

trigger decision The process by which trigger candidates are converted into trigger commands. 61, 63

WA105 DP demonstrator The $3 \times 1 \times 1\,\mathrm{m}^3$ WA105 dual-phase prototype detector at CERN. 7, 34

work breakdown structure (WBS) An organizational project management tool by which the tasks to be performed are partitioned in a hierarchical manner. 12

References

[1] DOE Office of High Energy Physics, "Mission Need Statement for a Long-Baseline Neutrino Experiment (LBNE)," tech. rep., DOE, 2009. LBNE-doc-6259.

[2] P. Derwent *et al.*, "Proton Improvement Plan-II." `http://projectx-docdb.fnal.gov/cgi-bin/RetrieveFile?=1232&filename=1.2%20MW%20Report_Rev5.pdf&version=3`, 2013.

[3] Particle Physics Project Prioritization Panel, "US Particle Physics: Scientific Opportunities; A Strategic Plan for the Next Ten Years," 2008. `http://science.energy.gov/~/media/hep/pdf/files/pdfs/p5_report_06022008.pdf`.

[4] S. Gardiner, B. Svoboda, C. Grant, and E. Pantic, "MARLEY (Model of Argon Reaction Low Energy Yields),".

[5] P. Antonioli, C. Ghetti, E. V. Korolkova, V. A. Kudryavtsev, and G. Sartorelli, "A Three-dimensional code for muon propagation through the rock: Music," *Astropart. Phys.* **7** (1997) 357–368, `arXiv:hep-ph/9705408 [hep-ph]`.

[6] V. A. Kudryavtsev, "Muon simulation codes MUSIC and MUSUN for underground physics," *Comput. Phys. Commun.* **180** (2009) 339–346, `arXiv:0810.4635 [physics.comp-ph]`.

[7] R. Veenhof, "GARFIELD, recent developments," *Nucl. Instrum. Meth.* **A419** (1998) 726–730.

[8] L. W. Nagel and D. Pederson, "SPICE (Simulation Program iwth Integrated Circuit Emphasis),".

[9] J. S. Marshall and M. A. Thomson, "The Pandora Software Development Kit for Pattern Recognition," *Eur. Phys. J.* **C75** no. 9, (2015) 439, `arXiv:1506.05348 [physics.data-an]`.

[10] I. Esteban, M. C. Gonzalez-Garcia, M. Maltoni, I. Martinez-Soler, and T. Schwetz, "Updated fit to three neutrino mixing: exploring the accelerator-reactor complementarity," *JHEP* **01** (2017) 087, `arXiv:1611.01514 [hep-ph]`.

[11] P. Huber and J. Kopp, "Two experiments for the price of one? – The role of the second oscillation maximum in long baseline neutrino experiments," *JHEP* **1103** (2011) 013, `arXiv:1010.3706 [hep-ph]`.

[12] J. C. Pati and A. Salam, "Is Baryon Number Conserved?," *Phys.Rev.Lett.* **31** (1973) 661–664.

[13] H. Georgi and S. Glashow, "Unity of All Elementary Particle Forces," *Phys.Rev.Lett.* **32** (1974) 438–441.

[14] S. Dimopoulos, S. Raby, and F. Wilczek, "Proton Decay in Supersymmetric Models," *Phys.Lett.* **B112** (1982) 133.

[15] P. Langacker, "Grand Unified Theories and Proton Decay," *Phys.Rept.* **72** (1981) 185.

[16] W. de Boer, "Grand unified theories and supersymmetry in particle physics and cosmology," *Prog.Part.Nucl.Phys.* **33** (1994) 201–302, `arXiv:hep-ph/9402266 [hep-ph]`.

[17] P. Nath and P. Fileviez Perez, "Proton stability in grand unified theories, in strings and in branes," *Phys.Rept.* **441** (2007) 191–317, `arXiv:hep-ph/0601023 [hep-ph]`.

[18] **Super-Kamiokande** Collaboration, H. Nishino *et al.*, "Search for Nucleon Decay into Charged Anti-lepton plus Meson in Super-Kamiokande I and II," *Phys. Rev.* **D85** (2012) 112001, `arXiv:1203.4030 [hep-ex]`.

[19] V. A. Kostelecky and M. Mewes, "Lorentz and CPT violation in neutrinos," *Phys.Rev.* **D69** (2004) 016005, `arXiv:hep-ph/0309025 [hep-ph]`.

[20] **Super-Kamiokande** Collaboration, K. Abe *et al.*, "Search for Matter-Dependent Atmospheric Neutrino Oscillations in Super-Kamiokande," *Phys.Rev.* **D77** (2008) 052001, `arXiv:0801.0776 [hep-ex]`.

[21] **Super-Kamiokande** Collaboration, K. Abe *et al.*, "Limits on sterile neutrino mixing using atmospheric neutrinos in Super-Kamiokande," *Phys.Rev.* **D91** (2015) 052019, `arXiv:1410.2008 [hep-ex]`.

[22] A. Kostelecky and M. Mewes, "Neutrinos with Lorentz-violating operators of arbitrary dimension," *Phys.Rev.* **D85** (2012) 096005, `arXiv:1112.6395 [hep-ph]`.

[23] A. Mirizzi, I. Tamborra, H.-T. Janka, N. Saviano, K. Scholberg, R. Bollig, L. Hudepohl, and S. Chakraborty, "Supernova Neutrinos: Production, Oscillations and Detection," *Riv. Nuovo Cim.* **39** no. 1-2, (2016) 1–112, `arXiv:1508.00785 [astro-ph.HE]`.

[24] K. Scholberg, "Supernova Signatures of Neutrino Mass Ordering," *J. Phys.* **G45** no. 1, (2018) 014002, `arXiv:1707.06384 [hep-ex]`.

[25] L. Hudepohl, B. Muller, H.-T. Janka, A. Marek, and G. Raffelt, "Neutrino Signal of

Electron-Capture Supernovae from Core Collapse to Cooling," *Phys.Rev.Lett.* **104** (2010) 251101, arXiv:0912.0260 [astro-ph.SR].

[26] A. Chatterjee, A. De Roeck, D. Kim, Z. G. Moghaddam, J.-C. Park, S. Shin, L. H. Whitehead, and J. Yu, "Search for Boosted Dark Matter at ProtoDUNE," arXiv:1803.03264 [hep-ph].

[27] M. Masud, A. Chatterjee, and P. Mehta, "Probing CP violation signal at DUNE in presence of non-standard neutrino interactions," *J. Phys.* **G43** no. 9, (2016) 095005, arXiv:1510.08261 [hep-ph].

[28] A. de Gouvea and K. J. Kelly, "Non-standard Neutrino Interactions at DUNE," *Nucl. Phys.* **B908** (2016) 318–335, arXiv:1511.05562 [hep-ph].

[29] P. Coloma, "Non-Standard Interactions in propagation at the Deep Underground Neutrino Experiment," *JHEP* **03** (2016) 016, arXiv:1511.06357 [hep-ph].

[30] Y. Farzan and M. Tortola, "Neutrino oscillations and Non-Standard Interactions," *Front.in Phys.* **6** (2018) 10, arXiv:1710.09360 [hep-ph].

[31] P. Minkowski, "$\mu \to e\gamma$ at a Rate of One Out of 10^9 Muon Decays?," *Phys. Lett.* **67B** (1977) 421–428.

[32] R. N. Mohapatra and G. Senjanovic, "Neutrino Mass and Spontaneous Parity Violation," *Phys. Rev. Lett.* **44** (1980) 912.

[33] T. Yanagida, "HORIZONTAL SYMMETRY AND MASSES OF NEUTRINOS," *Conf. Proc.* **C7902131** (1979) 95–99.

[34] M. Gell-Mann, P. Ramond, and R. Slansky, "Complex Spinors and Unified Theories," *Conf. Proc.* **C790927** (1979) 315–321, arXiv:1306.4669 [hep-th].

[35] R. N. Mohapatra and J. W. F. Valle, "Neutrino Mass and Baryon Number Nonconservation in Superstring Models," *Phys. Rev.* **D34** (1986) 1642.

[36] E. K. Akhmedov, M. Lindner, E. Schnapka, and J. W. F. Valle, "Dynamical left-right symmetry breaking," *Phys. Rev.* **D53** (1996) 2752–2780, arXiv:hep-ph/9509255 [hep-ph].

[37] E. K. Akhmedov, M. Lindner, E. Schnapka, and J. W. F. Valle, "Left-right symmetry breaking in NJL approach," *Phys. Lett.* **B368** (1996) 270–280, arXiv:hep-ph/9507275 [hep-ph].

[38] M. Malinsky, J. C. Romao, and J. W. F. Valle, "Novel supersymmetric SO(10) seesaw mechanism," *Phys. Rev. Lett.* **95** (2005) 161801, arXiv:hep-ph/0506296 [hep-ph].

[39] M. Blennow, P. Coloma, E. Fernandez-Martinez, J. Hernandez-Garcia, and J. Lopez-Pavon,

"Non-Unitarity, sterile neutrinos, and Non-Standard neutrino Interactions," *JHEP* **04** (2017) 153, `arXiv:1609.08637 [hep-ph]`.

[40] F. J. Escrihuela, D. V. Forero, O. G. Miranda, M. TâĹŽâĽĕrtola, and J. W. F. Valle, "Probing CP violation with non-unitary mixing in long-baseline neutrino oscillation experiments: DUNE as a case study," *New J. Phys.* **19** no. 9, (2017) 093005, `arXiv:1612.07377 [hep-ph]`.

[41] R. F. Streater and A. S. Wightman, *PCT, spin and statistics, and all that.* 1989.

[42] G. Barenboim and J. D. Lykken, "A Model of CPT violation for neutrinos," *Phys. Lett.* **B554** (2003) 73–80, `arXiv:hep-ph/0210411 [hep-ph]`.

[43] G. Barenboim, C. A. Ternes, and M. TâĹŽâĽĕrtola, "Neutrinos, DUNE and the world best bound on CPT violation," `arXiv:1712.01714 [hep-ph]`.

[44] **LSND** Collaboration, A. Aguilar-Arevalo *et al.*, "Evidence for neutrino oscillations from the observation of anti-neutrino(electron) appearance in a anti-neutrino(muon) beam," *Phys.Rev.* **D64** (2001) 112007, `arXiv:hep-ex/0104049 [hep-ex]`.

[45] **MiniBooNE** Collaboration, A. Aguilar-Arevalo *et al.*, "Improved Search for $\bar{\nu}_\mu \to \bar{\nu}_e$ Oscillations in the MiniBooNE Experiment," *Phys.Rev.Lett.* **110** (2013) 161801, `arXiv:1207.4809 [hep-ex]`.

[46] M. A. Acero, C. Giunti, and M. Laveder, "Limits on nu(e) and anti-nu(e) disappearance from Gallium and reactor experiments," *Phys. Rev.* **D78** (2008) 073009, `arXiv:0711.4222 [hep-ph]`.

[47] G. Mention, M. Fechner, T. Lasserre, T. A. Mueller, D. Lhuillier, M. Cribier, and A. Letourneau, "The Reactor Antineutrino Anomaly," *Phys. Rev.* **D83** (2011) 073006, `arXiv:1101.2755 [hep-ex]`.

[48] G. R. Dvali and A. Yu. Smirnov, "Probing large extra dimensions with neutrinos," *Nucl. Phys.* **B563** (1999) 63–81, `arXiv:hep-ph/9904211 [hep-ph]`.

[49] **MINOS** Collaboration, P. Adamson *et al.*, "Constraints on Large Extra Dimensions from the MINOS Experiment," *Phys. Rev.* **D94** no. 11, (2016) 111101, `arXiv:1608.06964 [hep-ex]`.

[50] W. Altmannshofer, S. Gori, M. Pospelov, and I. Yavin, "Neutrino Trident Production: A Powerful Probe of New Physics with Neutrino Beams," *Phys. Rev. Lett.* **113** (2014) 091801, `arXiv:1406.2332 [hep-ph]`.

[51] **CHARM-II** Collaboration, D. Geiregat *et al.*, "First observation of neutrino trident production," *Phys. Lett.* **B245** (1990) 271–275.

[52] **CCFR** Collaboration, S. R. Mishra *et al.*, "Neutrino tridents and W Z interference," *Phys.*

Rev. Lett. **66** (1991) 3117–3120.

[53] **WA105** Collaboration, S. Murphy, "Status of the WA105-3x1x1 m^3 dual phase prototype," tech. rep., 2017. `https://indico.fnal.gov/event/12345/session/1/contribution/5/material/slides/0.pdf`.

[54] R. Brun and F. Rademakers, "Root - an object oriented data analysis framework," *Nucl. Inst. And Meth. in Phys. Res. A* **389** (1997) .

[55] S. Agostinelli *et al.*, "Geant4 - a simulation toolkit," *Nuclear Instruments and Methods in Physics Research Section A: Accelerators, Spectrometers, Detectors and Associated Equipment* **506** no. 3, (2003) 250 – 303. `http://www.sciencedirect.com/science/article/pii/S0168900203013688`.

[56] J. Allison *et al.*, "Geant4 developments and applications," *IEEE Trans. Nucl. Sci.* **53** (2006) 270.

[57] C. Andreopoulos *et al.*, "The GENIE Neutrino Monte Carlo Generator," *Nucl. Instrum. Meth.* **A614** (2010) 87–104, `arXiv:0905.2517 [hep-ph]`.

[58] T. Golan, J. T. Sobczyk, and J. Zmuda, "NuWro: the Wroclaw Monte Carlo Generator of Neutrino Interactions," *Nucl. Phys. Proc. Suppl.* **229-232** (2012) 499.

[59] M. Abadi, A. Agarwal, P. Barham, E. Brevdo, Z. Chen, C. Citro, G. S. Corrado, A. Davis, J. Dean, M. Devin, S. Ghemawat, I. J. Goodfellow, A. Harp, G. Irving, M. Isard, Y. Jia, R. Józefowicz, L. Kaiser, M. Kudlur, J. Levenberg, D. Mané, R. Monga, S. Moore, D. G. Murray, C. Olah, M. Schuster, J. Shlens, B. Steiner, I. Sutskever, K. Talwar, P. A. Tucker, V. Vanhoucke, V. Vasudevan, F. B. Viégas, O. Vinyals, P. Warden, M. Wattenberg, M. Wicke, Y. Yu, and X. Zheng, "Tensorflow: Large-scale machine learning on heterogeneous distributed systems," *CoRR* **abs/1603.04467** (2016) , `arXiv:1603.04467`. `http://arxiv.org/abs/1603.04467`.

[60] F. Chollet, "Keras." `https://github.com/fchollet/keras`, 2015.

[61] Y. Jia, E. Shelhamer, J. Donahue, S. Karayev, J. Long, R. Girshick, S. Guadarrama, and T. Darrell, "Caffe: Convolutional architecture for fast feature embedding," in *Proceedings of the 22Nd ACM International Conference on Multimedia*, MM '14, pp. 675–678. ACM, New York, NY, USA, 2014. `http://doi.acm.org/10.1145/2647868.2654889`.

[62] **MINOS Collaboration** Collaboration, D. Michael *et al.*, "The magnetized steel and scintillator calorimeters of the MINOS experiment," *Nuclear Instruments and Methods in Physics Research Section A: Accelerators, Spectrometers, Detectors and Associated Equipment* **596** no. 2, (2008) 190 – 228. `http://www.sciencedirect.com/science/article/pii/S0168900208011613`.

[63] **MINERvA collaboration** Collaboration, B. Osmanov, "MINERvA Detector: Description and Performance." arXiv:1109.2855 [hep-ex], 2011.

[64] R. Acciarri *et al.*, "Design and construction of the microboone detector," *Journal of Instrumentation* **12** no. 02, (2017) P02017. http://stacks.iop.org/1748-0221/12/i=02/a=P02017.

[65] **NOvA** Collaboration, P. Adamson *et al.*, "First measurement of muon-neutrino disappearance in NOvA," *Phys. Rev.* **D93** no. 5, (2016) 051104, arXiv:1601.05037 [hep-ex].

[66] **MicroBooNE** Collaboration, R. Acciarri *et al.*, "Design and Construction of the MicroBooNE Detector," *JINST* **12** no. 02, (2017) P02017, arXiv:1612.05824 [physics.ins-det].

[67] **MicroBooNE** Collaboration, R. Acciarri *et al.*, "Noise Characterization and Filtering in the MicroBooNE Liquid Argon TPC," *JINST* **12** no. 08, (2017) P08003, arXiv:1705.07341 [physics.ins-det].

[68] **MicroBooNE** Collaboration, C. Adams *et al.*, "Ionization Electron Signal Processing in Single Phase LArTPCs I. Algorithm Description and Quantitative Evaluation with MicroBooNE Simulation," arXiv:1802.08709 [physics.ins-det].

[69] **MicroBooNE** Collaboration, R. Acciarri *et al.*, "Convolutional Neural Networks Applied to Neutrino Events in a Liquid Argon Time Projection Chamber," *JINST* **12** no. 03, (2017) P03011, arXiv:1611.05531 [physics.ins-det].

[70] **MicroBooNE** Collaboration, R. Acciarri *et al.*, "The Pandora multi-algorithm approach to automated pattern recognition of cosmic-ray muon and neutrino events in the MicroBooNE detector," *Eur. Phys. J.* **C78** no. 1, (2018) 82, arXiv:1708.03135 [hep-ex].

[71] **MicroBooNE** Collaboration, R. Acciarri *et al.*, "Michel Electron Reconstruction Using Cosmic-Ray Data from the MicroBooNE LArTPC," *JINST* **12** no. 09, (2017) P09014, arXiv:1704.02927 [physics.ins-det].

[72] **DUNE** Collaboration, R. Acciarri *et al.*, "Long-Baseline Neutrino Facility (LBNF) and Deep Underground Neutrino Experiment (DUNE)," arXiv:1512.06148 [physics.ins-det].

[73] Worcester, E., "Energy Systematics Studies," 2016. https://indico.fnal.gov/event/11718/contribution/4/material/slides/0.pdf.

[74] **LArIAT** Collaboration, F. Cavanna, M. Kordosky, J. Raaf, and B. Rebel, "LArIAT: Liquid Argon In A Testbeam." arXiv:1406.5560, 2014.

[75] **LAr1-ND, ICARUS-WA104, MicroBooNE** Collaboration, M. Antonello *et al.*, "A Proposal for a Three Detector Short-Baseline Neutrino Oscillation Program in the Fermilab Booster Neutrino Beam," arXiv:1503.01520 [physics.ins-det].

[76] **ArgoNeuT** Collaboration, R. Acciarri *et al.*, "A study of electron recombination using

highly ionizing particles in the ArgoNeuT Liquid Argon TPC," *JINST* **8** (2013) P08005, arXiv:1306.1712 [physics.ins-det].

[77] **ICARUS** Collaboration, S. Amoruso *et al.*, "Study of electron recombination in liquid argon with the ICARUS TPC," *Nucl. Instrum. Meth.* **A523** (2004) 275–286.

[78] M. Antonello, B. Baibussinov, P. Benetti, F. Boffelli, A. Bubak, *et al.*, "Experimental observation of an extremely high electron lifetime with the ICARUS-T600 LAr-TPC," *JINST* **9** no. 12, (2014) P12006, arXiv:1409.5592 [physics.ins-det].

[79] P. Cennini *et al.*, "Performance of a 3-ton liquid argon time projection chamber," *Nucl. Instrum. Meth.* **A345** (1994) 230–243.

[80] T. K. Warburton, *Simulations and Data analysis for the 35 ton Liquid Argon detector as a prototype for the DUNE experiment.* PhD thesis, Sheffield U., 2017. http://lss.fnal.gov/archive/thesis/2000/fermilab-thesis-2017-28.pdf.

[81] A. Ereditato, D. Goeldi, S. Janos, I. Kreslo, M. Luethi, C. Rudolf von Rohr, M. Schenk, T. Strauss, M. S. Weber, and M. Zeller, "Measurement of the drift field in the ARGONTUBE LAr TPC with 266 nm pulsed laser beams," *JINST* **9** no. 11, (2014) P11010, arXiv:1408.6635 [physics.ins-det].

[82] M. Auger *et al.*, "A Novel Cosmic Ray Tagger System for Liquid Argon TPC Neutrino Detectors," *Instruments* **1** no. 1, (2017) 2, arXiv:1612.04614 [physics.ins-det].

[83] **DUNE** Collaboration, B. Abi *et al.*, "The Single-Phase ProtoDUNE Technical Design Report," arXiv:1706.07081 [physics.ins-det].

[84] **ArgoNeuT** Collaboration, R. Acciarri *et al.*, "Measurement of ν_μ and $\bar{\nu}_\mu$ neutral current $\pi^0 \to \gamma\gamma$ production in the ArgoNeuT detector," *Phys. Rev.* **D96** no. 1, (2017) 012006, arXiv:1511.00941 [hep-ex].

[85] **MicroBooNE collaboration** Collaboration, "A Measurement of the Attenuation of Drifting Electrons in the MicroBooNE LArTPC," 2017. MICROBOONE-NOTE-1026-PUB,http://microboone.fnal.gov/wp-content/uploads/MICROBOONE-NOTE-1026-PUB.pdf.

[86] T. M. Collaboration, "Study of Space Charge Effects in MicroBooNE," tech. rep., 2016. http://microboone.fnal.gov/wp-content/uploads/MICROBOONE-NOTE-1018-PUB.pdf. MICROBOONE-NOTE-1018-PUB.

[87] T. M. Collaboration, "Establishing a Pure Sample of Side-Piercing Through-Going Cosmic-Ray Muons for LArTPC Calibration in MicroBooNE," tech. rep., 2017. http://microboone.fnal.gov/wp-content/uploads/MICROBOONE-NOTE-1028-PUB.pdf. MICROBOONE-NOTE-1028-PUB.

[88] **MicroBooNE** Collaboration, P. Abratenko *et al.*, "Determination of muon momentum in

the MicroBooNE LArTPC using an improved model of multiple Coulomb scattering," *JINST* **12** no. 10, (2017) P10010, arXiv:1703.06187 [physics.ins-det].

[89] **ICARUS** Collaboration, A. Ankowski *et al.*, "Energy reconstruction of electromagnetic showers from pi0 decays with the ICARUS T600 Liquid Argon TPC," *Acta Phys. Polon.* **B41** (2010) 103–125, arXiv:0812.2373 [hep-ex].

[90] **ICARUS** Collaboration, A. Ankowski *et al.*, "Measurement of through-going particle momentum by means of multiple scattering with the ICARUS T600 TPC," *Eur.Phys.J.* **C48** (2006) 667–676, arXiv:hep-ex/0606006 [hep-ex].

[91] **ICARUS** Collaboration, M. Antonello *et al.*, "Muon momentum measurement in ICARUS-T600 LAr-TPC via multiple scattering in few-GeV range," *JINST* **12** no. 04, (2017) P04010, arXiv:1612.07715 [physics.ins-det].

[92] G. Cancelo, F. Cavanna, C. O. Escobar, E. Kemp, A. A. Machado, A. Para, E. Segreto, D. Totani, and D. Warner, "Increasing the efficiency of photon collection in LArTPCs: the ARAPUCA light trap," *JINST* **13** no. 03, (2018) C03040, arXiv:1802.09726 [physics.ins-det].

[93] Z. Moss, J. Moon, L. Bugel, J. M. Conrad, K. Sachdev, M. Toups, and T. Wongjirad, "A Factor of Four Increase in Attenuation Length of Dipped Lightguides for Liquid Argon TPCs Through Improved Coating," arXiv:1604.03103 [physics.ins-det].

[94] Z. Moss, L. Bugel, G. Collin, J. M. Conrad, B. J. P. Jones, J. Moon, M. Toups, and T. Wongjirad, "Improved TPB-coated Light Guides for Liquid Argon TPC Light Detection Systems," *JINST* **10** no. 08, (2015) P08017, arXiv:1410.6256 [physics.ins-det].

[95] Y. Li *et al.*, "Measurement of Longitudinal Electron Diffusion in Liquid Argon," *Nucl. Instrum. Meth.* **A816** (2016) 160–170, arXiv:1508.07059 [physics.ins-det].

[96] M. Zeller *et al.*, "First measurements with ARGONTUBE, a 5m long drift Liquid Argon TPC," *Nucl. Instrum. Meth.* **A718** (2013) 454–458.

[97] **T2K ND280 TPC** Collaboration, N. Abgrall *et al.*, "Time Projection Chambers for the T2K Near Detectors," *Nucl. Instrum. Meth.* **A637** (2011) 25–46, arXiv:1012.0865 [physics.ins-det].

[98] J. G. Rogers, M. S. Andreaco, and C. Moisan, "A 7-MeV - 9-MeV isotopic gamma-ray source for detector testing," *Submitted to: Nucl. Instrum. Meth.* (1996) .

[99] http://svoboda.ucdavis.edu/experiments/aced/.

[100] R. Reifarth *et al.*, "Background identification and suppression for the measurement of (n,g) reactions with the DANCE array at LANSCE," *Nucl. Instrum. Meth.* **A531** (2004) 530–543, arXiv:1310.1884 [nucl-ex].